

## **INFORMATION TO USERS**

This manuscript has been reproduced from the microfilm master. UMI films the text directly from the original or copy submitted. Thus, some thesis and dissertation copies are in typewriter face, while others may be from any type of computer printer.

**The quality of this reproduction is dependent upon the quality of the copy submitted.** Broken or indistinct print, colored or poor quality illustrations and photographs, print bleedthrough, substandard margins, and improper alignment can adversely affect reproduction.

In the unlikely event that the author did not send UMI a complete manuscript and there are missing pages, these will be noted. Also, if unauthorized copyright material had to be removed, a note will indicate the deletion.

Oversize materials (e.g., maps, drawings, charts) are reproduced by sectioning the original, beginning at the upper left-hand corner and continuing from left to right in equal sections with small overlaps.

**ProQuest Information and Learning  
300 North Zeeb Road, Ann Arbor, MI 48106-1346 USA  
800-521-0600**

**UMI<sup>®</sup>**



A

**SYNTHESES AND CHARACTERIZATION OF NOVEL  
COPOLYMERS**

by

Dayi Xu

A dissertation submitted to the Graduate Faculty in Chemistry in  
partial fulfillment of the requirements for the degree of Doctor of  
Philosophy, The City University of New York.

2002

UMI Number: 3063899

Copyright 2002 by  
Xu, Dayi

All rights reserved.

**UMI<sup>®</sup>**

---

UMI Microform 3063899

Copyright 2002 by ProQuest Information and Learning Company.  
All rights reserved. This microform edition is protected against  
unauthorized copying under Title 17, United States Code.

---

ProQuest Information and Learning Company  
300 North Zeeb Road  
P.O. Box 1346  
Ann Arbor, MI 48106-1346

© 2002

DAYI XU

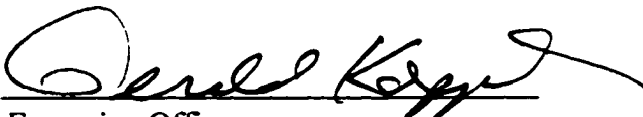
All Rights Reserved

This manuscript has been read and accepted for the Graduate Faculty in Chemistry in satisfaction of the dissertation requirement for the degree of Doctor of Philosophy.

Sept. 12, 2002  
Date

  
Chair of Examining Committee

9/19/2002  
Date

  
Executive Officer

Professor David C. Locke

Professor Steven Schwarz

Supervisory Committee

The University of New York

## Abstract

## SYNTHESES AND CHARACTERIZATION OF NOVEL COPOLYMERS

by

Dayi Xu

Adviser: Professor Nan-Loh Yang

A modified Wittig reaction was developed for the synthesis of soluble electroluminescent (EL) copolymers with uniform conjugate segments separated by flexible spacers. This new method of preparing macromolecular conjugate systems has important advantages over the conventional Wittig reactions. The trans-structured conjugate segment, essential for the electroluminescent property, was obtained without the conventionally-needed follow-up step of iodine-catalyzed isomerization, which can readily lead to radical cross-linking side-reactions. In this new synthesis route, triphenylphosphine used in the conventional Wittig reaction was replaced by triethyl phosphite, leading to efficient purification of the polymer product due to the water and alcohol solubility of its by-products. Soluble EL polymers with low glass transition temperature and emission in blue and yellow were synthesized. Poly-[1,10-decanedioxy-(2,6-dimethoxy-1,4-phenylene)-1,2-ethenylene-2,3-quinoxaline-1,2-ethenylene-(3,5,-dimethoxy-1,4-phenylene)] has an absorption maximum at 375 nm and emission maximum 499 nm. Poly[1,10-decanedioxy-(2,6-dimethoxy-1,4-phenylene)-1,2-ethenylene-9,10-anthracene-1,2-

ethenylene-(3,5,-dimethoxy-1,4-phenylene)] has an absorption maximum at 416 nm and emission maximum at 566 nm. These EL polymers were characterized using methods including one and two dimensional NMR, photoluminescence and DSC.

Three categories of functionalized polystyrene having electric charge, dipole, and hydrogen bond forming ability were synthesized. Polystyrenes sulfonated at a range of 2 to 30 % were prepared to give surface with charge densities up to  $0.15 \text{ C/m}^2$ ; the negatively charged polymer has the attributes to serve as a model extracellular matrix for protein adsorption and organization to gain fundamental information on tissue engineering. Acetylated polystyrene with dipole and polystyrene with hydroxyl group for interfacial hydrogen-bonding were synthesized for studies on interface including fracture toughness at polymer interfaces.

Random copolymers of methyl methacrylate and 3-(3, 5,7, 9, 11, 13, 15-heptacyclopentylpentacyclo [9. 5. 1.<sup>3.9</sup>. 1<sup>5.15</sup>. 1<sup>7.13</sup>] octasiloxa-1-nyl) propyl methacrylate (POSS-propyl methacrylate) were synthesized for the first time using atom transfer radical polymerization, resulting in narrow molecular weight distribution. This copolymer has the capability to serve as a very efficient compatibilizer for polystyrene/ poly (methyl methacrylate) immiscible blend.

## Acknowledgements

The author wishes to express his sincere appreciation to Professors Nan-Loh Yang, David Locke and Steven Schwarz for their expert advice, generous support, and assistance during this project. He acknowledges gratefully the support from the Center for Polymers at Engineered Interfaces (MRSEC, NSF), Chemistry Department at the College of Staten Island, the Graduate School and University Center, CUNY and the Department of Materials Science and Engineering at Stony Brook , SUNY.

## TABLE OF CONTENTS

	<u>PAGE</u>
<b>Abstract</b>	iv
<b>Thesis statement</b>	1
<b>Chapter 1. Soluble Electroluminescent Polymers</b>	3
<b>Introduction</b>	3
Basic Mechanism of Polymer EL process	5
Type and characteristics of EL polymers	7
The typical synthesis route of EL polymers	11
1. Fully conjugated EL polymers	11
2. Copolymers containing both conjugated and non-conjugated segments.	13
The mechanism of the Wittig reaction	15
<b>Experimental section</b>	22
I. Synthesis schemes of PPV-based copolymers	22
1. Synthesis of comonomers.	22
2. Synthesis of copolymers through Wittig reaction.	25
3. Synthesis of copolymers through modified Wittig reaction.	26
II. Syntheses procedure	27
Typical synthesis of dialdehyde compound	27

Typical synthesis of bis(triphenylphosphonium halide) monomer	27
Typical synthesis of bis(diethylphosphonate) monomers	28
Typical polycondensation by the Wittig reaction	28
Typical condensation with the modified Wittig reaction	29
<b>Instrumental analyses</b>	30
<b>Results and discussion</b>	31
Characterization of monomers	31
Characterization of the copolymer	40
Structure of the copolymers	40
2-D NMR analysis of the copolymer	51
GPC determination of molecular weight of copolymer	58
Thermal property of copolymers through	
DSC determination	60
UV and PL determination	64
<b>Conclusion</b>	69
<b>Chapter 2. Synthesis and characterization of functionalized Polystyrene</b>	70
<b>Background</b>	70
1. <b>Polystyrene with sulfonic acid group</b>	73
<b>Introduction</b>	73
<b>Experimental section</b>	75
1). <b>Synthesis of sulfonation of polystyrene</b>	75

2). Preparation of polystyrene with sodium and rubidium sulfonate	77
3) Characterization	78
<b>Result and discussion</b>	78
1. Solubility	78
2. Determination of sulfonation level	78
Sulfonated polystyrene as an extracellular matrix model	89
<b>Conclusion</b>	94
<b>2. Polystyrene with acetyl group</b>	95
<b>Introduction</b>	95
<b>Experimental section</b>	97
1). Synthesis- acetylation of polystyrene	97
2). Structural characterization	97
<b>Result and discussion</b>	98
<b>Conclusion</b>	98
<b>3. Polystyrene with hydroxyl group</b>	101
<b>Introduction</b>	101
<b>Experimental section</b>	104
Synthesis route- copolymerization and hydrolysis	104
Experimental procedure	105
1) Polymerization	105
2) Hydrolysis	106

3) structure characterization	106
<b>Results and discussion</b>	106
<b>Conclusion</b>	107
<b>Chapter 3. Polymethacrylate with POSS side group by atom transfer radical polymerization, ATRP</b>	110
<b>Introduction</b>	110
<b>Synthesis procedure</b>	114
<b>Results and discussion</b>	115
Polymethacrylate with POSS side group as a compatibilizer for polystyrene/poly(methyl methacrylate)blend	121
<b>Conclusion</b>	124
<b>Bibliography</b>	125

## **LIST OF FIGURES**

<u>No.</u>	<u>LEGEND</u>	<u>PAGE</u>
1-1.	<sup>1</sup> H-NMR spectra of $\alpha,\omega$ -dialdehyde monomers	33
1-2.	<sup>1</sup> H-NMR spectra of $\alpha,\omega$ -dialdehyde monomers	34
1-3.	<sup>1</sup> H-NMR spectra of triethylphosphite, <i>p</i> -dichloroxylylene and <i>p</i> -xylylenebis(diethylphosphonate)	37
1-4.	<sup>1</sup> H-NMR spectra of 2,3-bis(bromomethyl)-quinoxaline(A) and 2,3-dimethylenequinoxaline-bis(diethylphosphonate)	38
1-5.	<sup>1</sup> H-NMR spectra of 9,10-bis(chloromethyl) anthracene (A) and 9,10-dimethylene anthracene-bis(diethyl phosphonate)	39
1-6.	<sup>1</sup> H-NMR spectra of alternating copolymer with octylene and PPV segments  (A) unisomerized copolymer through Wittig reaction  (B) isomerized copolymer  (C) copolymer through modified Wittig reaction	41
1-7.	<sup>1</sup> H-NMR spectra of alternating copolymer with soft segments, hexyl(A), decyl (B), 2EO (C) and 3 EO (D).	44
1-8.	FT-IR spectra of alternating copolymers  (A) unisomerized copolymer through Wittig reaction	47

	(B) isomerized copolymer	
	(C) copolymer through modified Wittig reaction	
1-9.	IR spectra of alternating copolymers	48
	(A) unisomerized copolymer through Wittig reaction	
	(B) isomerized copolymer	
	(C) copolymer through modified Wittig reaction	
1-10.	<sup>1</sup> H-NMR spectrum of poly[1,10-decanedioxy-(2,6-dimethoxy-1,4-phenylene)-1,2-ethylene-2,3-quinoxaline-1,2-ethylene-(3,5-dimethoxy-1,4-phenylene)]	49
1-11.	<sup>1</sup> H-NMR spectrum of poly[1,3-methylenetetramethyldisiloxane dioxy-(2,6-dimethoxy-1,4-phenylene)-1,2-ethylene-1,4-phenylene-1,2-ethylene-(3,5-dimethoxy-1,4-phenylene)]	50
1-12.	<sup>1</sup> H-NMR (top) and <sup>13</sup> C-NMR spectra of poly[1,6-hexanedioxy-2,6-dimethoxy-1,4-phenylene-1,2-ethylene-1,4-phenylene-1,2-ethylene-3,5-dimethoxy-1,4-phenylene]. (600 MHz)	55
1-13.	2-D NMR spectrum of isomerized copolymer of poly[1,6-hexanedioxy-2,6-dimethoxy-1,4-phenylene-1,2-ethylene-1,4-phenylene-1,2-ethylene-3,5-dimethoxy-1,4-phenylene].	56
1-14.	HMQC 2D-NMR spectrum of poly[1,6-hexanedioxy-2,6-dimethoxy-1,4-phenylene-1,2-ethylene-1,4-phenylene-1,2-ethylene-3,5-dimethoxy-1,4-phenylene]. (600 MHz)	57
1-15.	DSC spectra of alternating copolymer with a soft segment of alkylene or EO and with conjugated segment of PPV.	62

- 1-16. DSC spectrum of poly[1,3-methylenetetramethyldisiloxane dioxo-(2,6-dimethoxy-1,4-phenylene)-1,2-ethenylene-1,4-phenylene-1,2-ethenylene-(3,5,-dimethoxy-1,4-phenylene)] 63
- 1-17. UV spectra of original poly[1,8-octanedioxy-2,6-dimethoxy-1,4-phenylene-1,2-ethenylene-1,4-phenylene-1,2-ethylene-3,5-dimethoxy-1,4-phenylene] (A) and its isomerized product (B). 65
- 1-18. Photoluminescence spectra of poly[1,8-octanedioxy-2,6-dimethoxy-1,4-phenylene-1,2-ethenylene-1,4-phenylene-1,2-ethylene-3,5-dimethoxy-1,4-phenylene]. 66
1. unisomerized copolymer through Wittig reaction.
  - 2 isomerized copolymer.
  3. copolymer through modified Wittig reaction
- 1-19 Photoluminescence spectrum of poly- poly[1,10-decanedioxy-(2,6-dimethoxy-1,4-phenylene)-1,2-ethenylene-9,10-anthracene-1,2-ethenylene-(3,5,-dimethoxy-1,4-phenylene)] 67
- 1-20. Photoluminescence spectrum of poly- poly[1,10-decanedioxy-(2,6-dimethoxy-1,4-phenylene)-1,2-ethenylene-2,3-quinoxaline-1,2-ethenylene-(3,5,-dimethoxy-1,4-phenylene)] 68
- 2-1 Proton NMR spectra of polystyrene (A) and sulfonated polystyrene (B) 80
- 2-2. <sup>1</sup>H-NMR spectrum of poly-styrene-co-(sodium styrenesulfonate) 81

2-3.	Comparison of FT-IR spectrum between sulfonated polystyrene(A) and original polystyrene(B).	84
2-4.	FT-IR spectrum of sulfonated polystyrene (15 mole %sulfonation).	85
2-5.	FT-IR spectrum of 60% sulfonated Polystyrene.	86
2-6.	The FT-IR spectrum of higher sulfonated polystyrene dried in vacuum oven at 35°C, for 24h.	87
2-7	Adsorbed fibronectin mass as a function of surface charge density.	88
2-8.	<sup>1</sup> H-NMR spectra of acetylated polystyrene (7 mole %) and its original polystyrene(top).	99
2-9.	FT-IR spectra of acetylated polystyrene (A) and its original polystyrene( B)	100
2-10.	<sup>1</sup> H-NMR spectra of polystyrene (A), poly-styrene-co-4-acetoxystyrene(C) and polystyrene-co-4-hydroxystyrene (10 mole %)(B).	108
2-11.	FT-IR spectra of polystyrene-co-4-acetoxystyrene (A) and its hydrolyzed product, polystyrene-co-4-hydroxystyrene (B)	109
3-1.	<sup>1</sup> H-NMR spectra of ATRP copolymerization solution of methyl methacrylate and propyl-POSS methacrylate (toluene as solvent, A is that after 36 h; and B is that after 72 h)	116

- 3-2.  $^1\text{H-NMR}$  spectrum of random copolymer of methyl methacrylate and POSS-propyl methacrylate ( 3 mole %). 117
- 3-3. GPC spectrum of copolymer of methyl methacrylate and propyl-POSS methyl methacrylate (2 mole %). 120
- 3-4 Interfacial tension calculated from observed contact angles as a function of POSS concentrations 122
- 3-5. Schematic of PMMA (solid) and PS (dashed) chains in a blend when functionalized POSS is grafted onto the PMMA chains. In this case, the functional groups (cyclopentyl) interact more favorably with the PS than the PMMA monomers. 123

## **LIST OF TABLES**

<b><u>No.</u></b>	<b><u>LEGEND</u></b>	<b><u>PAGE</u></b>
1-1.	The features and display screen benefit of EL polymers	4
1-2	Chemical shift of $\alpha,\omega$ -dialdehyde monomers on $^1\text{H-NMR}$	31
1-3	Melting point of $\alpha,\omega$ -dialdehyde monomers	35
1-4	Microstructure of copolymers	42
1-5	Results of GPC analysis of copolymers	59
1-6.	Glass transition temperature, $T_g$ , of EL copolymers	60
2-1	Sulfonating extent of some samples	82
2-2	Sulfonation of polystyrene in $\text{C}_2\text{H}_4\text{Cl}_2$ with acetyl sulfonate	82
3-1	The GPC results of copolymers	119

## LIST OF SCHEMES

<u>No.</u>	<u>LEGEND</u>	<u>PAGE</u>
1-1.	General route of polymerization of fully conjugated EL polymers	12
1-2.	Typical Wittig reaction for the formation of C=C bond.	13
1-3.	The radical mechanism of iodine-catalyzed isomerization	14
1-4.	Mechanism of conventional Wittig reaction.	15
1-5.	Illustration of cis- or trans- olefin forming path.	17
1-6.	Mechanism of modified Wittig reaction using triethyl phosphite.	19
1-7.	Illustration of trans-olefin formation through modified Wittig reaction using triethyl phosphite.	20
1-8.	The reaction of preparation of triphenylphosphium monomers.	22
1-9	The reaction of preparation of $\alpha,\omega$ -dialdehyde monomers with soft segment.	23
1-10.	The reaction of preparation of diphosphonate monomer.	24
1-11.	The synthesis route of copolymer through the Wittig reaction.	25
1-12.	The synthesis route through the modified Wittig reaction	26
2-1.	Reaction of polystyrene with electrophilic reagents.	71
2-2.	Sulfonation of polystyrene using acetyl sulfate	75

2-3.	Reaction of acetyl anhydride with concentrated sulfuric acid to form acetyl sulfate.	75
2-4.	The reaction of sulfonated polystyrene with acetate salt.	77
2-5.	Mechanism of acetylation of polystyrene through Friedel-Crafts reaction.	96
2-6.	Preparation of polystyrene with <i>p</i> -hydroxyl group	104
3-1	Transition-metal-catalyzed ARTP	112
3-2.	Copolymerization of methyl methacrylate and POSS-propyl methacrylate.	113

## **SYNTHESES AND CHARACTERIZATION OF NOVEL COPOLYMERS**

### **Thesis statement**

The focuses of this thesis are on developing new synthetic methods for novel copolymers having desired properties targeted for significant applications. The three chapters to follow report findings in synthetic routes for copolymers which were examined for their merits in the areas ranging from electroluminescence, polymer interfaces to tissue engineering.

Chapter 1 describes a new modified Wittig reaction developed for the copolymer synthesis of soluble electroluminescent materials. In comparison with other reported polymer investigations, this newly developed method has two main advantages: 1. All trans-structured PPV segment, essential for electroluminescent property, was obtained without the conventionally needed follow-up step of iodine-catalyzed isomerization, which can readily lead to radical cross-linking side-reaction; 2. In this synthesis route, triphenylphosphoshine used in conventional Wittig reaction was replaced by triethyl phosphite, leading to

efficient purification of polymer product due to water and alcohol solubility of its by-product. The mechanism of the reaction was discussed in detail.

Chapter 2 details the synthesis of three kinds of functionalized polystyrene, with electric charge, dipole, and hydrogen-bonding forming ability. Polystyrene sulfonated at a range of 2 to 30 % were prepared to give surface with charge density up to  $0.15 \text{ C/m}^2$ ; the negatively charged polymer has the attributes to serve as a model extracellular matrix for protein adsorption and organization. Acetylated polystyrene with dipole and polystyrene with hydroxyl group for interfacial hydrogen-bonding were synthesized for studies on interface including fracture toughness at polystyrene (PS) and Styrene acrylonitrile (SAN) interfaces.

Chapter 3 reports a procedure for the synthesis, for the first time, of random copolymer of methyl methacrylate with polyhedral oligomeric silsesquioxane monomer (POSS-propyl methacrylate) having narrow chain molecular weight distribution using atom transfer radical polymerization (ATRP). This copolymer has the capability as a very efficient compatibilizer for polystyrene/ poly (methyl methacrylate) immiscible blend.

## **Chapter 1.**

# **Soluble Electroluminescent Polymers**

## **Introduction**

The electroluminescence (EL) polymer, also so-called light emitting polymer (LEP), has attracted extensive recent attention <sup>[1-11]</sup>, because of its appealing scientific nature and potential applications for display devices including large area lighting. EL polymers exhibit radiative emission (normally in the visible range) under an electric field in a direct energy conversion process.

EL phenomena were first found in inorganic materials in the 1930s <sup>[12]</sup> and in organic materials in the 1960s <sup>[13]</sup>. Unlike inorganic materials, EL devices using organic compounds so far are almost exclusively of the charge injection type. Recently, much effort has been directed to the improvement of brightness, efficiency and longevity of devices especially by utilizing blends and by introducing charge carrier transport layers between the electrodes and the emitter. Compared with inorganic systems, the organic LEDs offer greater choice of materials and more facile modification of molecular structure for fine tuning properties, such as emission color, and the organic EL polymers can be processed

readily into large area film. Some attributes and advantages of EL polymers are listed in Table 1- 1.

Table 1-1. The attributes and display screen benefit of EL polymers.

<b>LEP Attributes</b>	<b>Display Screen Benefit</b>
The processability of the polymer materials – especially in this case the ability to ink-jet the active materials of a device.	This will considerably simplify the manufacturing process.
The fact that a large number of process steps are common with LCD manufacture means a lot of exiting manufacturing plant can be used in LEP manufacture.	Reduces cost and risk to the manufacturer.
LEPs are itself emissive, which means that a large number of components used in a LCD such as polarisers. colour filters and backlights are not needed.	This reduces cost and has other benefits for the overall thickness and weight of the LEP display which are considerably reduced.
LEPs are Lambertian emitters.	The displays show a 180-degree

Continue	viewing angle up, down and side-to-side.
LEPs are driven by low DC voltage.	Voltages are suitable for use with TFT active matrix drivers. It is also important for portable applications, as no voltage converters are required.
The LEP and TFT switch very fast.	The display can show true video, without the blurring and submarining seen on LCDs.
The finished devices are solid state.	Very rugged and robust -ideal for portable environments. This also saves weight and overall thickness in the product packaging.

*From: [www.cdtltd.co.uk/seikotvtech.html](http://www.cdtltd.co.uk/seikotvtech.html)(1998)*

### **Basic Mechanism of Polymer EL process**

In a polymer EL device, a chromophoric polymer film is sandwiched between two electrodes, a transparent high work function anode, which is often indium-tin-oxide (ITO), and a low work function metal cathode. On applying an

appropriate forward DC bias, the polymer film emits light, which can be observed through the transparent anode.

In the first step of the process charge carriers of opposite sign are injected from the two electrodes into the polymer emitter film: electrons are injected from the cathode and holes from the anode. The carrier flux is a function of the electric field and the electronic properties of the respective electrodes in relation to those of polymer. To achieve injection, a field of  $10^5$ -  $10^6$  V/cm is necessary to sustain the process for chromophore layer of the order of 100 nm thick.

In the second step, the charge carriers migrate in the polymer film under the influence of the field and interact within the emitter film to form excited state molecules (excitons). Charge carriers may lose their energy in non-radiative decay processes, such as, multi-photon emission, Auger processes, or surface recombination. These concepts have been extensively studied in inorganic systems and may also apply to polymer systems, though relatively little detailed information is available.

In the third step, a singlet-singlet radiative decay takes place with photon emission. The singlet state exciton generated in the second step may undergo two types of decays: radiative and non-radiative. In the non-radiative decay, the exciton may lose its energy by dissociation into an electron-hole pair or by processes such as photon scattering, collision ionization, defect scattering, and field ionization, it may also undergo photon emission and lose energy in a thermal burst or transfer energy to "impurities" or convert into a triplet state by intersystem crossing and

eventually lose energy non-radiatively. In the radiative decay process, the released photon has an energy characterized by the energy gap between the LUMO and the HOMO of the chromophore. For organic polymeric chromophores, this energy gap ranges from 1.4 to 3.3 eV, corresponding to light of wavelength between 890 and 370 nm. This spectral width covers the visible light range.

### **Type and characteristics of EL polymers**

The first requirement for achieving high performance in the EL cells is good quality of the emitter films. Organic or inorganic low molar mass chromophores often suffer from their less than perfect film forming properties, causing deterioration in the emitter layer because of recrystallization.

Tang and Vanslyke were the first to report on the high-performance EL devices composed of a vacuum-sublimed double-layer dye film (emissive and hole-transport layers) <sup>[14]</sup>. Since then, various multilayered structure devices, fluorescent dyes, and electrode materials have been studied to improve the efficiency and stability of the devices <sup>[15-19]</sup>. Chihaya Adachi et al <sup>[20]</sup> examined 15 non-polymer organic compounds with blue fluorescence, which were deposited on a pre-cleaned ITO glass substrate by vacuum deposition. Except a few with lower symmetry or with bulky substituents, other typical organic scintillators did not give dense thin films. The surfaces of the evaporated films appeared to be rugged, and the growth of about 1  $\mu\text{m}$  scale large crystals was observed. Poor quality of these emitter films resulted in inferior EL cell characteristics. In general, organic compounds with blue

fluorescence have simple molecular structure with high symmetry and with few substituents. Thus, such molecules possess a tendency to give large crystals, even when they are forced to form thin film.

However, one of the problems associated with such devices is the lifetime of the cell. Although a lifetime of 100 h has been reported <sup>[14]</sup>, a much longer lifetime is required for practical use. The degradation of the cell is partly caused by crystallization of organic dyes. The cell structure with two organic layers contains an interface between the two organic layers where only the weak van der Waals force exists between the layers. Such interface may not be physically strong enough for long term use of the devices; therefore, one-layer-type device rather than two-layer-type device may achieve an improvement of structural stability.

Most of polymeric materials have the excellent ability to form single-layer film, because of their large intermolecular force.

Three categories of EL polymer systems are known: (1) polymers doped with low molar mass dyes; (2) fully conjugated polymers; and (3) copolymers or homopolymers containing both conjugated and non-conjugated segments in the backbone or polymers with side group chromophores.

The works reported on the doped polymers with low molar mass dyes are so far sparse. An improvement in the organic dyes system is to use less crystalline polymeric materials, and the utility of poly(methylphenysiline)<sup>[21]</sup>, and poly(vinylcarbazole)<sup>[22]</sup> as the hole transport layer. However, there still is the

interface problem, because of the compatibility of the dyes with polymer matrix. Devices obtained from using multiple compounds, including dye-doped polymer thin film system, are conventionally prepared by the solvent-dependent method such as spin-coating or casting. These methods, although convenient, have been proven to be difficult for obtaining a large-area and uniform pinhole-free thin film [23]. Some organic electroluminescent devices based on molecularly doped polymer were fabricated experimentally using poly(methyl methacrylate) molecularly doped with triphenyldiamine derivative and tris (8-quinolinolato) aluminum(III) complex [24]. Jwo-Huei Jou et al [25] reported an approach for preparing single-layer molecularly doped EL polymer thin film.

Studies of other two kinds of conjugated polymers are drawing significant attention because they are free of problems related to crystallization, aggregation, or heat stability. These problems have so far posed factors that are detrimental to the quality of evaporated films made with low molecular weight compounds. [26]

Burroughes et al. [27] first demonstrated the light-emitting property of fully conjugated poly (*p*-phenylenevinylene)(PPV) through fabricating a green-emitting diode(LED) using this polymer in the emitting layer. Since then a number of polymer LEDs have been reported, using different conjugated polymers [28-37] emitting in various portions of the visible spectrum.

Fully conjugated polymers such as polyphenylene vinylene and its substituted analogues have an extended conjugated molecular structure. By varying the structure, one can change the effective conjugation length and energy gap,

which results in chromophores giving EL emission at different wavelengths. Polymers such as PPV and its analogues typically yield EL emission in the relatively longer wavelength region (green, yellow, orange and red) though poly(p-phenylene) (PP) and poly(9-alkylfluorene) and their derivatives give blue light at lower efficiency and brightness. Conjugated polymers may have chromophores with different energy gaps because the effective length of conjugation is statistically distributed. However, in the mixture, chromophores with lower energy gaps will be the emitting species because of energy transfer.

There are some fully conjugated EL polymers with improved solubility by introducing long alkyl side groups on the aromatic ring. However, the side group enhances the steric hindrance and leads also to the decrease of the planarity<sup>[38-42]</sup>.

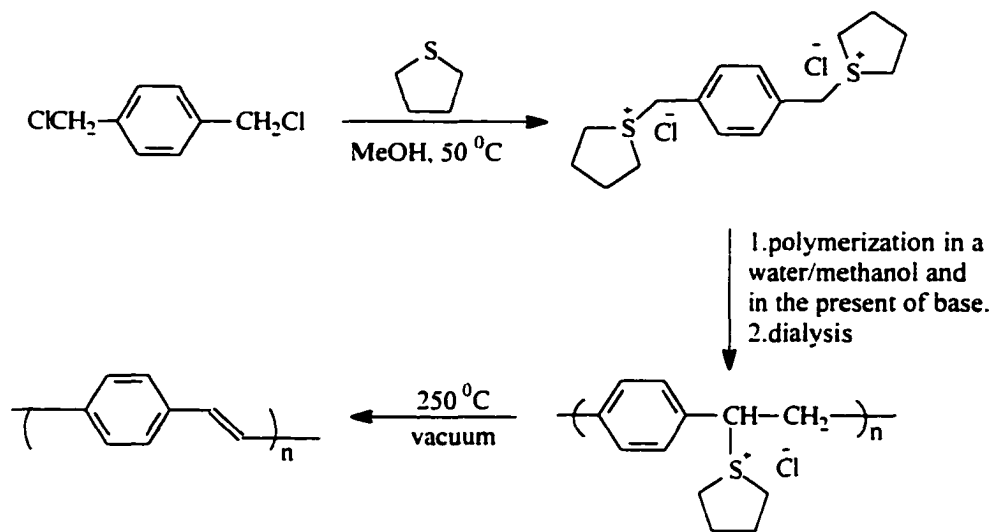
The copolymers with conjugated and non-conjugated segments may be designed to have uniform length chromophores. For this type of polymer, one may design a short wavelength EL polymer more readily because all of the chromophores can have the same structure and length and, therefore, the same energy gap. Longer wavelength EL polymers can also be designed based on the same principle. This design is similar to sequencing conjugated dye molecular segments with non-conjugated spacers, yielding polymer material with good film forming and mechanical properties. This type of polymer can have amorphous and uniform character as well as appropriate thermal properties when the proper spacer is selected. In addition, spacers help to isolate chromophores and confine exciton formation and consequently enhance EL efficiency<sup>[43-45]</sup>.

Polymer materials have an obvious advantage in being capable of forming large homogeneous emitter films. Most known polymers have relatively low photoluminescent (PL) efficiency in the solid state compared with organic dyes, though data in this area are sparse. Some studies have related EL efficiency to solid state PL efficiency of a material. From a material aspect, effort has been directed toward finding higher efficiency polymers. An analogue of PPV has been found to have 4 % EL efficiency, which is comparable to that of good organic low molar dyes. As mentioned previously, designing a molecular structure with isolated chromophores may also improve the efficiency of polymer EL. On the other hand, device performance is related to many other parameters in addition to material PL efficiency. Obviously, the charge carrier injection process itself affects the efficiency of the device. One of the most important tasks is to achieve a balance in carrier injection <sup>[46-47]</sup>.

### **The typical synthesis route of EL polymers**

#### **1. Fully conjugated EL polymers**

The first fully conjugated EL polymer, PPV, reported in 1990 <sup>[27]</sup> is insoluble in any organic solvent due to its rigid structure. Therefore, the insoluble PPV films are synthesized, using a solution-processable precursor non-conjugated polymer to spin-coat thin films and then thermally converting to conjugated polymer (typically  $\geq 250$  °C, in vacuum, for 10 h) via the sulfonium salt pyrolysis. The route is depicted as follows:



Scheme 1-1. General route of polymerization of fully conjugated EL polymers

Introduction of long side chains on the aromatic rings of a fully conjugated polymer improves its solubility remarkably <sup>[48-54]</sup>. Some PPV-like derivatives bearing long alkyl or alkoxy chains were prepared as soluble polymers with high molecular weight by the same method of sulfonium salt pyrolysis shown above, such as poly[2-methoxy-5-(2-ethylhexyloxy)-1,4-phenylenevinylene] <sup>[49]</sup> (MEH-PPV) and poly(2,5-diheptyl-1,4-phenylenevinylene) (HpPPV) <sup>[50]</sup>.

Other typical syntheses for soluble fully conjugated polymers are Wittig method <sup>[51]</sup> and Gilch method <sup>[54]</sup>. However, the polymer product from Wittig method using triphenylphosphine was mixture of cis- and trans-isomers, which has to be transformed into all of trans-structure by iodine isomerization <sup>[51]</sup>.

## 2. Copolymers containing both conjugated and non-conjugated segments.

Soluble alternating copolymers with both soft segment and PPV segment on main chain are synthesized through condensation of comonomers.

Up to now, most of works reported <sup>[43,55-56]</sup> on the synthesis of alternating copolymer were completed through the Wittig reaction <sup>[57]</sup> using triphenylphosphine. In the Wittig reaction, an aldehyde or ketone is treated with a phosphorus ylide to give an olefin.



Scheme 1-2. Typical Wittig reaction for the formation of C=C bond.

Z. Yang et al <sup>[43]</sup> emphasized that low molar mass conjugated organic molecules with photoluminescence maxima in the blue region often show parallel electroluminescence around the same wavelength <sup>[20,58]</sup> and that small molecules can be blended into an inert polymeric matrix to give a light-emitting layer in a LED device. <sup>[59]</sup>

They specifically synthesized a copolymer containing alternating rigid and flexible blocks in which the former have a molecular structure analogous to the

appropriate low molar mass conjugated molecules while the latter are blocks of polyethylene. i.e., poly[1,8-octanedioxy-2,6-dimethoxy-1,4-phenylene-1,2-ethenylene-1,4-phenylene-1,2-ethylene-3,5-dimethoxy-1,4-phenylene].

However, their copolymer contains the mixture of cis- and trans-stereomeric conjugated PPV segment after condensation. The copolymer with most of trans structure must be obtained through iodine atom catalyzed cis-trans isomerization. Only trans conjugated system is planar and gives high quantum efficiencies in electroluminescent process. The cis-isomer is markedly distorted from planarity.

It has been found from the present work that the copolymer after iodine isomerization still contains a small amount of cis-isomer and is susceptible to aging under the influence of air. This is because the iodine atom catalyzed isomerization is an equilibrium radical reaction mechanism. Meanwhile, some cross-linking side product can be formed during isomerization.



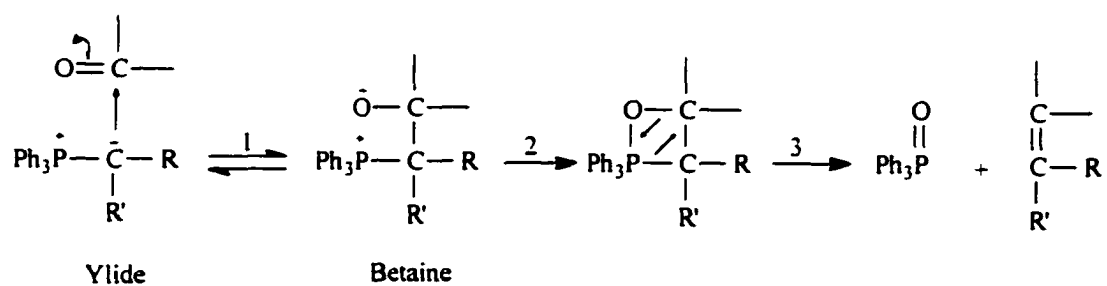
Scheme 1-3. The radical mechanism of iodine-catalyzed isomerization.

These problems could be avoided if we can develop a method, which gives all trans isomer directly in condensation without the isomerization.

### The mechanism of the Wittig reaction

The Wittig reaction affords an invaluable method for the conversion of a carbonyl compound to an olefin. Question is why the Wittig reaction with triphenylphosphine always gives a mixture of trans- and cis- isomers, and if we could find a method, which gives all trans-isomers.

The mechanism of the key process of the Wittig reaction consists of at least two and perhaps three steps <sup>[60]</sup>:

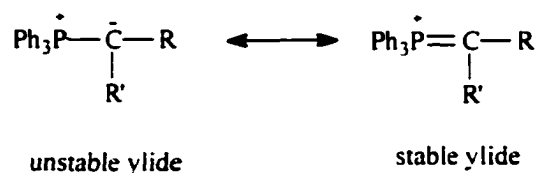


Scheme 1-4. Mechanism of conventional Wittig reaction.

Step 1 may or not be an equilibrium reaction. Steps 2 and 3 constitute an elimination of Ph<sub>3</sub>PO, and they may take place simultaneously. Either step 1 or step 2-3 may be rate-determining.

Question is when step 1 is faster than steps 2-3 or vice versa, what its effect on olefin structure.

The ylide is increased in stability (and decreased in reactivity) by the presence of electron-withdrawing groups on the carbon (R and R' groups). Another factor is the presence of electron-donating groups, like benzene ring, on the phosphorus. These groups will stabilize the ylide canonical form of the resonance hybrid at the expense of the C=P form by decreasing the positive charge on the phosphorus:

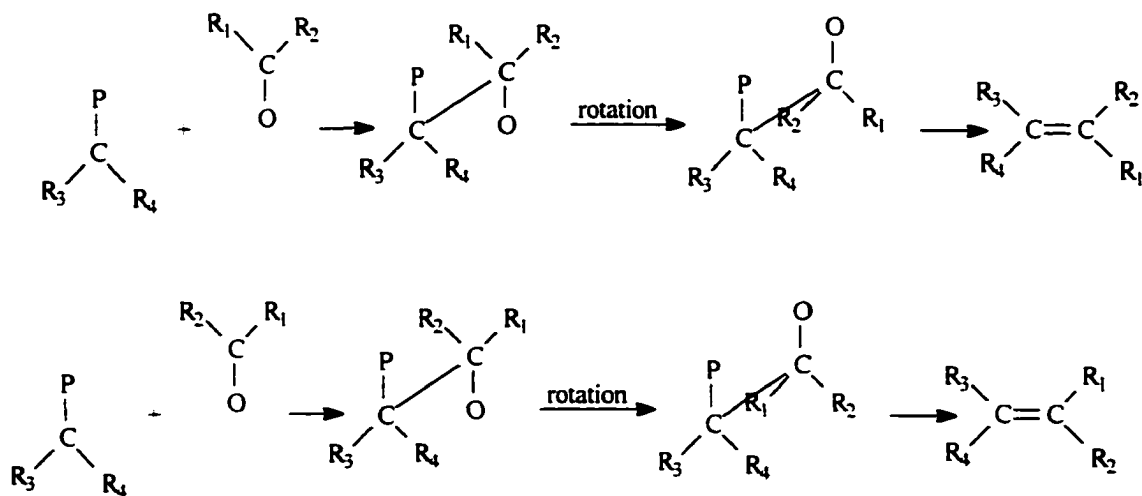


This decrease of the reactivity of the ylide can explain, for example, why trialkyl phosphorus ylides are more reactive than the triaryl variety.

On the other hand, once the betaine is formed, these factors work in precisely the opposite direction. Electron-withdrawing groups on the carbon increase the reactivity of the betaine, because they stabilize (by conjugation) the newly forming double bond; and electron-donating substituents on the phosphorus decrease the reactivity of the betaine, since they decrease the positive charge on the phosphorus and make it less attractive to the negative oxygen.

From all of above analyses, the first step in triphenylphosphine reaction may be slower and, gives the unstable betaine with higher reactivity, which completes the steps 2-3 faster.

These considerations make possible at least some conclusions about the stereochemistry of the reaction. In the Wittig reaction with the triphenylphosphine, step 1 may be irreversible or where the reversibility is not important because of the high reactivity of the forming betaine. If the betaine has two asymmetric carbons, the diastereomer formed is determined by the way the ylide and carbonyl compound lining up. Once the betaine is formed, the stereochemistry of olefin is determined by the fact that elimination is cis as following.

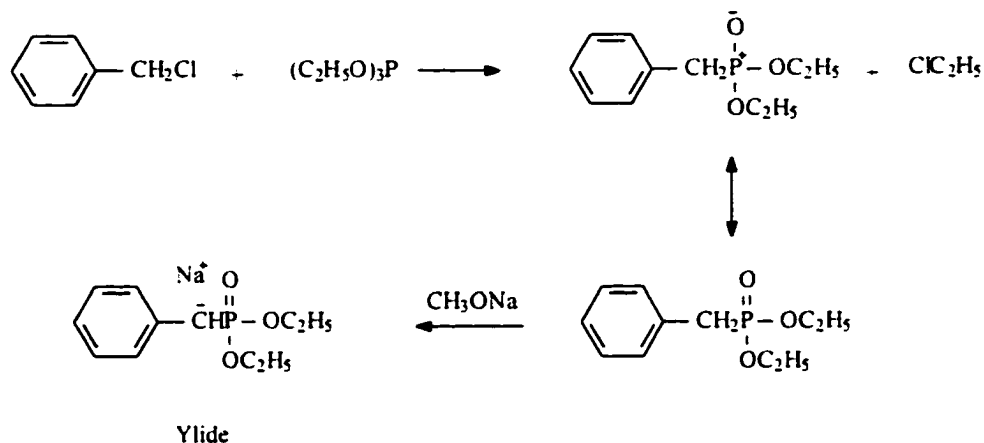


Scheme 1-5. Illustration of cis- or trans- olefin forming path.

From this discussion, it may be predicted that ylide formed from triphenylphosphine and ordinary aldehydes and ketones should give cis or mixtures of cis and trans olefin. This is why most of alternating copolymers with PPV segments have cis- and trans- conjugated isomers obtained from the Wittig condensation reaction with triphenylphosphine.

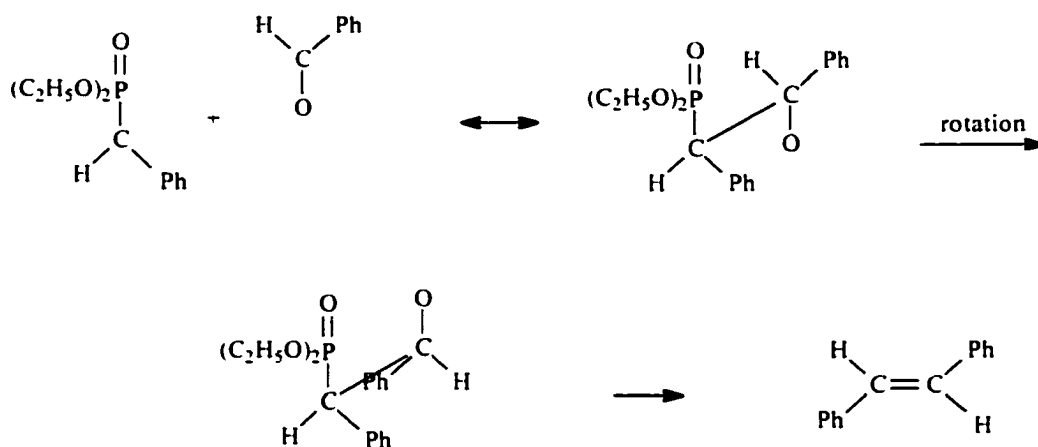
Based on the mechanism of the Wittig reaction discussed, it may be predicted also that the entire trans copolymer could be prepared by replacing triphenylphosphine with other phosphinelike compounds with electron-withdrawing groups on the phosphorus. In this case, where the betaine formation is reversible, and only the thermodynamically more stable diastereomer will be predominantly formed before elimination occurs, and this diastereomer will normally give the trans olefin.

In general organic synthesis, the Wittig reaction has also been carried out with other type of ylides, the most important being prepared from phosphonates.<sup>[61]</sup> one of phosphonate is prepared from triethylphosphite.



Scheme 1-6. Mechanism of modified Wittig reaction using triethyl phosphite.

Unlike triphenyl ylide, the phosphorus has no more positive charge, because of the formation of O=P bond and electron-donating group, C<sub>2</sub>H<sub>5</sub>O, which will increase the reactivity of the ylide by decreasing the positive charge on the phosphorus. Meanwhile, they also decrease the reactivity of the betaine, since they decrease the positive charge on the phosphorus, and make it less attractive to the negative oxygen of the carbonyl compound, leading to difficulty forming cis-structure thermodynamically through rotation. This modified Wittig reaction with triethylphosphite may give all trans product, because there are reversible step 1 and slow steps 2-3.



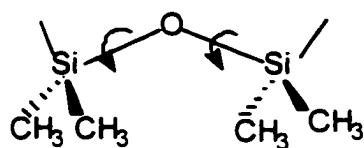
Scheme 1-7. Illustration of trans-olefin formation through modified Wittig reaction using triethyl phosphite.

One goal in the present research is to find a method to preparing the alternating copolymer with all-trans PPV segment without an additional isomerization step.

On other hand, the copolymers reported up to now still have high  $T_g$ , even they have excellent solubility in some organic solvent. This may limit their application and processability. Therefore, the second focus is on lowering its  $T_g$  by

introducing longer ethylene segment or more flexible segment such as ether and siloxane segment.

Silicon properties can be interpreted in terms of structural characteristics. The silicon-oxygen chain that constitutes the backbone of these polymers is predominantly responsible for their uniqueness. A segment of methylsiloxane chain is shown below:



Commonly accepted bond angles are: C-Si-C = 112 °, Si-C-Si = 143°, and O-Si-O = 110°; bond lengths are Si-C = 0.188 nm, and Si-O = 0.163 nm. The siloxane chain flexes, and its segmental rotation is fairly free about the Si-O axis, especially with small substituents e.g., methyl, on the silicon atom. Rotation is also free about the Si-C axis in methyl silicon compounds. As a result of such freedom of motion, the intermolecular distances between methyl silicon chains are greater than between hydrocarbons, and intermolecular forces are smaller. The small rotational barriers contribute to properties such as low modulus, low glass-transition temperature, and high permeability.

## Experimental section

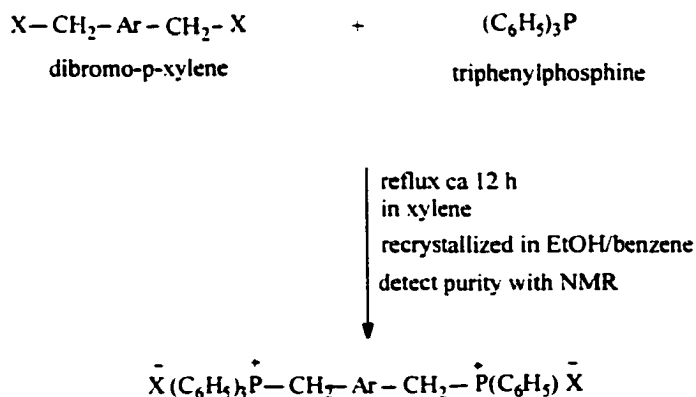
### I. Synthesis schemes of PPV-based copolymers

Copolymer samples containing blue-emitting segment were prepared through the Wittig reaction between  $\alpha,\omega$ -dialdehyde and bis (triphenylphosphonium halide), and through the modified Wittig reaction between  $\alpha,\omega$ -dialdehyde and bis (phosphonate) comonomers.

Synthetic Schemes are depicted as follows.

#### 1. Synthesis of comonomers.

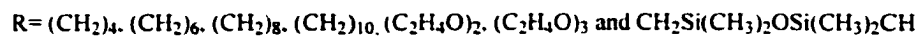
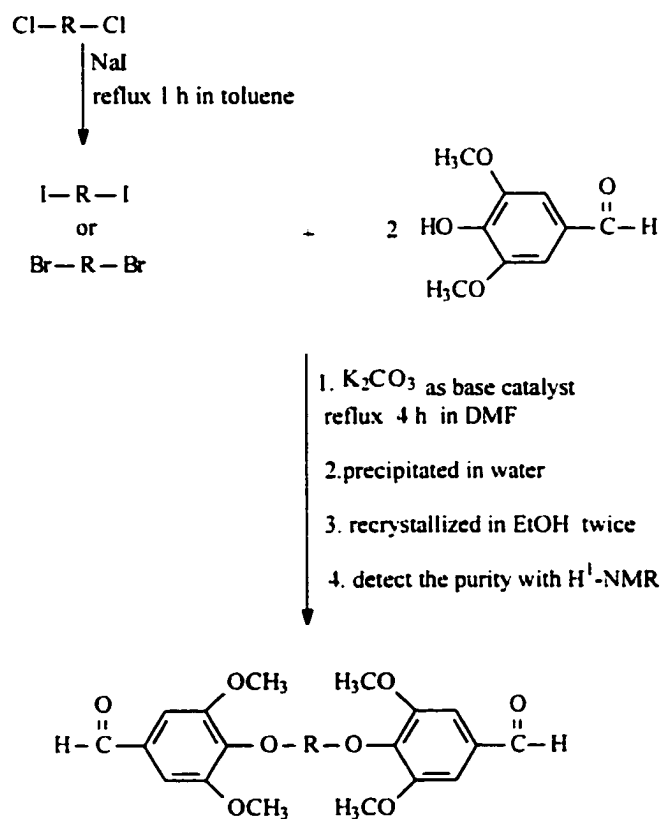
#### Bis(triphenylphosphonium halide) compounds for the Wittig reaction



Scheme 1-8. The reaction of preparation of triphenylphosphonium monomers.

Ar = benzene ring

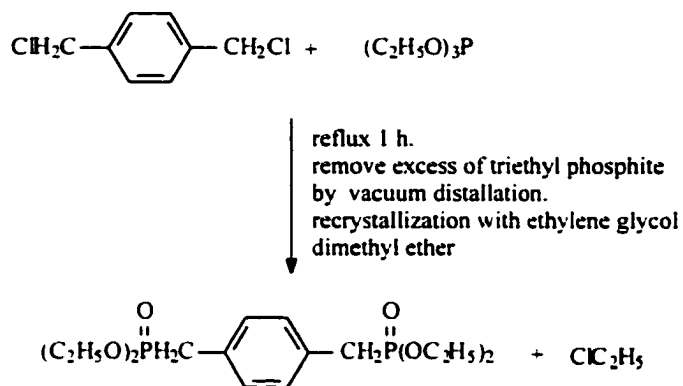
**$\alpha,\omega$ -Dialdehyde compound:**



Scheme 1-9. The reaction of preparation of  $\alpha,\omega$ -dialdehyde monomers with soft segment.

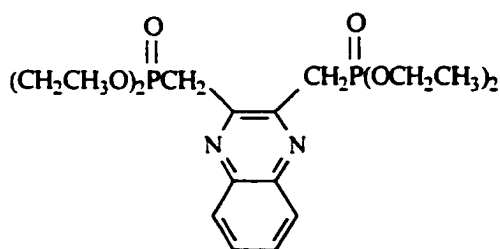
### Preparation of phosphonates for the modified Wittig reaction

The synthetic scheme of p-xylene diethylphosphonate is as following,

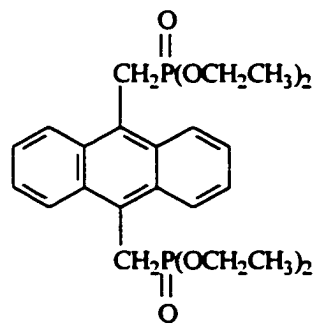


Scheme 1-10. The reaction of preparation of diphosphonate monomer.

Through the same scheme, 2,3-dimethylenequinoxaline-bis(diethylphosphonate) and 9,10-dimethylene anthracene-bis(diethyl phosphonate) were prepared.

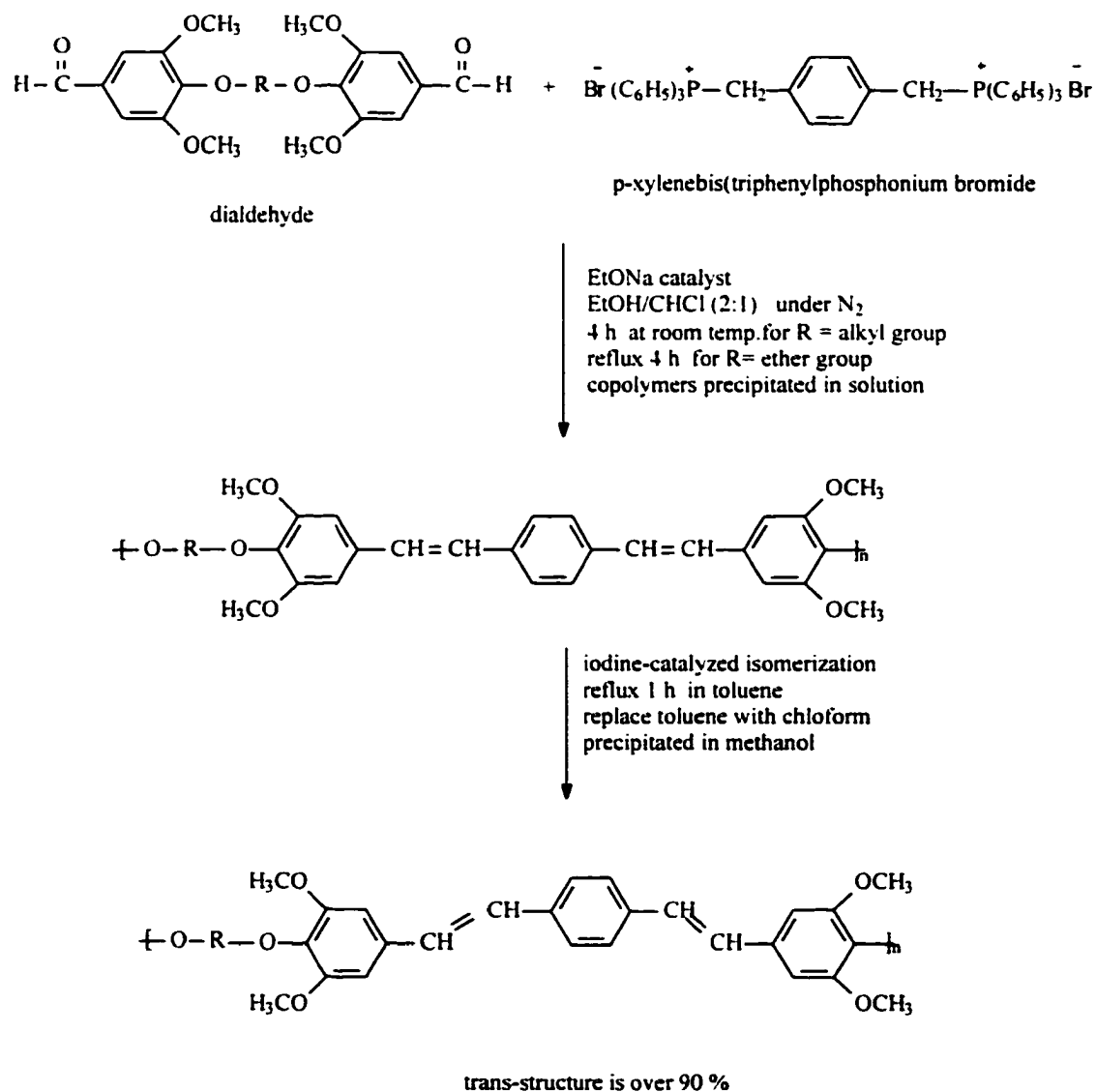


2,3-dimethylenequinoxaline-  
bis(diethylphosphonate)



9,10-dimethylene anthracene-  
bis(diethyl phosphonate)

## 2. Synthesis of copolymers through Wittig reaction.

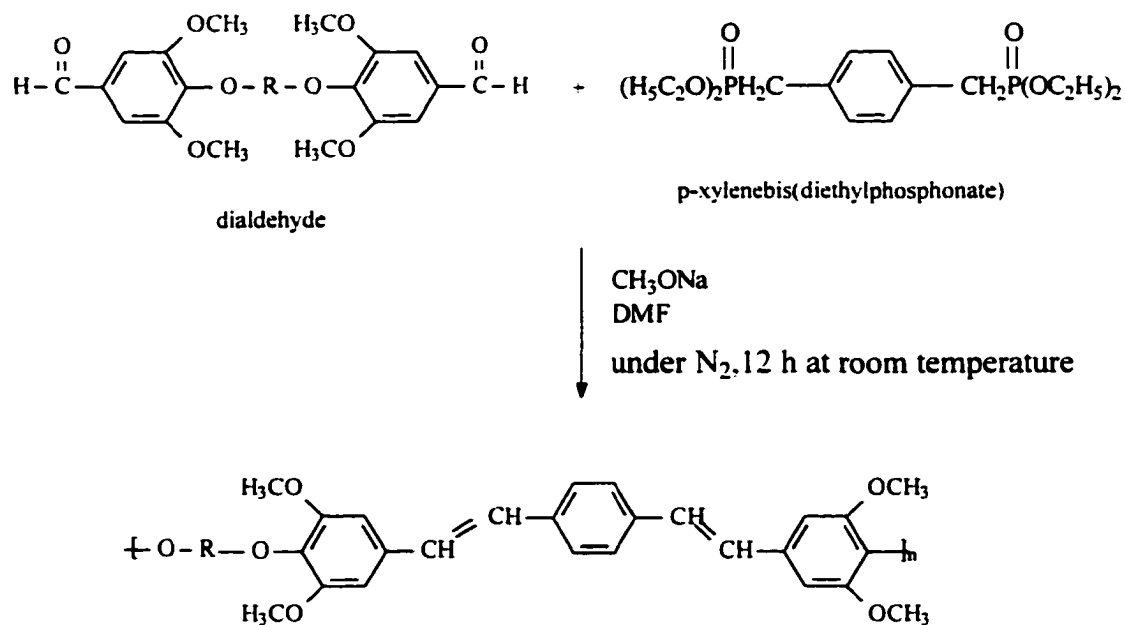


Scheme 1-11. The synthesis route of copolymer through the Wittig reaction.

The product from this synthesis is a mixture of trans and cis structures. The polymer with all trans-structure (> 90 %) was obtained by isomerization through reflux in I<sub>2</sub> toluene solution.

### 3. Synthesis of copolymers through the modified Wittig reaction.

The synthetic scheme of copolymerization of dialdehyde comonomer and di(phosphonate) comonomer is as following.



Scheme 1-12. The synthesis route through the modified Wittig reaction.

## II. Syntheses procedure

### Typical synthesis of dialdehyde compound

A solution of 4-hydroxy-3,5-dimethoxybenzaldehyde (3.64 g, 0.02 mole) and  $\alpha,\omega$ -dibromoalkane (0.01 mole) in 150 ml of DMF was stirred and heated to reflux. A total of 3.0 g (0.022 mole) of potassium carbonate was added in small portions. The solution was stirred and refluxed for 4 h after the completion of addition. The resulting mixture was poured into 2 L of distilled water. The precipitate was collected after standing 4 h, dried in air at room temperature, and recrystallized from ethanol to give the pure product,  $\alpha,\omega$ -bis(4-formyl-2,6-dimethoxyphenoxy) alkane.

If the dialdehyde monomer was made from dichloride compound, sodium iodide was employed to increase the yield of the product.

### Typical synthesis of bis(triphenylphosphonium halide) monomer

Triphenylphosphine (0.026 mole) was dissolved in 10 ml of dry xylene with stirring, and then 0.012 mole of *p*-dibromomethylbenzene was added. The

solution was refluxed for about 12 h under nitrogen protection. The product was precipitated in solution, filtered and recrystallized with ethanol/benzene solvent. The yield is about 98%. The purity was determined through  $^1\text{H-NMR}$ .

### **Typical synthesis of bis(diethylphosphonate) monomers**

0.03 mole of dichloromethyl compound and 0.1 mole of triethylphosphite were added in a 100ml round flask with condenser and dry tube. The mixture was refluxed for about 3 h and then the excess of unreacted triethylphosphite was removed by vacuum distillation at 140 °C. The crude product was recrystallized twice with ethylene glycol dimethyl ether, the yield is about 85%. The purity of bis(diethylphosphonate) crystal was established using  $^1\text{H-NMR}$ .

### **Typical polycondensation by the Wittig reaction**

Dialdehyde (0.005 mole) and 1,4-xylenebis(triphenylphosphonium bromide) (0.005 mole) were dissolved in 100 ml of anhydrous ethanol-chloroform (3:1) solvent, followed by dropwise addition of 0.012 mole of sodium ethoxide into the solution. The mixture solution was stirred for 4 h at room temperature, and then 5 ml of 2% HCl were added into the solution. The paste-like product was collected

and thoroughly washed with ethanol/water (3:1) mixed solvent to remove the by-products triphenylphosphine oxide and sodium bromide. In some case, it is necessary to reprecipitate the product.

The copolymer was isomerized into all-trans configuration by refluxing for 1 h in toluene in the presence of a catalytic amount of iodine. And then the isomerized product was precipitated in 200 ml of 90% ethanol and dried in a vacuum oven at 40 °C for about 1 week.

#### **Typical condensation with the modified Wittig reaction**

p-Xylenebis(diethylphosphonate) (1 g ,2.63 mmol) was dissolved in 8 ml of DMF in 100 ml round flask at room temperature under the protection of nitrogen. 0.34 g of sodium methoxide was added into the solution and the solution became dark red immediately. And then 10 ml DMF solution with 2.63 mmol of dialdehyde monomer was added dropwise into the flask over 0.5 h under N<sub>2</sub>. The solution changed to bright yellow. The reaction was carried out about 10 hours at room temperature. The copolymer was precipitated in methanol/water (50/50), and vacuum dried for 48 h at 40 °C.

### **Instrumental analyses**

The  $^1\text{H}$ -NMR and 2-D NMR spectra were obtained on a Varian UNITY 200 and Varian INOVA 600 spectrometers. The samples were dissolved in  $\text{CDCl}_3$ ; chemical shift is referred to TMS.

GPC measurements were obtained on a Waters Model 150C with a refractometer and using THF as solvent. Polystyrene standards (Aldrich Co.) were used for calibration.

The DSC determination was performed on a Du Pont DSC-2910 and heating rate is  $10\text{ }^\circ\text{C}/\text{min}$ .

FT-IR spectra were taken on a Magna 550 FT-IR spectrometer equipped with OMNIC operation software.

The UV-VIS spectra were recorded on a Cary 1E UV-Visible Spectrometer. Photoluminescence (PL) spectra were recorded on a FluoroMax-3.

Melting point of comonomers was determined on a Fisher-Johns melting point apparatus.

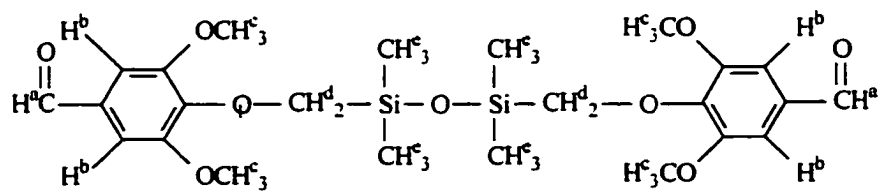
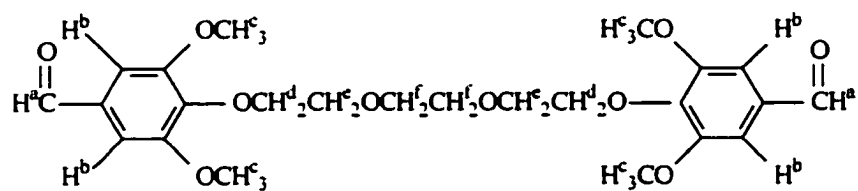
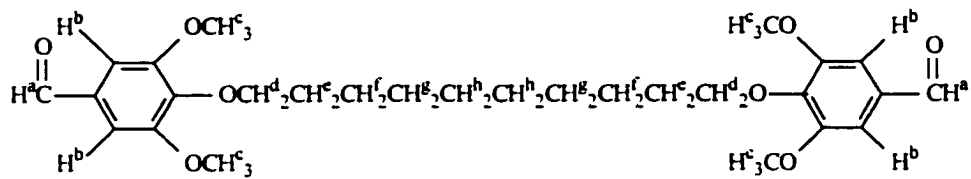
## Results and Discussion

### Characterization of comonomers

Seven dialdehyde monomers containing ether, siloxane and alkyl segments with different length were prepared. Their structure was characterized with  $^1\text{H-NMR}$ . The spectra are shown in Figures 1-1 and 1-2. The assignments of the chemical shifts of all of protons are completed based on the reference <sup>[62]</sup>. The results are listed in Table 1-2.

Table 1-2. Chemical shift of  $\alpha,\omega$ -dialdehyde monomers on  $^1\text{H-NMR}$  (ppm)

R	H <sup>a</sup>	H <sup>b</sup>	H <sup>c</sup>	H <sup>d</sup>	H <sup>e</sup>	H <sup>f</sup>	H <sup>g</sup>	H <sup>h</sup>
(CH <sub>2</sub> ) <sub>4</sub>	9.87	7.12	3.90	4.15	1.98			
(CH <sub>2</sub> ) <sub>6</sub>	9.87	7.13	3.91	4.09	1.80	1.54		
(CH <sub>2</sub> ) <sub>8</sub>	9.87	7.12	3.91	4.07	1.76	1.45	1.39	
(CH <sub>2</sub> ) <sub>10</sub>	9.86	7.12	3.91	4.07	1.75	1.41	1.32	1.32
(CH <sub>2</sub> CH <sub>2</sub> O) <sub>2</sub>	9.86	7.12	3.91	4.25	3.81			
(CH <sub>2</sub> CH <sub>2</sub> O) <sub>3</sub>	9.86	7.12	3.91	4.25	3.81	3.72		
CH <sub>2</sub> Si(CH <sub>3</sub> ) <sub>2</sub>								
OSi	9.87	7.13	3.90	3.82	0.25			
(CH <sub>3</sub> ) <sub>2</sub> CH <sub>2</sub>								



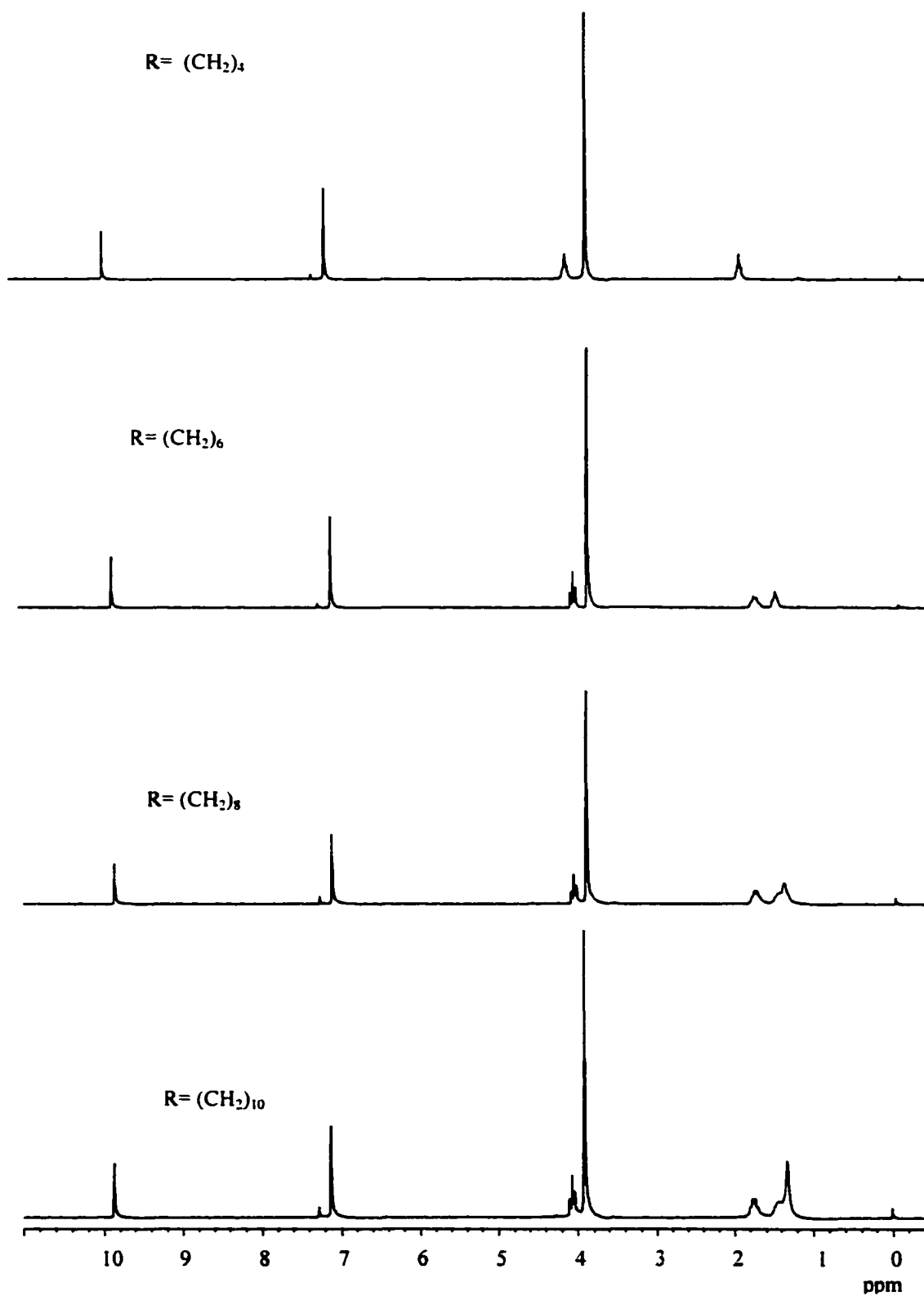


Figure 1-1.  $^1\text{H-NMR}$  spectra of  $\alpha,\omega$ -dialdehyde monomers

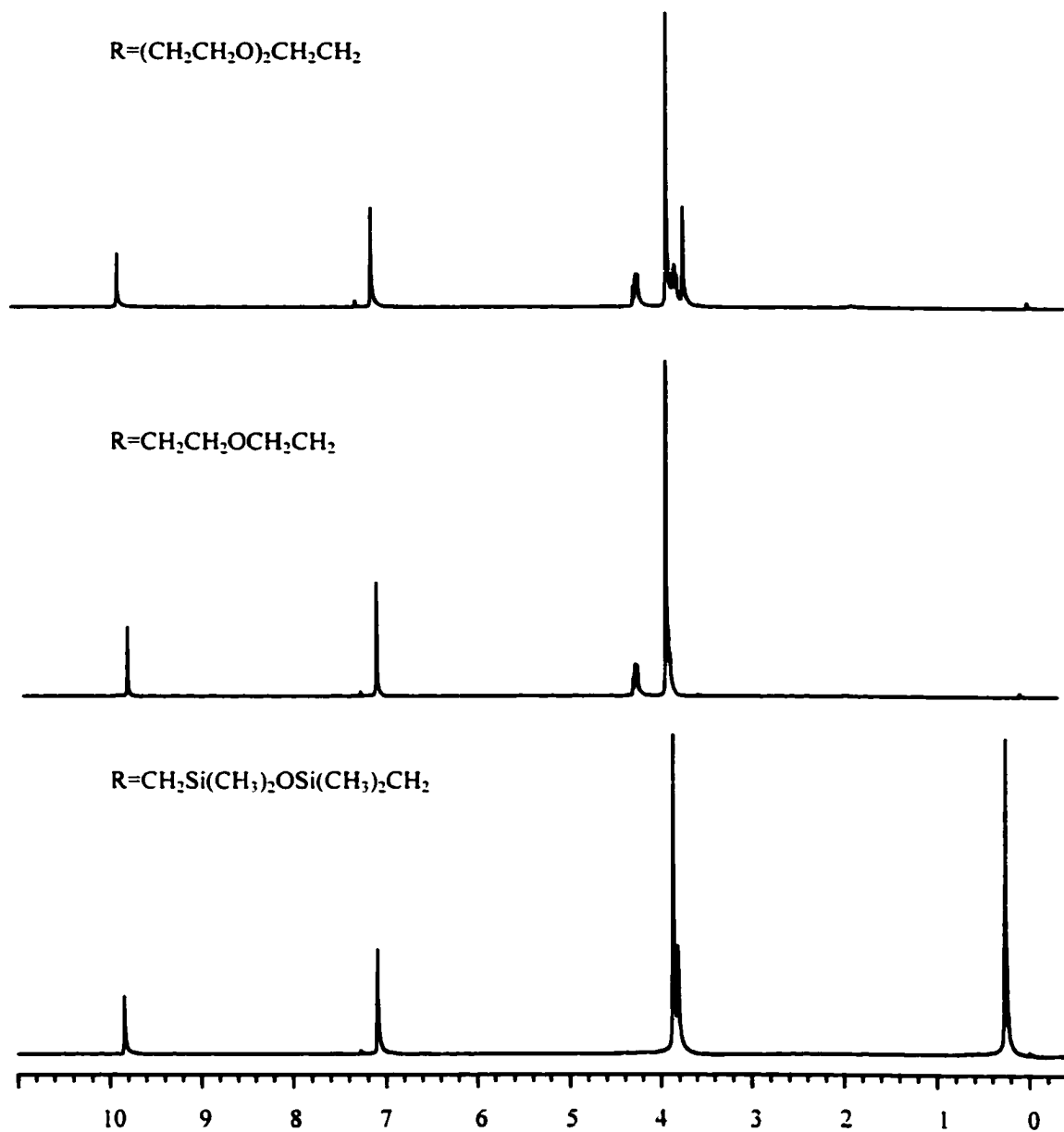
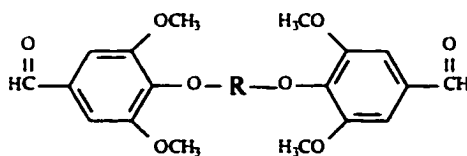


Figure 1-2.  $^1\text{H}$ -NMR spectra of  $\alpha,\omega$ -dialdehyde monomers.



The melting points of seven  $\alpha,\omega$ -dialdehyde monomers were determined with the Thomas-Hoover UniMelt melting point apparatus. The results were listed in the Table 1-3.

Table 1-3. Melting point of  $\alpha,\omega$ -dialdehyde monomers

R	m.p. °C
(CH <sub>2</sub> ) <sub>4</sub>	124-125
(CH <sub>2</sub> ) <sub>6</sub>	99-100
(CH <sub>2</sub> ) <sub>8</sub>	93-94
(CH <sub>2</sub> ) <sub>10</sub>	87-88
(CH <sub>2</sub> CH <sub>2</sub> O) <sub>2</sub>	105-106
(CH <sub>2</sub> CH <sub>2</sub> O) <sub>3</sub>	81-82
CH <sub>2</sub> Si(CH <sub>3</sub> ) <sub>2</sub> OSi(CH <sub>3</sub> ) <sub>2</sub> CH <sub>2</sub>	88-89

The *p*-xylylenebis(triphenylphosphonium bromide) was purchased from Aldrich Co. *p*-Xylylenebis(diethylphosphonate), 2,3-dimethylenequinoxaline-bis(diethylphosphonate) and 9,10-dimethylene anthracene-bis(diethyl phosphonate) were prepared and its structure was identified using <sup>1</sup>H-NMR.

The proton spectrum of *p*-xylylenebis(diethylphosphonate) was assigned by comparing with the proton NMR spectra of *p*-dichloroxylylene and triethylphosphite, which are shown in the Figure 1-3. The chemical shifts of each hydrogen of *p*-xylylenebis(diethylphosphonate) are: H<sup>a</sup>, 7.22 ppm; H<sup>b</sup>, 3.08 and 2.20 ppm; H<sup>c</sup>, 4.00 ppm; and H<sup>d</sup>, 1.22 ppm. The two H<sup>b</sup> have different chemical shifts. This indicates that two hydrogen atoms connected to the same carbon next to P=O are not equivalent, because the phosphorus atom forms a cone with carbon atom and oxygen atoms. And the tetrahedral structure of the carbon renders one hydrogen atom inside the cone and another outside of the cone. The melting point of *p*-xylylenebis(diethyl phosphonate) is 72-73 °C.

Figures 1-4 and 1-5 show the <sup>1</sup>H-NMR spectrum of 2,3-dimethylenequinoxaline-bis(diethylphosphonate) and 9,10-dimethylene anthracene-bis(diethyl phosphonate), respectively. Comparing with the proton NMR spectrum of their starting materials, the spectrum of the monomer products were assigned. Two hydrogen atoms connected with the carbon of C-P give two different chemical shifts also, as in *p*-xylylene-bis(diethyl phosphonate): 3.922 ppm and 4.032 ppm for 2,3-dimethylenequinoxaline-bis(diethylphosphonate) and 4.189 ppm and 4.290 ppm for 9,10-dimethylene anthracene-bis(diethyl phosphonate). Their melting points are 90-90.5 °C and 158-159 °C, respectively.

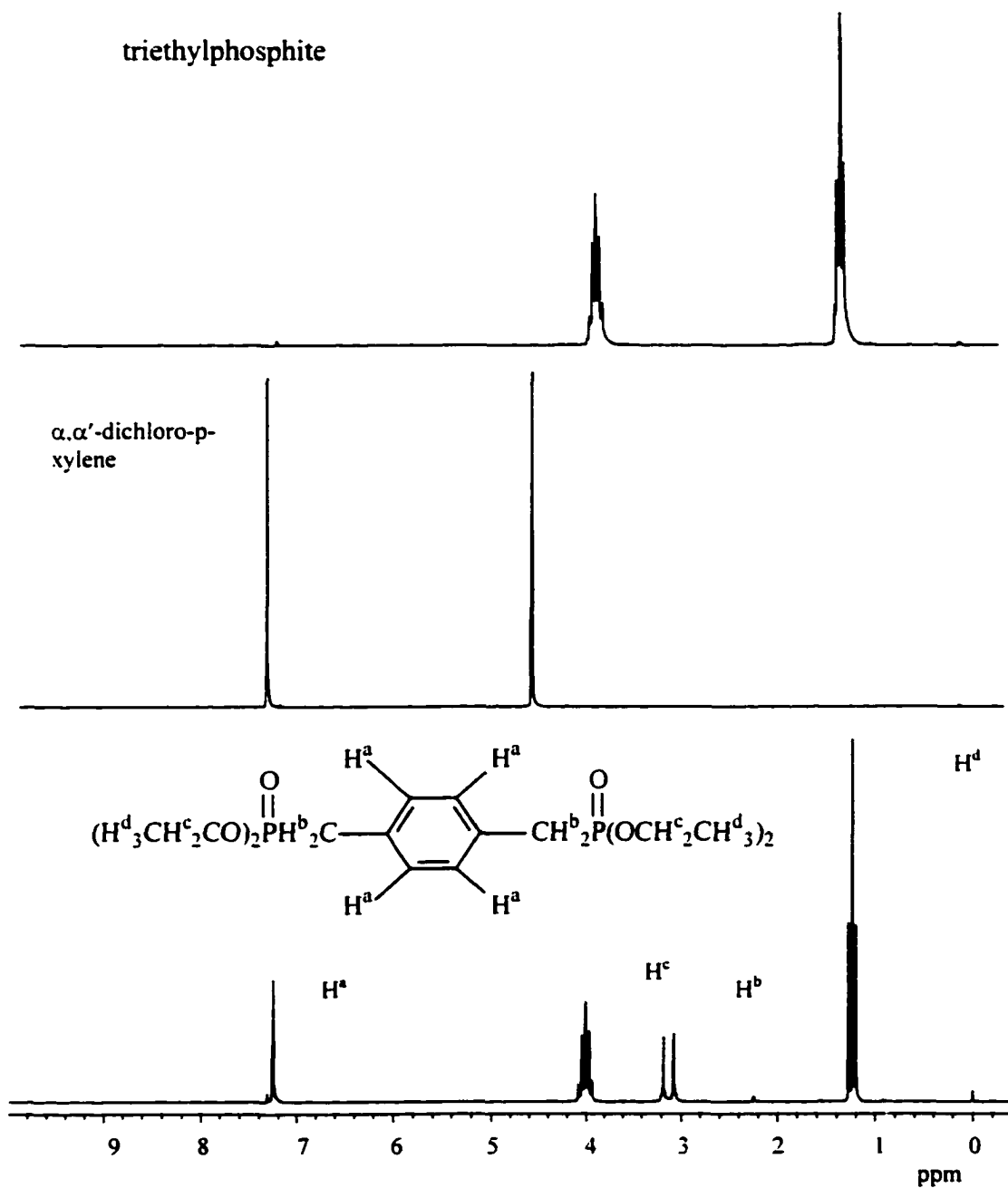


Figure 1-3. The  $^1\text{H}$ -NMR spectra of triethylphosphite, *p*-dichloroxylylene and *p*-xylylenebis(diethylphosphonate)

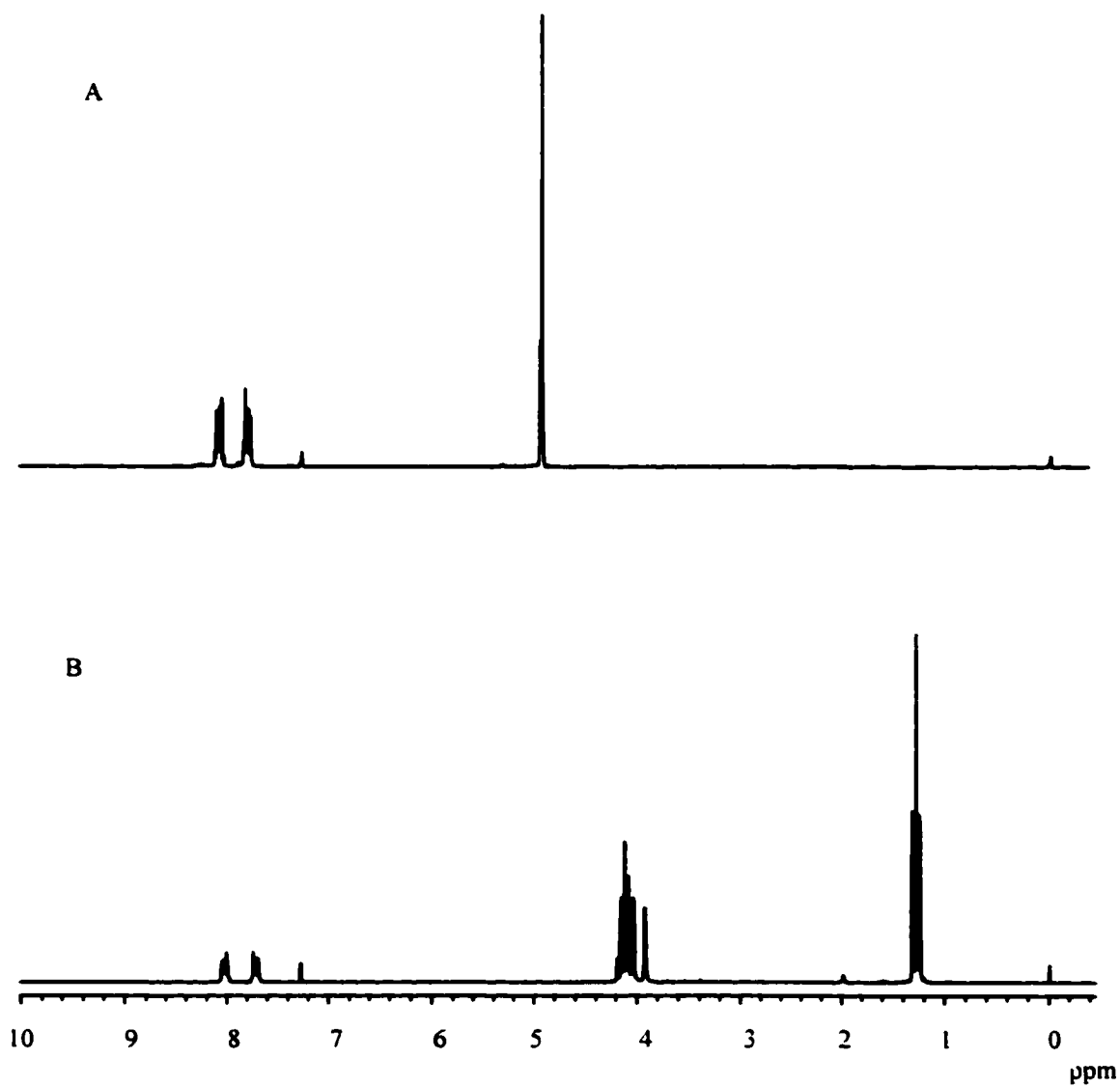


Figure 1-4. <sup>1</sup>H-NMR spectra of 2,3-bis(bromomethyl)-quinoxaline (A) and 2,3-dimethylenequinoxaline-bis(diethylphosphonate) (B)

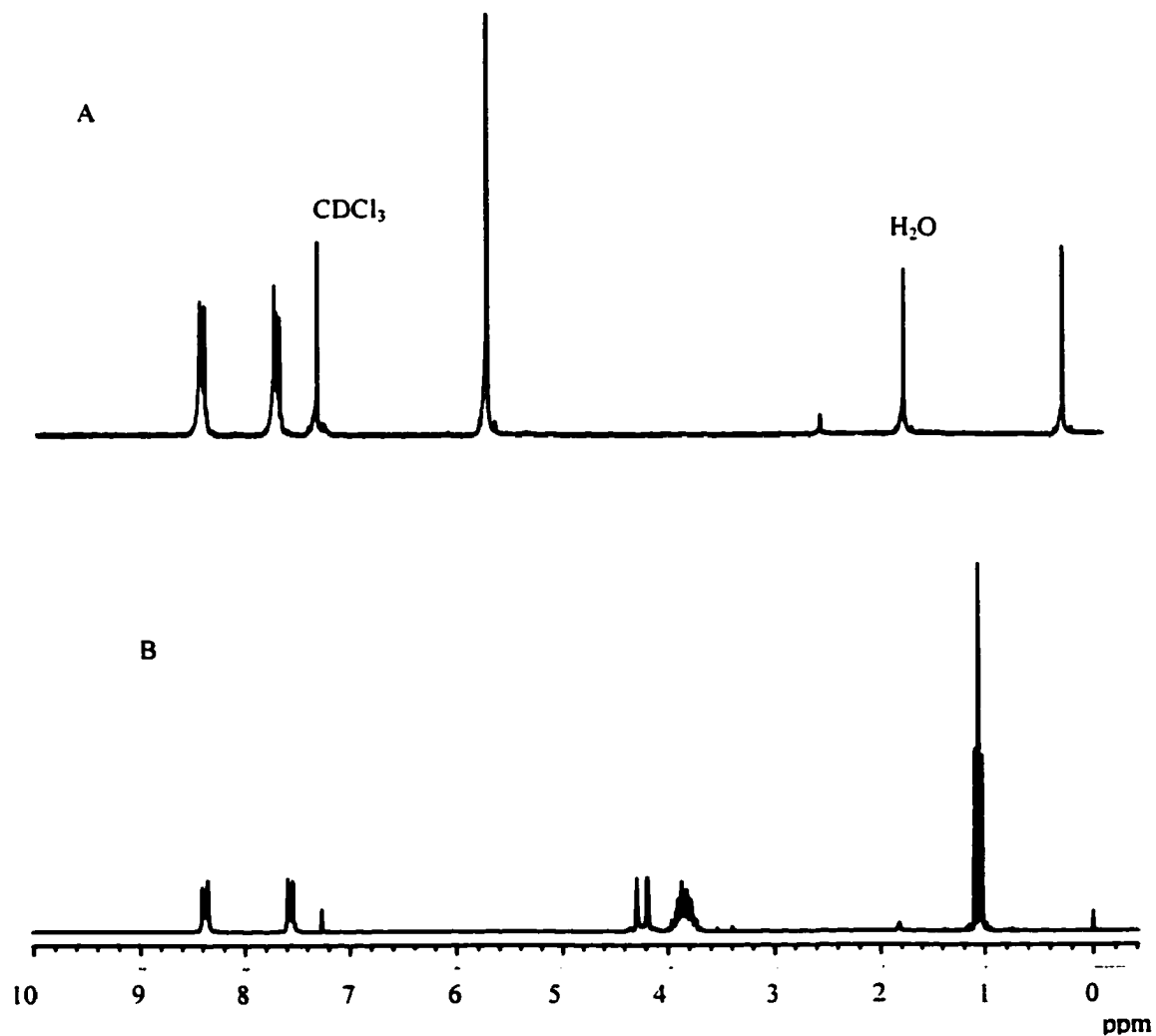


Figure 1-5.  $^1\text{H-NMR}$  spectra of 9,10-bis(chloromethyl)anthracene (A) and 9,10-dimethylene anthracene-bis(diethyl phosphonate) (B)

### **Characterization of the copolymer**

NMR and IR were used for characterizing the structure of the copolymer; GPC was used for determining the molecular weight and molecular weight distribution of copolymers; UV-Visible spectrophotometer and PL were used for optical property determination; and DSC was used for thermal property determination.

### **Structure of the copolymers**

Figure 1-6 shows proton NMR spectra of copolymer products, poly[1,8-octanedioxy-(2,6-dimethoxy-1,4-phenylene)-1,2-ethenylene-1,4,-phenylene-1,2-ethenylene-(3,5.-dimethoxy-1,4-phenylene) (A) made with Wittig reaction, and its product ( B) of iodine-catalyzed isomerization; copolymer (C), which is as same as A. was prepared through the modified Wittig reaction with triethyl phosphite to replace triphenyl phosphine.

Copolymer A gives a more complicated proton NMR spectrum. From the calculation of spin-spin coupling constant of hydrogen of vinyl, this polymer has been shown to contain almost same amount of trans-isomer and cis-isomer. After isomerization, the product gives a simpler proton NMR spectrum (Figure 1-6. B).

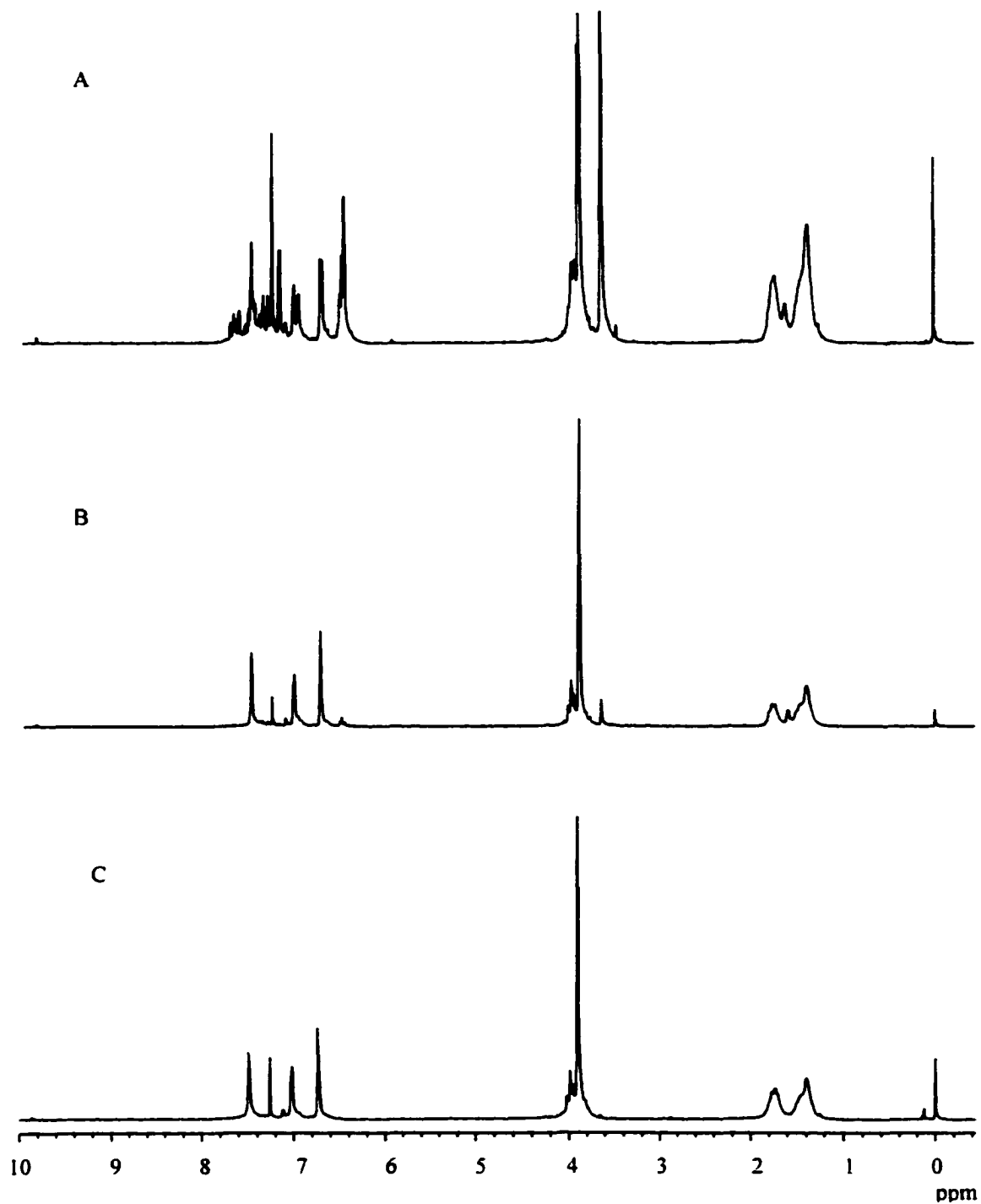


Figure 1-6.  $^1\text{H}$ -NMR spectra of alternating copolymer with octylene and PPV segments.

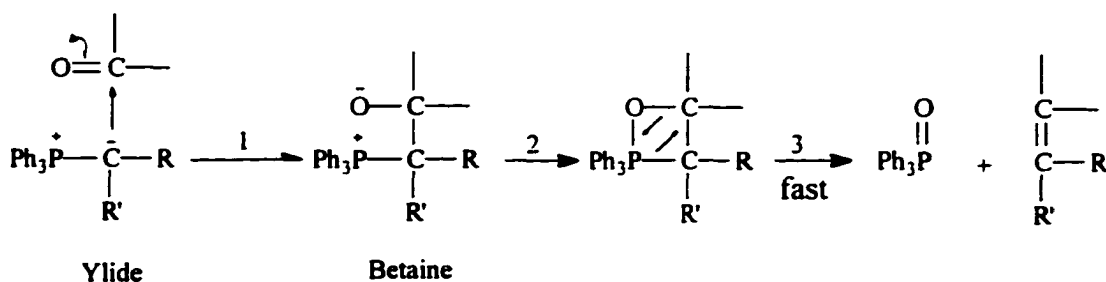
- A. unisomerized copolymer through Wittig reaction.
- B. isomerized copolymer.
- C. copolymer through modified Wittig reaction

The spin-spin coupling constant indicates the isomerized product containing almost all trans conjugated segments. Comparing both  $^1\text{H-NMR}$  spectra of a copolymer before and after isomerization, the signals of methoxyl at 3.56 ppm, methine at 6.95, 7.30 and 7.40 ppm, aromatic ring at 6.50 and 7.20 ppm from *cis*-isomer structure diminishes conspicuously after isomerization. Therefore, the microstructure of copolymers was obtained from the integral ratios of the signals at 3.90 ppm and 3.65 ppm as Table 1-4.

Table 1-4. Microstructure of copolymers

R	trans/cis	trans/cis
	Before isomerization	After isomerization
Butylene	53/47	93/7
Hexylene	55/45	92/8
Octylene	51/49	91/9
Decylene	44/56	97/3
Diethylene glycol	48/52	98/2
Triethylene glycol	44/56	91/9
Tetramethyldisiloxane	58/42	----

The data in the Table 1-4 has shown that the mechanism of the Wittig reaction using triphenylphosphine is dynamically controlling process consisting of three steps:



The presence of electron-donating groups, benzene ring, on the phosphorus increase the reactivity of Ylide and make the formation of the betaine random irreversibly in step 1. Meanwhile, the  $(\text{Ph})_3\text{P}=\text{O}$  is good leaving group, because of its large size. This results in the formation of both trans and cis conjugated microstructure.

In this study, a critical shortcoming of the conventional method was found that a certain level of cross-linking polymer was formed during isomerization step, most likely due to radical nature of the iodine-catalyzed isomerization. On standing, even the linear polymer isolated from the isomerization process showed cross-linking, perhaps due to trace iodine residue.

The proton NMR spectrum shows that the product directly from the modified Wittig reaction, using triethyl phosphite, has all trans conjugated microstructure without additional isomerization step. (Figures 1-6 and 1-7).

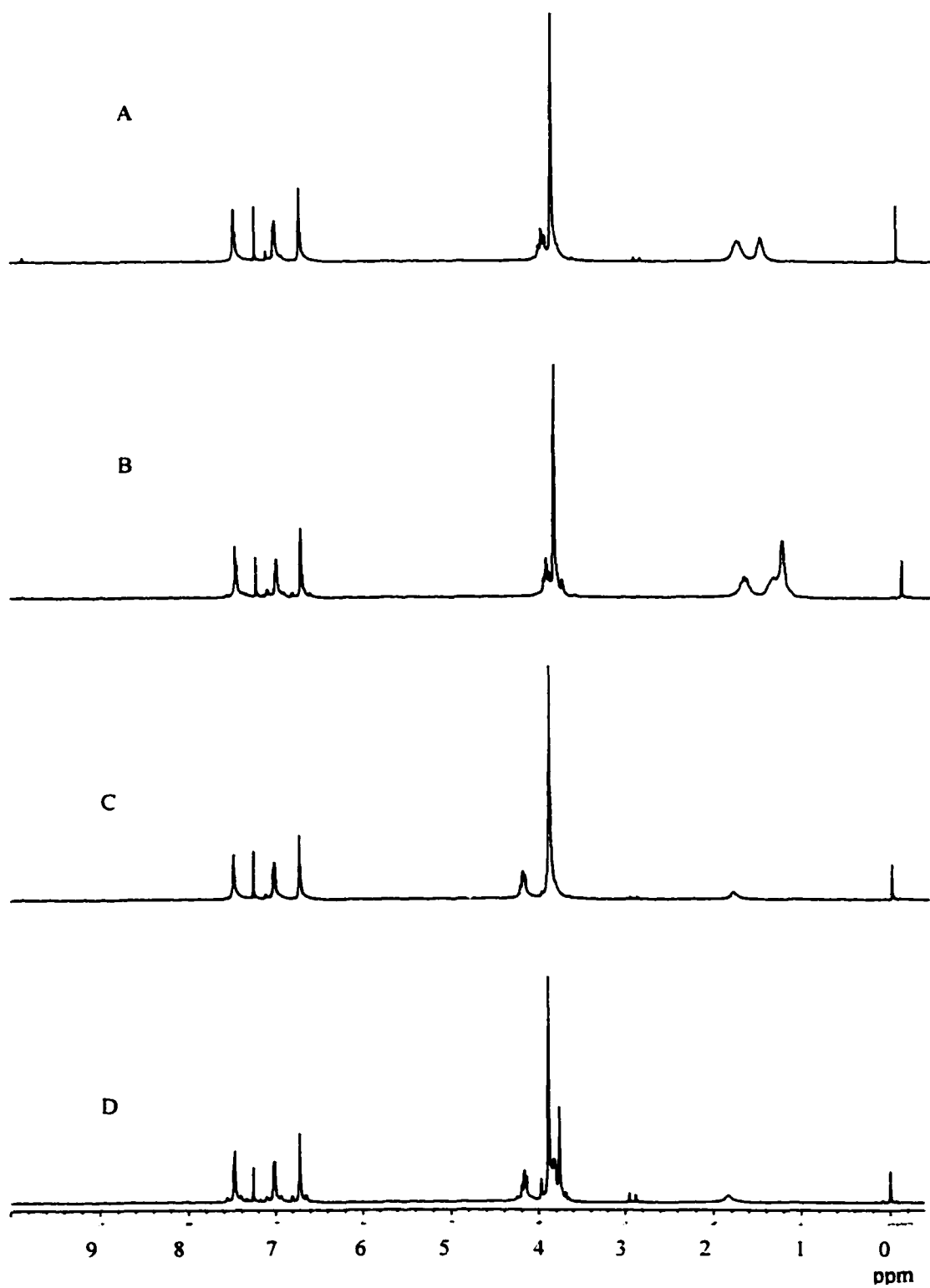
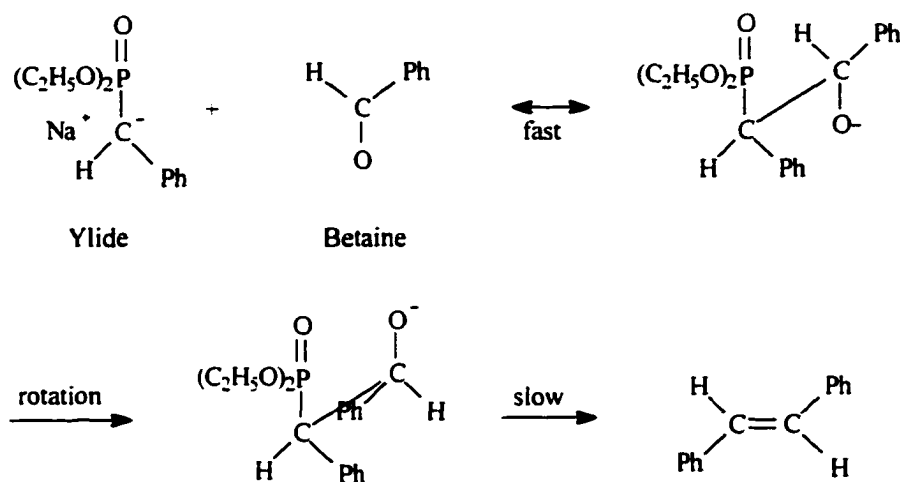


Figure 1-7.  $^1\text{H-NMR}$  spectra of alternating copolymers with soft segments, hexyl (A), Decyl (B), 2EO (C) and 3EO(D) (from modified Wittig reaction)

Figures 1-8 and 1-9 represent the FT-IR spectra of poly[1,8-octanedioxy-(2,6-dimethoxy-1,4-phenylene)-1,2-ethenylene-1,4-(3,5-dimethoxy-1,4-phenylene)] (A) made through the Wittig reaction, and its product (B) of iodine-catalyzed isomerization; copolymer (C) prepared through the modified Wittig reaction. They support the result from NMR determination. The product through the Wittig reaction gives strong absorption peaks from cis vinyl units at 748, 721 and 696  $\text{cm}^{-1}$ , besides absorption of trans vinyl units at 959  $\text{cm}^{-1}$  in the fingerprint range. The isomerized product and the copolymer through the modified Wittig reaction give only strong absorption at 959  $\text{cm}^{-1}$  without observable absorption from the cis vinyl units.

Figure 1-7 shows that all of alternated copolymers with different soft segments synthesized using modified Wittig reaction contain only trans conjugated segments. These experimental results indicated that the coupling of the Ylide made from triethylphosphite with carbonyl component underwent reversible step 1 mechanism, in which the step 2-3, formation of carbon-carbon double bond and elimination of sodium diethylphosphonate, is slower than step 1. This is because the leaving group is smaller and the phosphorus in the betaine has no more positive charge to attract to the negative oxygen of the original carbonyl group.



The  $^1\text{H-NMR}$  spectra (Figures 1-10 and 1-11) of poly[1,10-decanedioxy-(2,6-dimethoxy-1,4-phenylene)-1,2-ethenylene-2,3-quinoxaline-1,2-ethenylene-(3,5,-dimethoxy-1,4-phenylene)] and poly[1,3-methylene tetramethyldisiloxane dioxy-(2,6-dimethoxy-1,4-phenylene)-1,2-ethenylene-1,4,-phenylene-1,2-ethenylene-(3,5,-dimethoxy-1,4-phenylene)] also show that the modified Wittig condensation gives conjugated segments with trans microstructure, using quinoxaline to replace benzene ring or using methylsiloxane to replace hydrocarbon compounds.

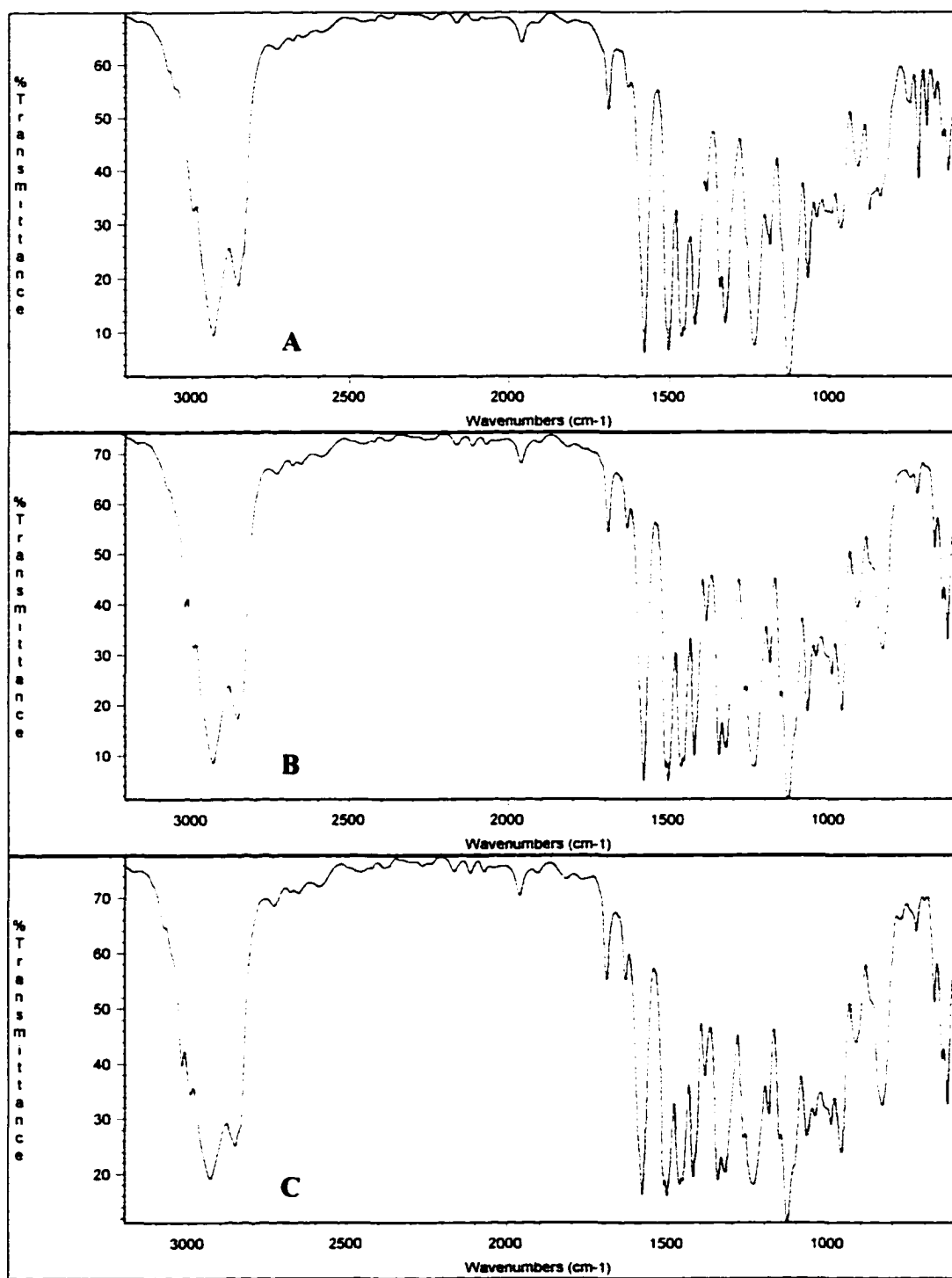


**Figure 1-8. FT-IR spectrum of alternating copolymers**  
A. unisomerized copolymer through Wittig reaction.  
B. isomerized copolymer.  
C. Copolymer through modified Wittig reaction.

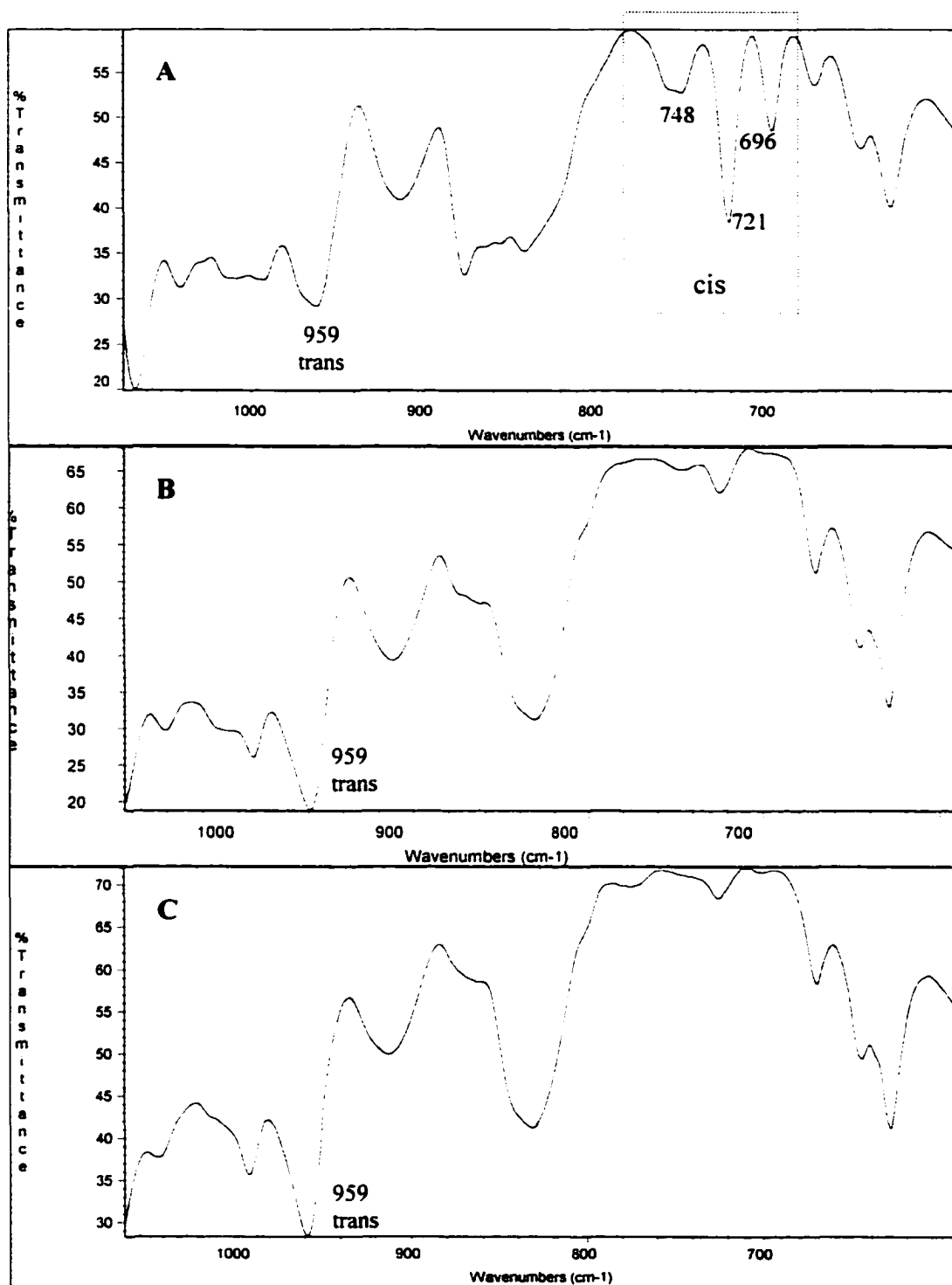


Figure 1-9. FT-IR spectrum of alternating copolymers  
 A. unisomerized copolymer through Wittig reaction.  
 B. isomerized copolymer.  
 C. copolymer through modified Wittig reaction

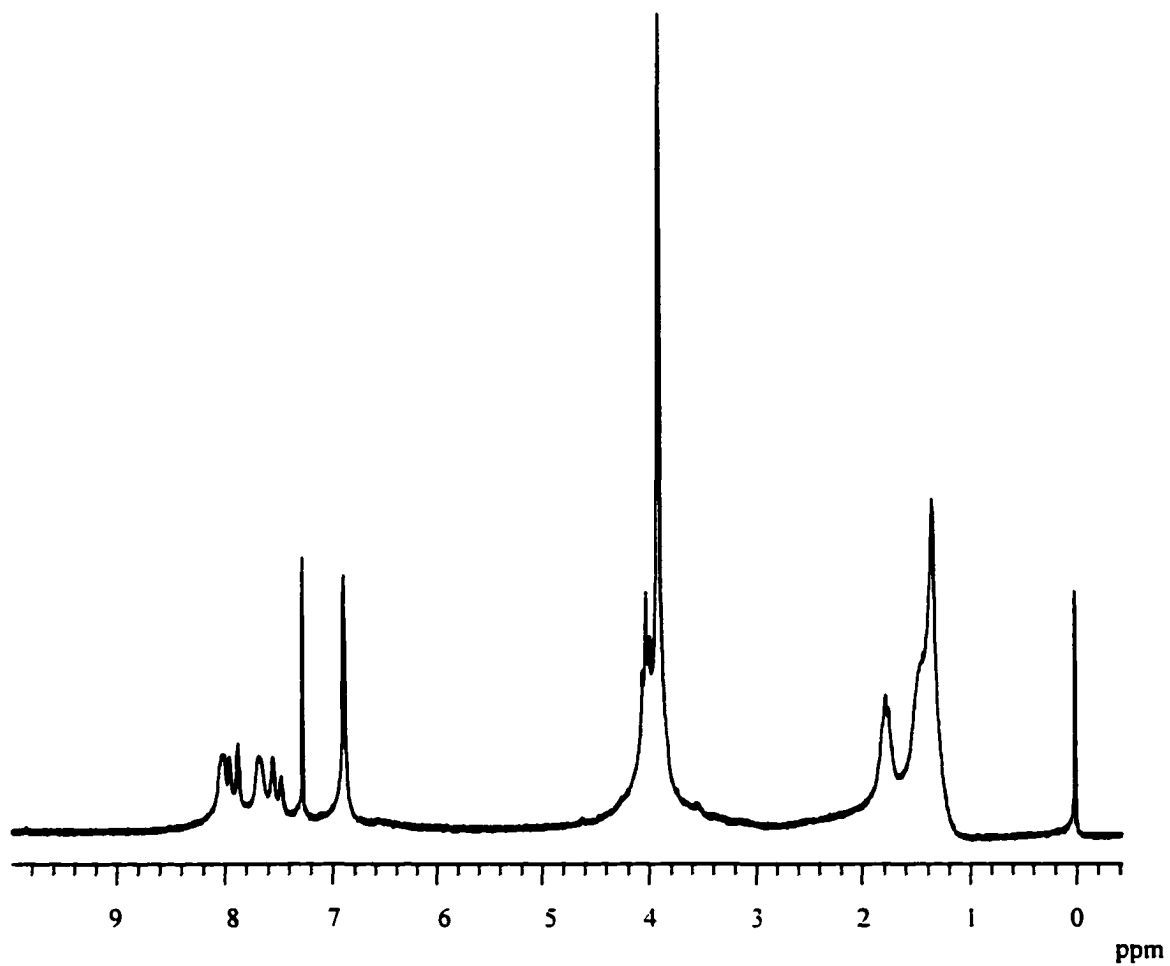


Figure 1-10.  $^1\text{H-NMR}$  spectrum of of poly- [1,10-decanedioxy-(2,6-dimethoxy-1,4-phenylene)-1,2-ethenylene-2,3-quinoxaline-1,2-ethenylene-(3,5,-dimethoxy-1,4-phenylene)]

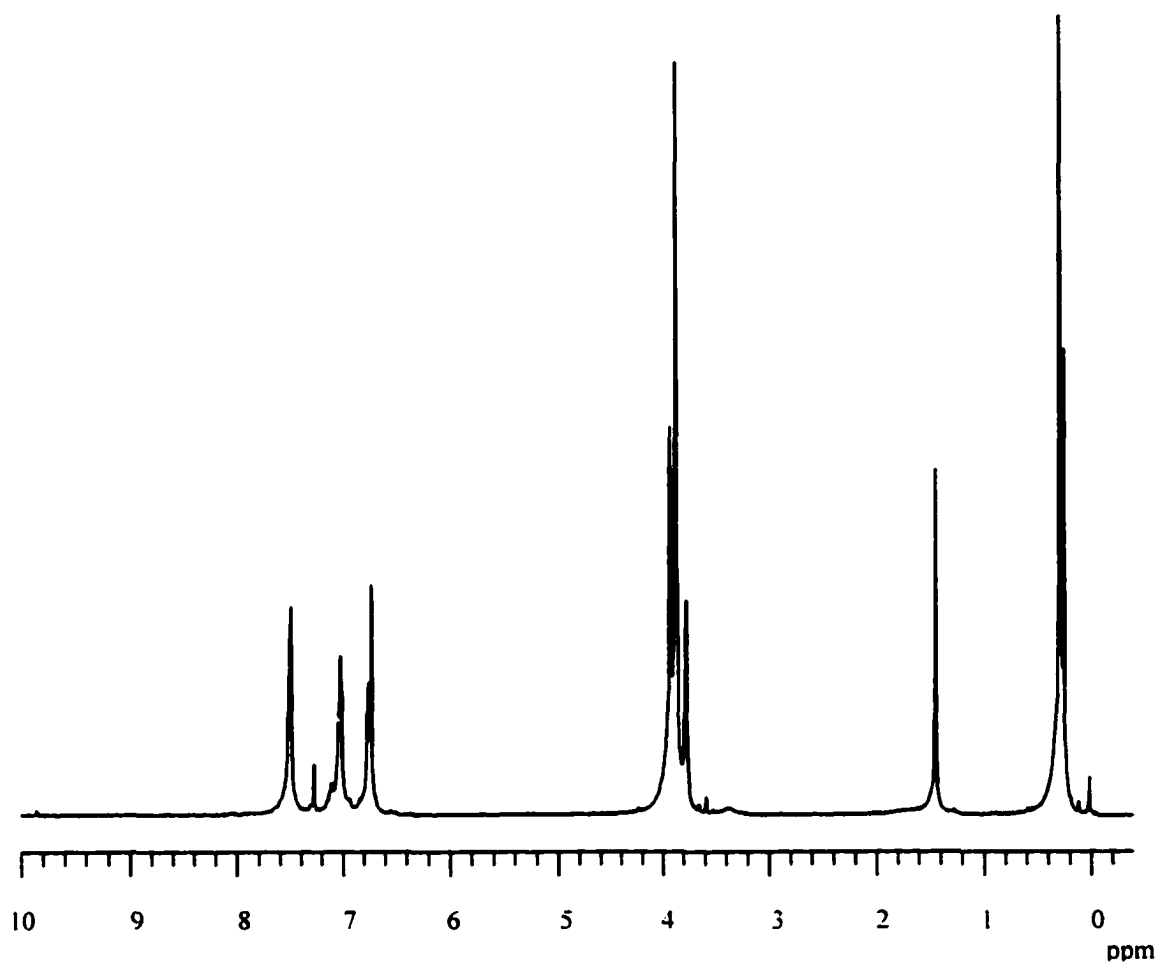


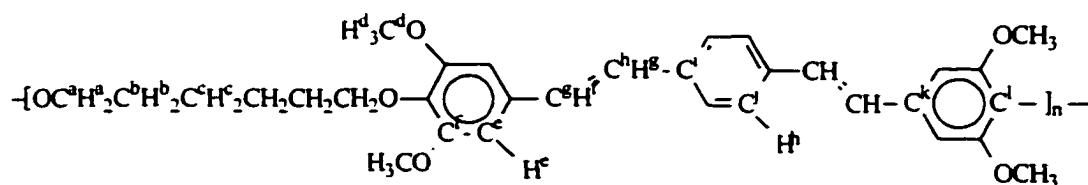
Figure 1-11.  $^1\text{H-NMR}$  spectrum of poly[1.3-methylenetetramethyldisiloxanedioxy-(2,6-dimethoxy-1,4-phenylene)-1,2-ethynylene-1,4-phenylene-1,2-ethynylene-(3,5-dimethoxy-1,4-phenylene)]

## 2-D NMR analysis of copolymer

The proton and carbon NMR spectrum of polymerization product are somewhat complicated as shown in Figure 1-12 of copolymer of poly[1,6-hexanedioxy-2,6-dimethoxy-1,4-phenylene-1,2-ethynylene 1,4-phenylene-1,2-ethylene-3,5-dimethoxy-1,4-phenylene].

Heteronuclear multi bond correlation (HMBC) and heteronuclear multiple-quantum coherence (HMQC) two-dimensional NMR spectroscopy were used for assignment of chemical shift of protons and carbons of the copolymer and determination of the microstructure of the copolymer.

There should be chemical shift signal of eight kinds of hydrogen nuclear and twelve kinds of carbon nuclear of copolymer of poly[1,6-hexanedioxy-2,6-dimethoxy-1,4-phenylene-1,2-ethynylene-1,4-phenylene-1,2-ethylene-3,5-dimethoxy-1,4-phenylene], named  $H^a$  to  $H^h$  and  $C^a$  to  $C^l$ , respectively, as shown as following figures:



HMQC 2D spectrum (Figure 1-14) gives the correlation between hydrogen and carbon connected through bond and HMBC 2D spectrum (Figure 1-13) gives that information for 2- or 3- bond connection.

Methoxyl group,  $\text{H}^{\text{d}}_3\text{C}^{\text{d}}\text{O}-$ , on the benzene ring was used as the starting point for assignment. From  $^1\text{H}$ -NMR spectra of monomer and copolymer, peak area integrations show that the proton chemical shift of  $\text{H}^{\text{d}}$  is 3.90 ppm and the chemical shift of  $\text{C}^{\text{d}}$  is 56.37 ppm from HMQC.  $\text{H}^{\text{d}}$  has also correlation with  $\text{C}^{\text{f}}$ , which connects  $\text{H}^{\text{d}}$  through three bonds and gives chemical shift at 153.88 ppm shown on HMBC spectrum.  $\text{C}^{\text{f}}$  has no coherence signal on HMQC, because it has no hydrogen atom connected to it directly, but  $\text{C}^{\text{f}}$  has another correlation with the  $\text{H}^{\text{e}}$ , which has chemical shift at 6.74 ppm. From HMQC,  $\text{C}^{\text{e}}$  connected to  $\text{H}^{\text{e}}$  has chemical shift at 103.99 ppm.  $\text{C}^{\text{e}}$  has a correlation with  $\text{H}^{\text{f}}$ , which gives signal at 6.98 ppm (from HMBC) and connected to  $\text{C}^{\text{g}}$  (126.95 ppm, from HMQC). Another hydrogen,  $\text{H}^{\text{g}}$ , on the double bond gives signal at 7.03 ppm, which correlated with  $\text{C}^{\text{g}}$  from HMBC and connected with  $\text{C}^{\text{h}}$ , 128.83 ppm, from HMQC.

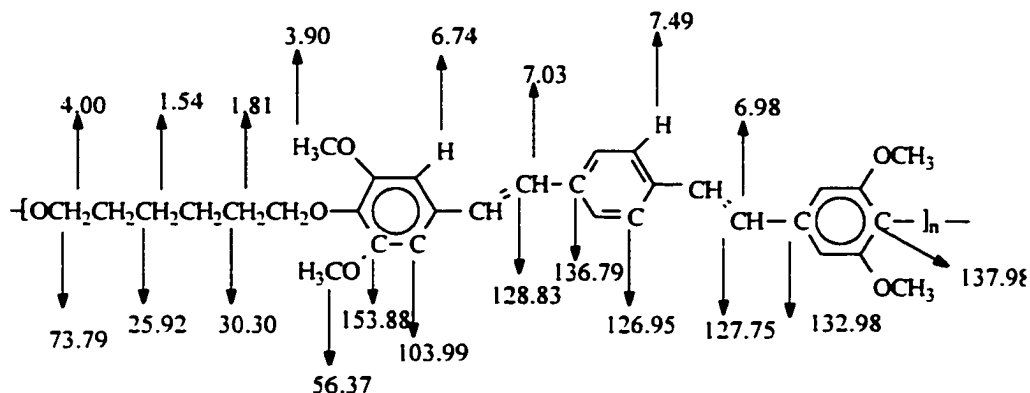
The signal, 132.98 ppm, can be determined from  $\text{C}^{\text{k}}$ , according to its correlation with  $\text{H}^{\text{f}}$ , 6.98 ppm, and  $\text{H}^{\text{e}}$ , 6.74 ppm, through two bonds. Meanwhile, it has no coherence signal on HMQC 2D spectrum.

Another carbon,  $C^l$ , on the p-position of  $C^k$ , with 137.98 ppm, is established by correlation with  $H^e$ , and no coherence signal on HMQC.

Two kinds of carbon,  $C^i$  and  $C^j$  on the middle phenylene unit can be assigned at 136.79 ppm and 126.95 ppm, respectively, because the carbon with 136 ppm has no connecting hydrogen atom and whereas the carbon with 126.95 ppm has connecting hydrogen,  $H^h$ , with 7.49 ppm. Even though they have same correlation with  $H^g$ , 7.09 ppm and  $H^h$ , 7.49 ppm.

The chemical shift of  $H^a$ ,  $H^b$ ,  $H^c$ ,  $C^a$ ,  $C^b$ , and  $C^c$ , is assigned at 4.00, 1.81, 1.54, 73.79, 30.30 and 25.92 ppm, respectively, because only  $H^a$  can have correlation with  $C^l$ , 137.98 ppm, through three bonds, and  $C^c$  can have three correlation with  $H^a$ , 4.00 ppm, through three bonds and with  $H^b$ , 1.81 ppm, and another non-connecting  $H^c$ , 1.54 ppm, through two bonds. The connecting relation among of  $H^a$  and  $C^a$ ,  $H^b$  and  $C^b$ ,  $H^c$  and  $C^c$  can be obtained from HMQC 2D spectrum.

Based on the detailed explanation above, assignment can be summarized the following depiction:



From 2D NMR spectroscopy, the chemical shift of two hydrogen atoms on the double bond,  $H^f$  and  $H^g$ , are 6.98 and 7.03 ppm respectively. The spin-spin coupling constant  $J_{H-H}$  of the  $H^f$  and  $H^g$  is 17.3 Hz from proton NMR spectrum. Therefore, the isomerized copolymer has mainly trans-structure.

HMQC has shown also that in addition to  $H^d$ , the carbon,  $C^d$ , of methoxyl group connects with another kind of hydrogen, which gives chemical shift at 3.62 ppm and has large integral as well as  $H^d$  before isomerization. This hydrogen can be considered from methoxyl group on the benzene ring, which connected to cis-double bond. Therefore, the integral ratio of hydrogen atoms at 3.90 and 3.62 ppm can be used for calculation of the ratio of trans- and cis- microstructure.

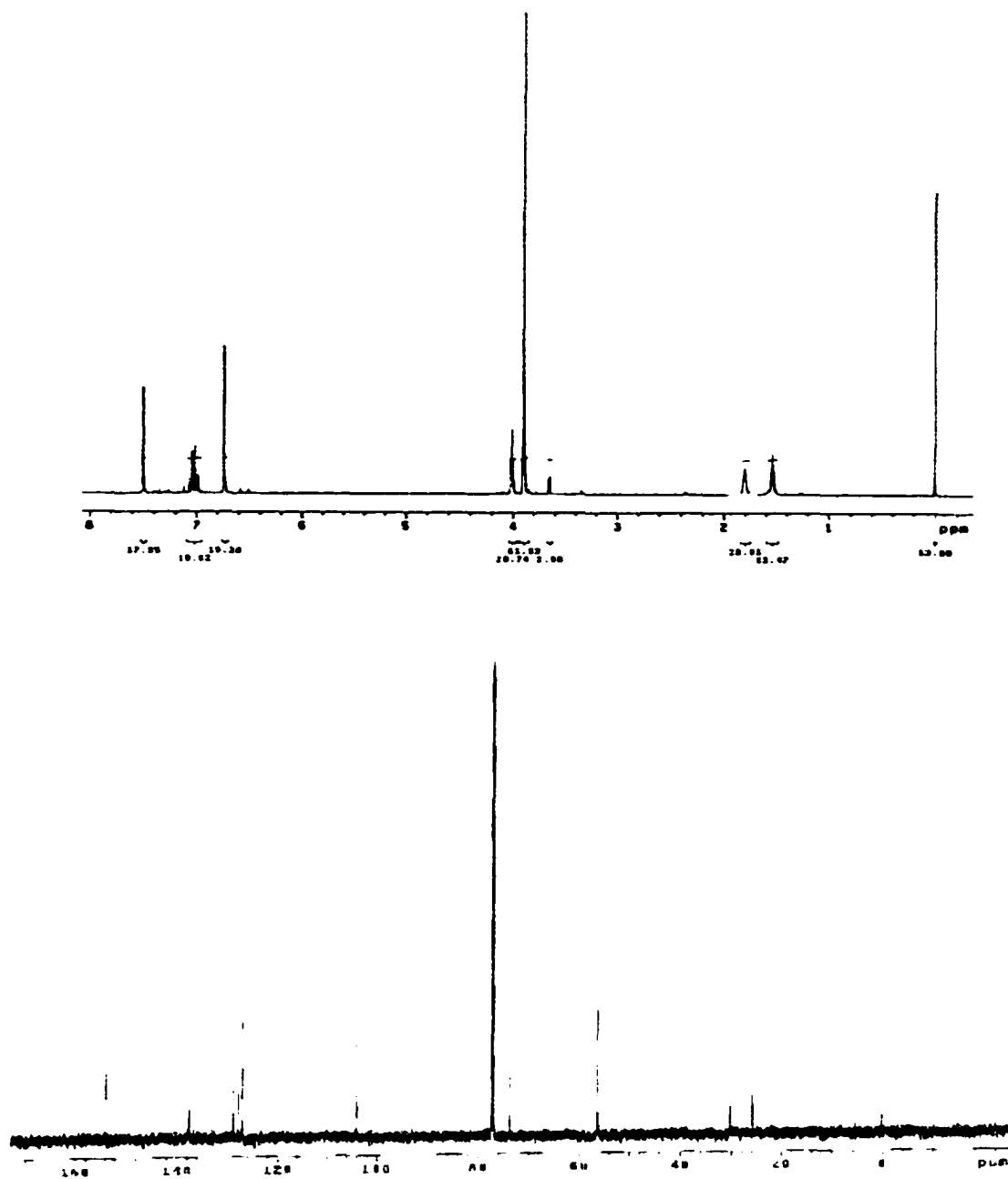


Figure 1-12.  $^1\text{H-NMR}$  (top) and  $^{13}\text{C-NMR}$  spectra of poly[1,6-hexanedioxy-2,6-dimethoxy-1,4-phenylene-1,2-ethenylene-1,4-phenylene-1,2-ethylene-3,5-dimethoxy-1,4-phenylene]. (600 MHz)

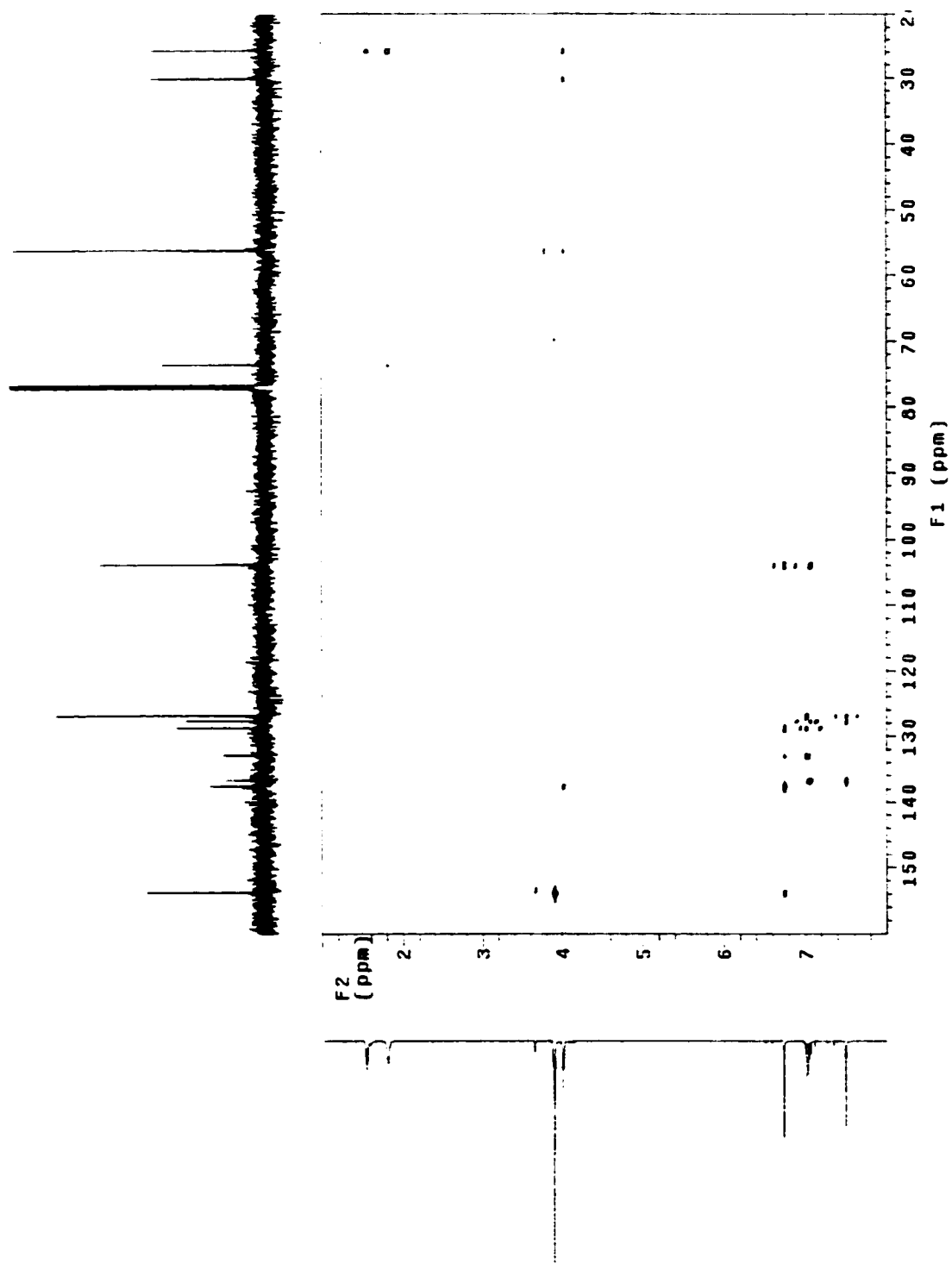


Figure 1-13. 2-D NMR spectrum of isomerized copolymer of poly[1,6-hexanedioxy-2,6-dimethoxy-1,4-phenylene-1,2-ethenylene-1,4-phenylene-1,2-ethylene-3,5-dimethoxy-1,4-phenylene].

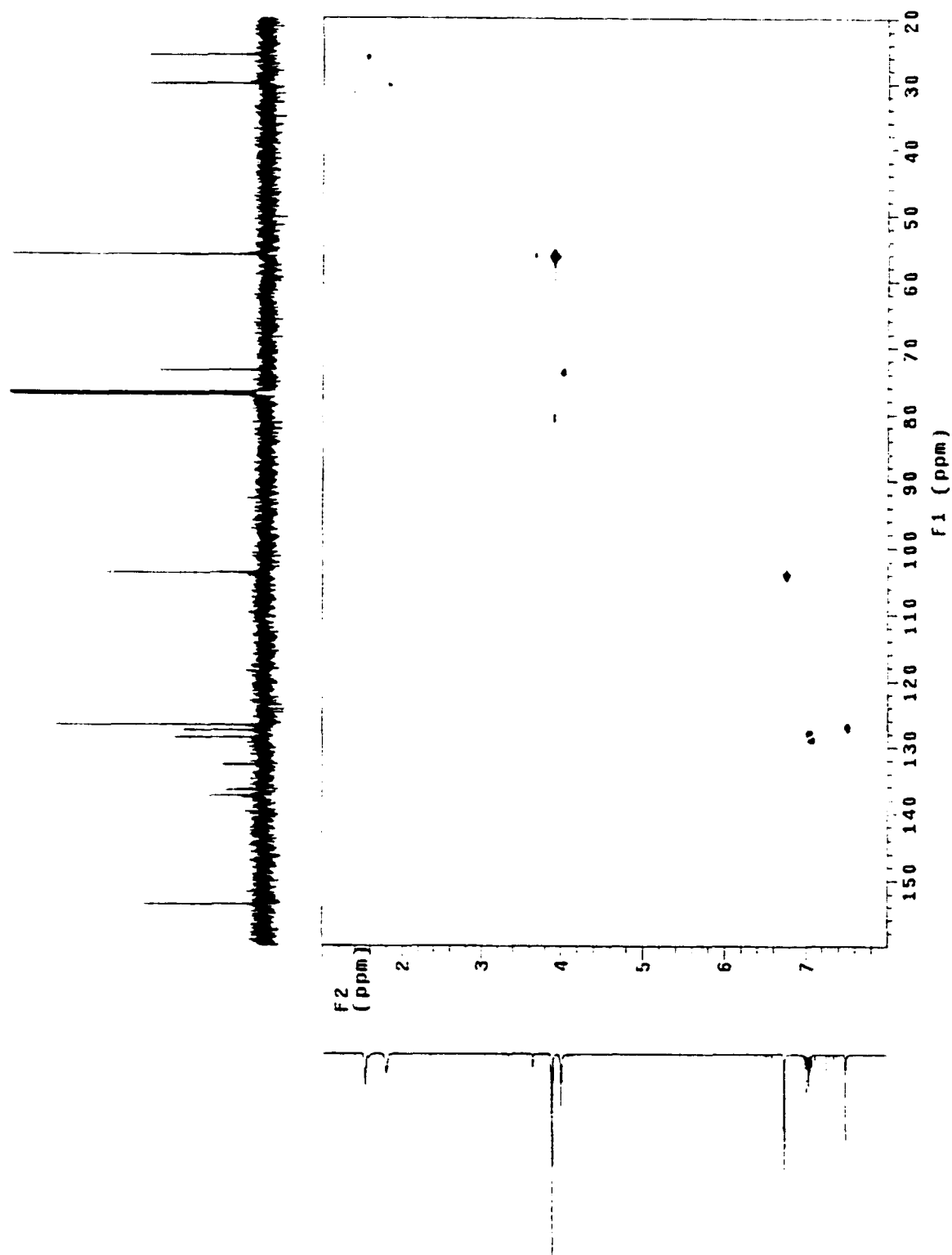


Figure 1-14. HMQC 2D-NMR spectrum of poly[1,6-hexanedioxy-2,6-dimethoxy-1,4-phenylene-1,2-ethenylene-1,4-phenylene-1,2-ethylene-3,5-dimethoxy-1,4-phenylene]. (600 MHz)

### **GPC determination of Molecular weight of copolymers**

Both the alternating copolymers synthesized through the Wittig reaction and the modified Wittig reaction has high molecular weight, which can give good processability of film-formation

The GPC results (calibration using polystyrene standard) are listed in Table 1-5. The molecular weight of copolymers through the Wittig condensation is in range from 34k to 97k for alkylene soft segments. For copolymers having glycol segment, the molecular weight is relatively lower, in range of about 20k. But, the molecular weight of the copolymer containing dimethylsiloxane segments is only 2.8k in paste state and high MW polymer was not formed in the polycondensation using anthracenyltriphenylphosphonium chloride.

However, the molecular weight of copolymers synthesized through the modified Wittig reaction are somewhat lower than that through the Wittig reaction for the copolymers with alkyl soft segments and higher for the copolymer with siloxane segment.

The results of GPC examination showed that the molecular weight of copolymers may be dependent on the solubility of copolymer in the polymerization

Table 1-5. Results of GPC analysis of EL copolymers

<i>Copolymers</i>		<i>Wittig reaction</i>		<i>Modified Wittig reaction</i>	
R	Ar	Mn	MWD	Mn	MWD
-(CH <sub>2</sub> ) <sub>4</sub> O-	Benzene ring	34,000	1.67	-	-
-(CH <sub>2</sub> ) <sub>6</sub> O-	Benzene ring	49,000	1.77	-	-
-(CH <sub>2</sub> ) <sub>8</sub> O-	Benzene ring	54,000	1.89	30,000	1.90
-(CH <sub>2</sub> ) <sub>10</sub> O-	Benzene ring	97,000	1.67	33,000	1.65
-(CH <sub>2</sub> CH <sub>2</sub> O) <sub>2</sub> .	Benzene ring	17,000	1.89	-	-
-(CH <sub>2</sub> CH <sub>2</sub> O) <sub>3</sub> .	Benzene ring	22,000	1.53	-	-
CH <sub>2</sub> Si(CH <sub>3</sub> ) <sub>2</sub> OSi (CH <sub>3</sub> ) <sub>2</sub> CH <sub>2</sub> O	Benzene ring	2,800	1.65	9,300	1.52
-(CH <sub>2</sub> ) <sub>10</sub> O-	Quinoxaline	-	-	15,000	1.83
-(CH <sub>2</sub> ) <sub>10</sub> O-	Anthracene	-	-	8,000	1.63

solvent. In the conventional Wittig condensation, the less polar mixed solvent of ethanol and chloroform were employed; the modified method used a strong polar solvent dimethylformamide to avoid reaction of sodium methoxide with chloroform.

### Thermal property of copolymers through DSC determination

The DSC experiments were carried out at heating rate 10 °C/min. The spectra of DSC are shown in Figure 1-15 and 1-16. The glass transition temperatures,  $T_g$ , of copolymers are tabulated as following.

Table 1-6. Glass transition temperature,  $T_g$ , of copolymers.

<i>Copolymers</i>		<i>Wittig reaction</i>		<i>Modified Wittig reaction</i>	
R	Ar	Mn	$T_g$	Mn	$T_g$
-(CH <sub>2</sub> ) <sub>4</sub> O-	Benzene ring	34,000	95.8	-	-
-(CH <sub>2</sub> ) <sub>6</sub> O-	Benzene ring	49,000	93.73	-	-
-(CH <sub>2</sub> ) <sub>8</sub> O-	Benzene ring	54,000	81.45	30,000	84.05
-(CH <sub>2</sub> ) <sub>10</sub> O-	Benzene ring	97,000	75.95	33,000	-
-(CH <sub>2</sub> CH <sub>2</sub> O) <sub>2</sub> .	Benzene ring	17,000	84.00	-	-
-(CH <sub>2</sub> CH <sub>2</sub> O) <sub>3</sub> .	Benzene ring	22,000	74.64	-	-
CH <sub>3</sub> Si(CH <sub>3</sub> ) <sub>2</sub> OSi (CH <sub>3</sub> ) <sub>2</sub> CH <sub>2</sub> O	Benzene ring	2,800	-	9,300	84.14
-(CH <sub>2</sub> ) <sub>10</sub> O-	Quinoxaline	-	-	15,000	96.97
-(CH <sub>2</sub> ) <sub>10</sub> O-	Anthracene	-	-	8,000	-

The glass transition temperature reflects the flexibility of polymer chain. From the experimental data, the flexibility of copolymers increases with increasing length of soft alkyl segment and the contribution of glycol segment for flexibility of polymer chain is larger than alkyl segment.

$T_g$  of the copolymer with tetramethyldisiloxane segment is 84.14 °C, which is equal to that of the copolymer with octylene segment. A lower  $T_g$  can be expected, if longer siloxane chain can be synthesized. Unfortunately, proper starting material for such syntheses are not available

The DSC data show that the copolymers, especially those obtained through the modified Wittig coupling reaction, have well defined low temperature endotherms. This indicates that the conjugated segments of the alternating copolymers have a observable level of order arrangement.

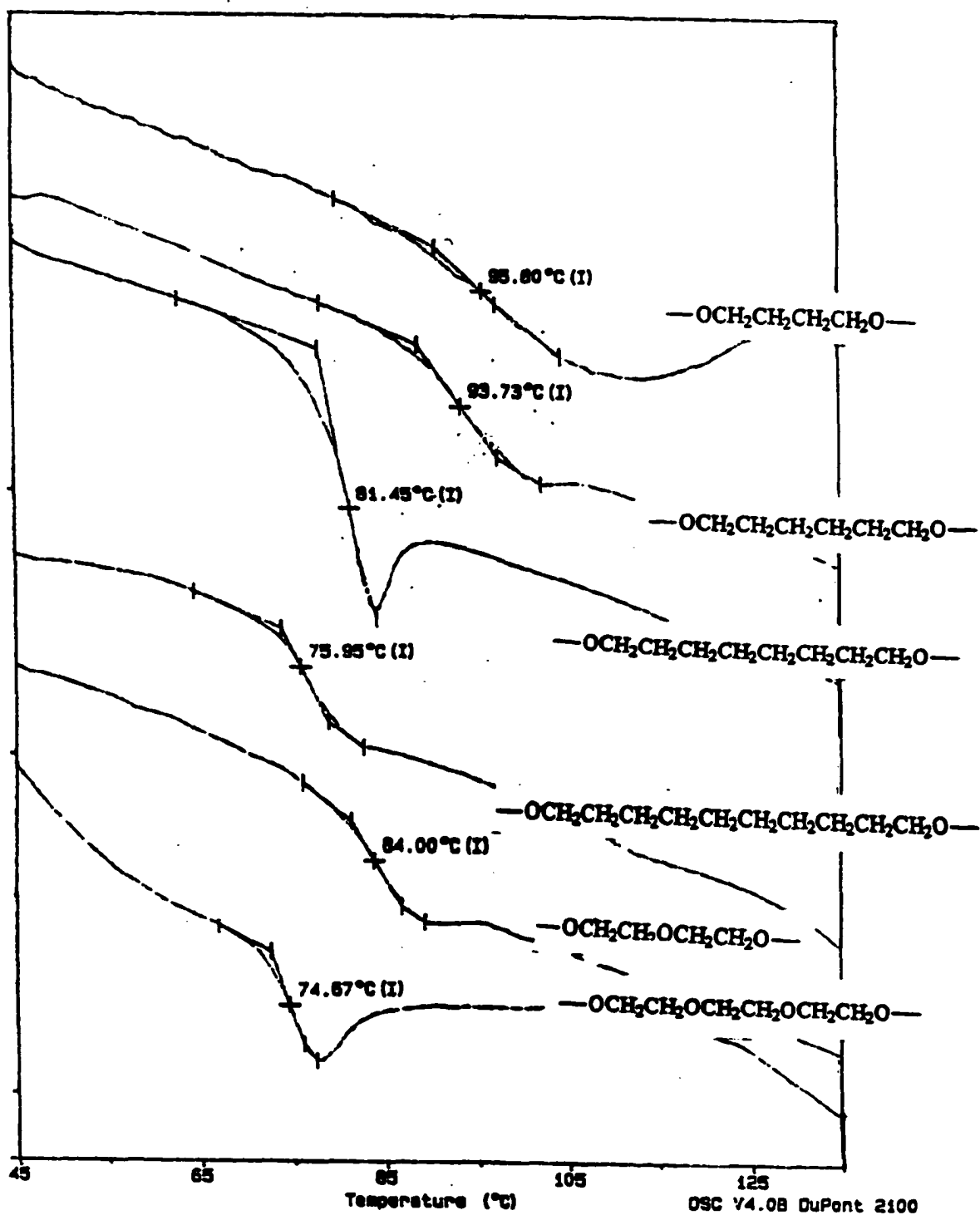


Figure 1-15. DSC spectra of alternating copolymer with a soft segment of alkylene or EO and with conjugated segment of PPV.

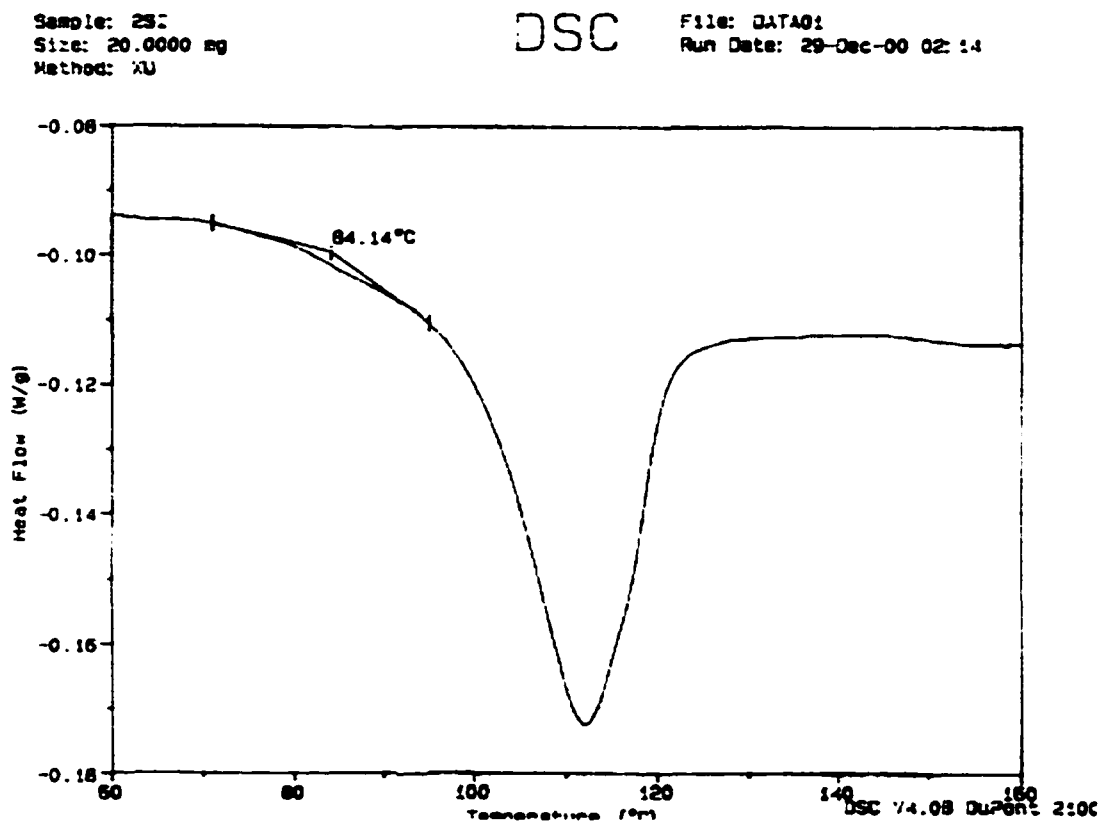


Figure 1-16. DSC spectrum of poly[1,3-methylenetetramethyldisiloxanedioxy-(2,6-dimethoxy-1,4-phenylene)-1,2-ethenylene-1,4-phenylene-1,2-ethenylene-(3,5-dimethoxy-1,4-phenylene)]

### UV and PL determination.

Although THF solutions of both nascent copolymer and isomerized copolymer made through the Wittig reaction with PPV segments have same UV absorption maximum at 375 nm (Figure 1-17), the *trans* -copolymer has larger absorption coefficient,  $\epsilon = 12.2 \times 10^4$  L/mole cm, compared with unisomerized copolymer,  $\epsilon = 3.4 \times 10^4$  L/mole cm. The alternating PPV copolymer made through the modified Wittig reaction has the same UV absorption maximum, 375 nm, and higher absorption coefficient,  $\epsilon = 13.2 \times 10^4$  L/mole cm.

Early reported work indicated that the same result could be obtained from determining both photoluminescence and electroluminescence.<sup>[63]</sup>

PL (photoluminescent) determination (Figure 1-18) indicated that the copolymer emits in the blue, i.e. 440 nm.

Poly- [1,10-decanedioxy-(2,6-dimethoxy-1,4-phenylene)-1,2-ethenylene-2,3-quinoxaline-1,2-ethenylene-(3,5,-dimethoxy-1,4-phenylene)] gives UV absorption, at 375 nm, and emitting light at 499 nm (Figure 1-20), which gives yellow color.

Poly[1,10-decanedioxy-(2,6-dimethoxy-1,4-phenylene)-1,2-ethenylene-9,10-anthracene-1,2-ethenylene-(3,5,-dimethoxy-1,4-phenylene)] has UV absorption, at 416 nm, and gives emitting light with wavelength at 566 nm, which will appear yellow-green color. (Figure 1-19.)

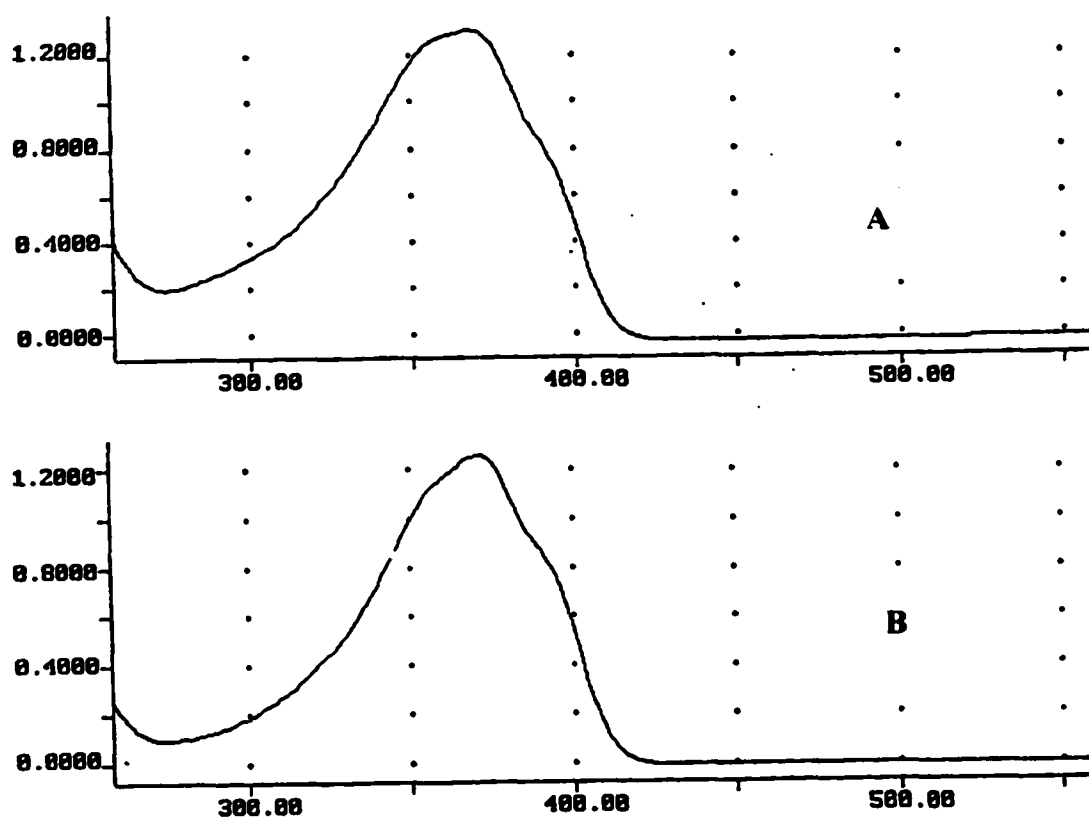


Figure 1-17. UV spectra of original poly[1,8-octanedioxy-2,6-dimethoxy-1,4-phenylene-1,2-ethenylene-1,4-phenylene-1,2-ethylene-3,5-dimethoxy-1,4-phenylene] (A) and its isomerized product (B).

Max. absorption wavelength 370-371 nm

The molar extinction coefficient:  $\epsilon = 3.4 \times 10^4$  L/mole cm (A) and  $\epsilon = 12.2 \times 10^4$  L/mole cm (B).

2D Graph 4

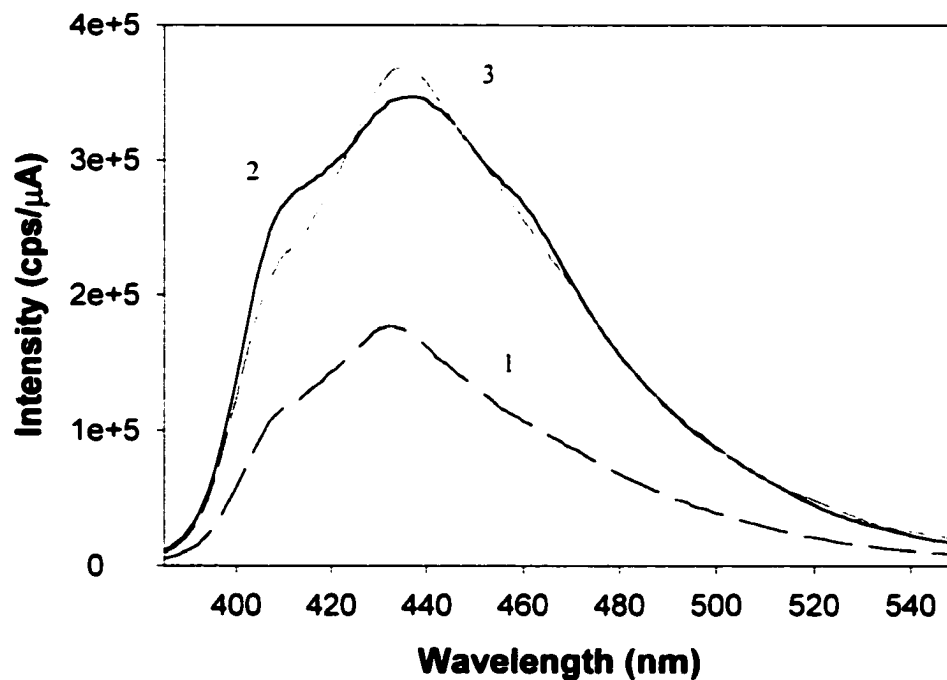


Figure 1-18. Photoluminescence spectra of poly[1,8-octanedioxy-2,6-dimethoxy-1,4-phenylene-1,2-ethynylene-1,4-phenylene-1,2-ethylene-3,5-dimethoxy-1,4-phenylene].

1. unisomerized copolymer through Wittig reaction.
2. isomerized copolymer.
3. copolymer through modified Wittig reaction

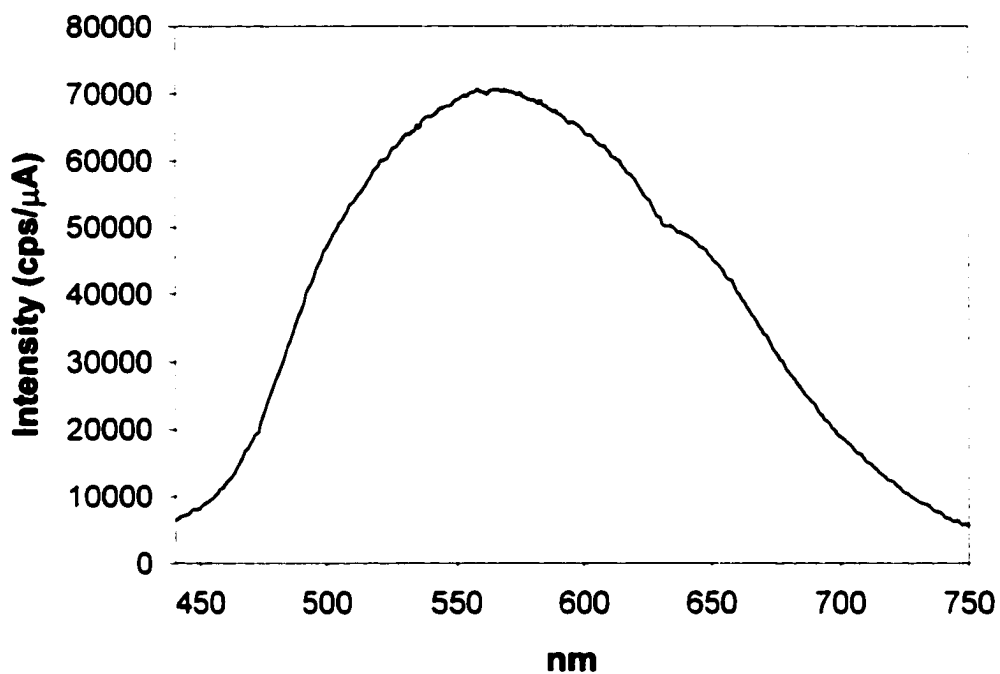


Figure 1-19. Photoluminescence spectrum of poly- poly[1,10-decanedioxy-(2,6-dimethoxy-1,4-phenylene)-1,2-ethenylene-9,10-anthracene-1,2-ethenylene-(3,5,-dimethoxy-1,4-phenylene)]

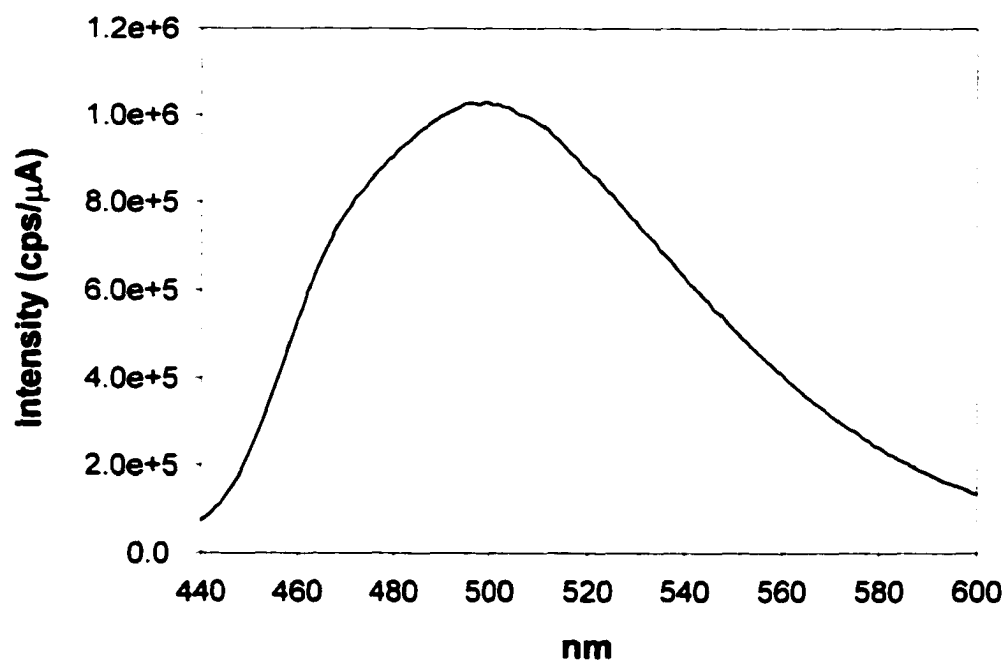


Figure 1-20. Photoluminescence spectrum of poly-poly[1,10-decanedioxy-(2,6-dimethoxy-1,4-phenylene)-1,2-ethenylene-2,3-quinoxaline-1,2-ethenylene-(3,5-dimethoxy-1,4-phenylene)]

## **Conclusion**

The modified Wittig reaction was applied successfully to the synthesis of soluble alternating PPV-like copolymers with significant advantages over the conventional Wittig method. The modified method gives all-trans microstructure of the conjugated segments without additional isomerization step. Unlike the conventional method, no cross-linking was observed. The Wittig method gives triphenylphosphine oxide as a side-product, while the side-product of the modified method, phosphate, can be removed much more efficiently because of its solubility in water, methanol and ethanol.

The methylsiloxane as soft segment in the alternating copolymers can reduce the glass transition temperature in comparison with alkyl segment with the same length, however, short siloxane segment chain has no significant effect.

## **Chapter 2.**

### **Synthesis and characterization of functionalized polystyrene**

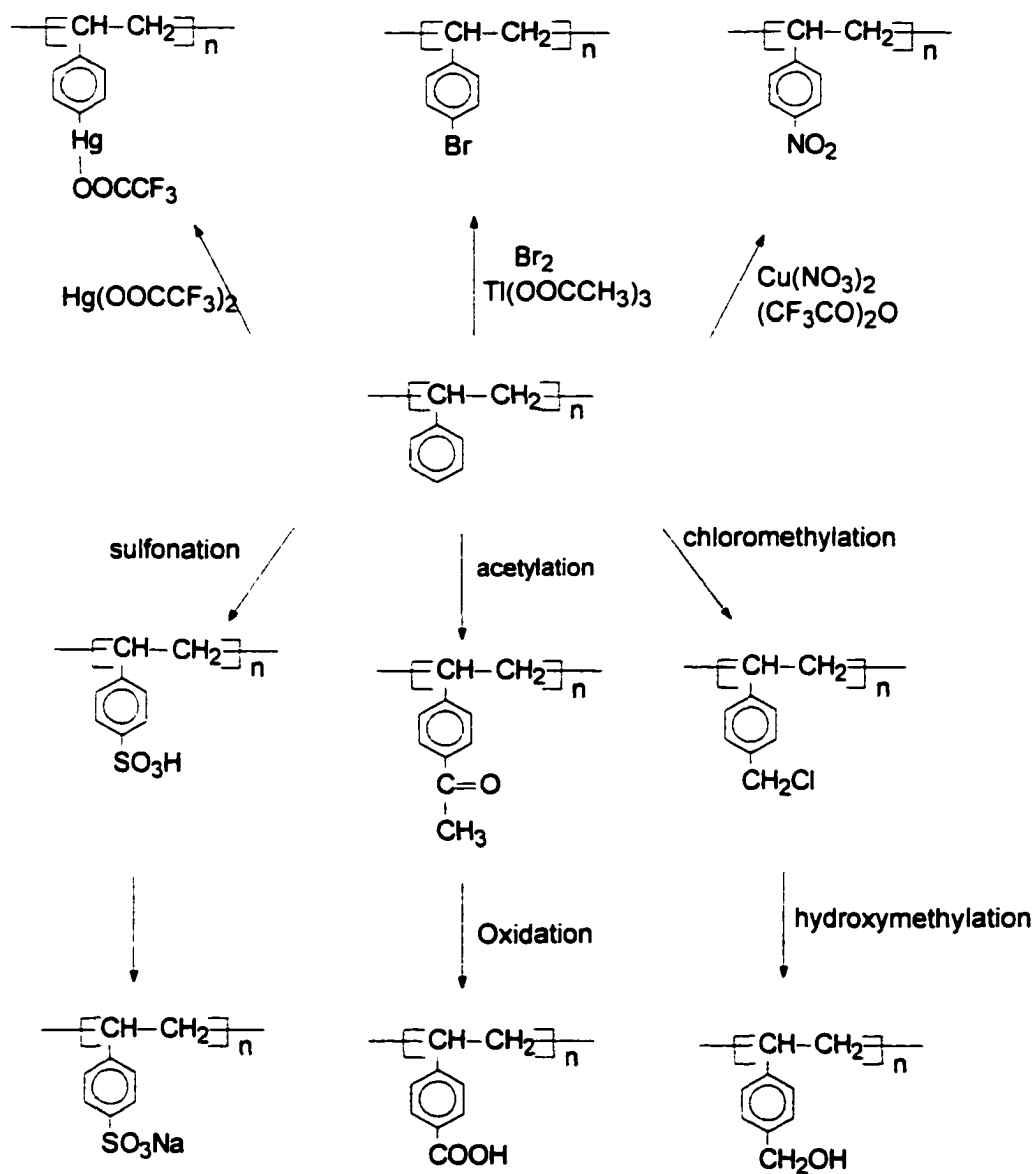
#### **Background**

Functionalization of polymer materials is an important area in polymer science. Polymers can provide new properties and applications through chemical or physical modifications. One of most commonly chosen polymer for modification study is polystyrene.

Polystyrenes with various functional groups have been applied to create interesting polymer interface, and used in large-scale industrial applications, e.g. ion-exchange.

Functionalized polystyrene can be obtained through a broad scope of reactions involving electrophilic reagents reacting directly with polystyrene or copolymerization of styrene with other vinylphenyl monomers containing a functional group. Scheme 2-1 shows the typical direct electrophilic reactions of polystyrene.

In the present work, polystyrenes carrying functionalities with electric charge, dipole, and hydrogen-bonding forming ability were prepared through copolymerization and polymer reactions:



Scheme 2-1. Reaction of polystyrene with electrophilic reagents.

1. *Polystyrene with strong acid group, i.e. sulfonic acid group.* Sulfonated polystyrene, or poly (styrene-co-styrenesulfonic acid), has been synthesized through directly sulfonation of polystyrene using acetyl sulfonate.
2. *Polystyrene with a dipole group, i.e. acetyl group.* Typical Friedel-Crafts acylation was employed for preparation of this polymer.
3. *Polystyrene with hydrogen-bonding forming group, i.e. hydroxyl group.* The polymer was prepared through copolymerization of styrene with vinylphenyl acetate and followed by hydrolysis reaction of the ester group

Polystyrene sulfonated at different levels synthesized here was applied as a model extracellular matrix (ECM) for protein adsorption and organization, to gain fundamental information for processes involved in tissue engineering. The other two polymers were used to explore fundamental interaction at polymer interfaces.

## 1. Polystyrene with sulfonic acid group

### Introduction

Due to broad range of their technological applications, polymers and copolymers of (styrenesulfonic acid) have been receiving a considerable attention for many years and still there is growing interest in the subject <sup>[1-20,32,70,71]</sup>.

Earlier, sulfonation of polystyrene was used for manufacturing cation-exchange resin. The polystyrene with different levels of sulfonic acid group gives the polymer novel properties, including ion-exchange capability

The polystyrene/polypyridine interfaces can be reinforced after partial sulfonation of polystyrene <sup>[21]</sup>. Reactivity was incorporated into the system by lightly sulfonating the polystyrene component, providing acid functionality which is coreactive with basic pyridine nitrogen of polypyridine.

Sulfonation of polystyrene can form a gradient-index medium useful for light-focusing purpose <sup>[22]</sup>. The refractive index of sulfonated polystyrene varies with the degree of sulfonation and that the refractive index of the fully sulfonated polystyrene is lower by ca. 0.06 at 436 nm compared with that of pure polystyrene.

Sulfonation of polystyrene changes the solubility of polystyrene, decreases the melting point and degree of crystallinity for syndiotactic polystyrene <sup>[23]</sup>.

Compatibility of blend of polystyrene and an amorphous polyamide was improved by low level of polystyrene sulfonation.<sup>[24,25]</sup> Hydrogen bonding between amide groups and either sulfuric acid or metal sulfonate groups lowers the interfacial tension between both polymers, leading to a much finer size of the dispersed phase in the blend. At relatively high sulfonate-amide ratios, two polymers formed a miscible blend. The miscibility of polystyrene and poly (methyl methacrylate) blend was enhanced through ionic interaction by sulfonation of polystyrene as well<sup>[26]</sup>.

A large number of sulfonation methods for linear polystyrene has been developed:

1. homogeneously using a complex between triethyl phosphate and sulfur trioxide<sup>[27]</sup>;
2. heterogeneously with 100 % sulfuric acid in presence of  $\text{Ag}_2\text{SO}_4$ <sup>[28]</sup>;
3. homogeneously with sulfuric acid(95-97%) and  $\text{P}_2\text{O}_5$  in cyclohexane<sup>[29]</sup>;
4. homogeneously with acetyl sulfate in dichloroethane<sup>[30]</sup>;
5. homogeneously with lauric acid- $\text{SO}_3$  in cyclohexane<sup>[31]</sup>;

All of above methods were examined in this study and the method using acetyl sulfate was found to be the most efficient way to prepare lightly sulfonated polystyrene, because it is easy to control sulfonation level and the product is easy to purify.



And then the acetyl sulfonate reacts with the benzene ring of styrene unit.

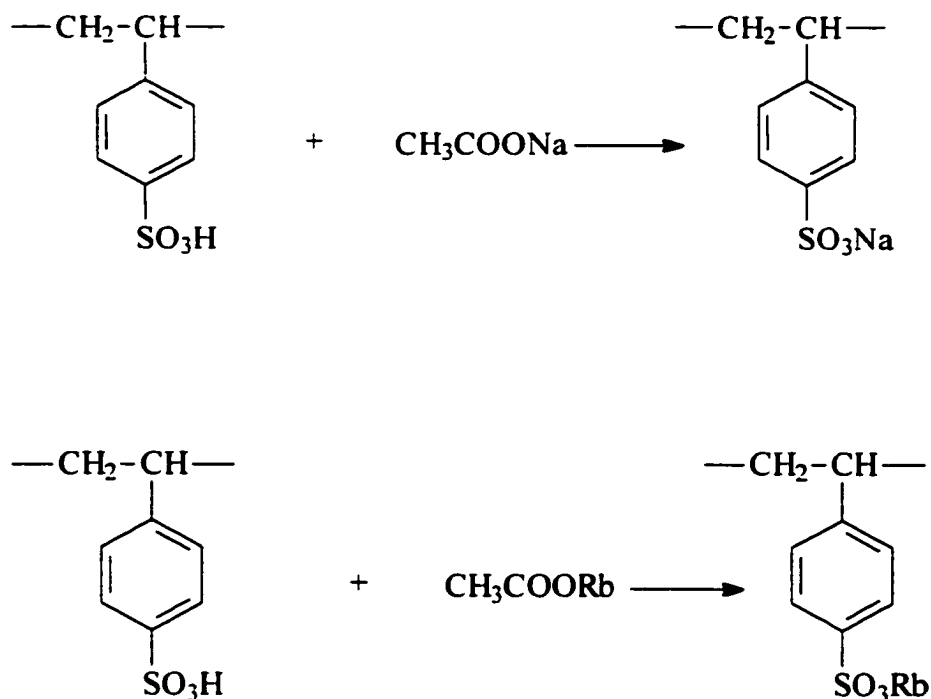
### **Experimental procedure**

Polystyrene (1 g) was dissolved in 30 ml of dichloroethane in a 100 ml-round three-necked flask. Acetic anhydride with concentrated sulfuric acid (molar ratio of 1.6:1) was added at room temperature. The reaction was allowed to proceed for 1 h at 50 °C and then terminated by the addition of ethanol.

Solvent, by-products methyl acetate, acetic acid and unreacted acid and ethanol were removed by steam stripping for 2 h. The products with less than 25 % sulfonation were isolated based on their insolubility in water. For the polystyrene at higher sulfonation level, the purification was carried out through dialysis for about one week.

The products were dried in a vacuum oven at 60 °C for 48 h, giving a light-yellow product.

## 2). Preparation of polystyrene with sodium and rubidium sulfonate



Scheme 2-4. The reaction of sulfonated polystyrene with acetate salt..

### Procedure

Sodium acetate- methanol solution or rubidium acetate methanol solution in excess amounts was added into sulfonated polystyrene/1,2-dichloroethane solution. The mixture was stirred for about 6 h and then the polymer is precipitated in methanol or precipitated in cold cyclohexane to obtain highly sulfonated polymer which was further purified using dialysis in redistilled water. The samples were dried in vacuum oven at 60°C for 24 h.

A series of samples with different extents of sulfonation, from 60 % to 1 %, were prepared.

### **3). Characterization**

Proton NMR and IR were employed for the characterization of sulfonation degree of polystyrene.

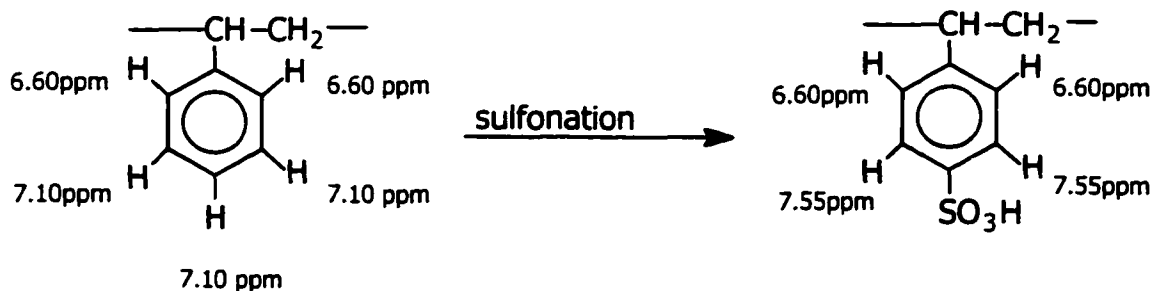
## **Result and discussion**

### **1. Solubility.**

After sulfonation, the solubility of the polystyrene was changed. The product at sulfonation level lower than 10% can be dissolved in mixed solvent of chloroform/methanol (3:1), but cannot be dissolved in chloroform alone. Highly sulfonated polymers can be dissolved in methanol or water.

### **2. Determination of sulfonation level.**

Most of publications used elemental analysis to determine the extent of sulfonation.  $^1\text{H-NMR}$  was used for the present work. The electron-withdrawing sulfonic acid group causes a downfield shift in the chemical shift of the nearby hydrogen atoms:



The extent of sulfonation was determined from the integrated areas of resonance peaks at 6.60, 7.10 or 7.55 ppm.

$$\text{Sulfonated units \%} = \frac{I_{7.55}}{I_{6.60}} \times 100 \quad \text{or} \quad \frac{I_{6.60} - \frac{2}{3} I_{7.10}}{I_{6.60}} \times 100$$

where,  $I_{6.60}$ ,  $I_{7.10}$  and  $I_{7.55}$  are the integrated intensities of the signals at 6.60, 7.10 and 7.55 ppm, respectively.

Figures 2-1 represents the spectra of polystyrene and sulfonated polystyrene respectively. Table 2-1 shows the extent of sulfonation for three samples by NMR and by elemental analysis. Data from the two methods are in good agreement.

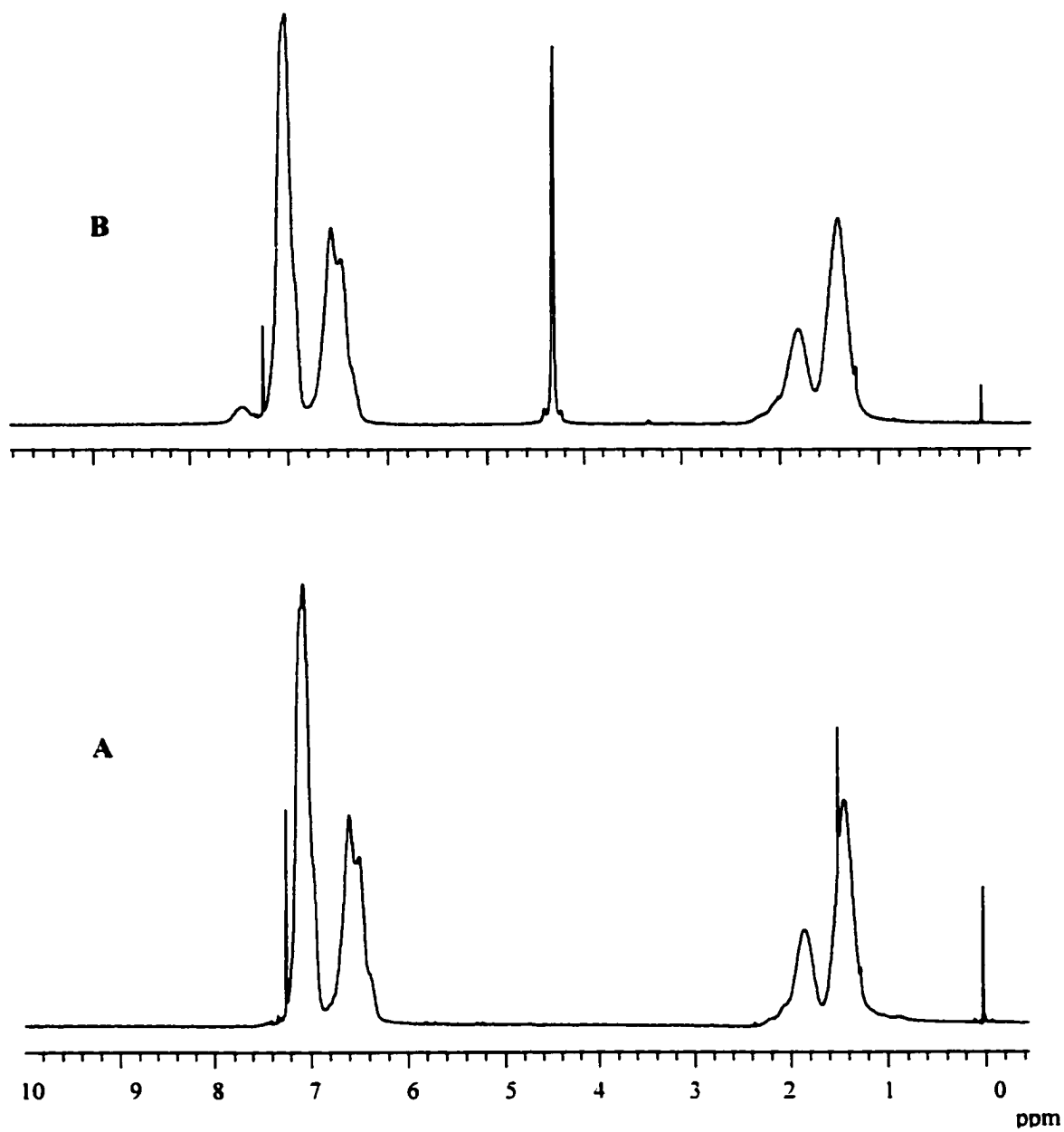


Figure 2-1. <sup>1</sup>H-NMR spectra of polystyrene (A) and sulfonated polystyrene (B)

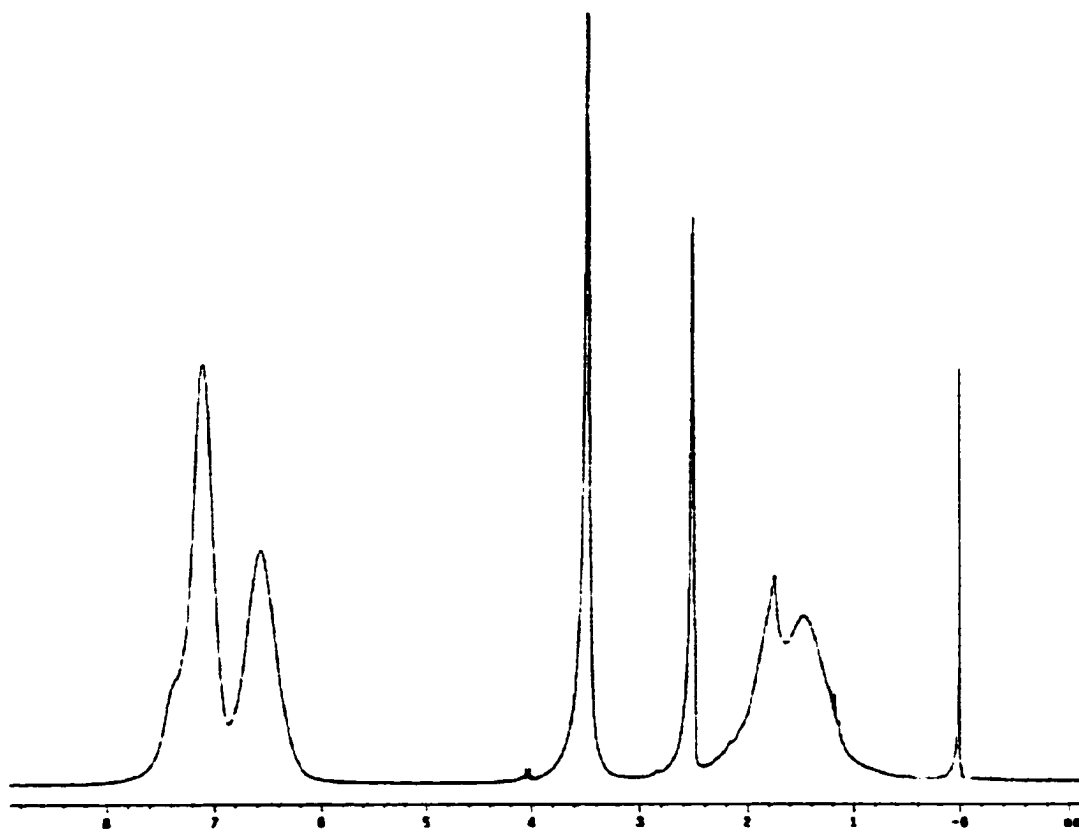


Figure 2-2.  $^1\text{H-NMR}$  spectrum of poly-styrene-co-(sodium styrenesulfonate)  
(DMSO as solvent)

Table 2-1 Sulfonating extent of some samples

Samples	<sup>1</sup> H-NMR	Elemental analysis a)
PSS#14	10.5 %	10.1 %
PSS#17-1	31.1 %	30.5 %
PSS#18	36.0 %	34.0 %

note a) by E+R Microanalytical Laboratory, Inc.

The experimental results (Table 2-2 ) shows that the method of homogeneous sulfonation with acetyl sulfonate is efficient for preparing lightly-sulfonated polystyrene.

Table 2-2. Sulfonation of Polystyrene in C<sub>2</sub>H<sub>4</sub>Cl<sub>2</sub> with Acetyl Sulfonate (50 °C)

Samples	Theory	Anal. by NMR
PSS# 12a)	15 %	10.5 %
PSS#11a)	30 %	15.3 %
PSS#16a)	86 %	26.8 %
PSS#17	86 %	31.1 %
PSS#18	100 %	36.0 %

a). Preparing sulfonating reagent first and then adding into the polystyrene solution.

The NMR resonance of the hydrogen of sulfonic acid functionality does not appear downfield in  $^1\text{H}$ -NMR spectrum and the signal of hydroxyl group of methanol, impurity of methanol- $d_4$ , appears downfield to its normal position, most likely due to the interaction of -OH with  $-\text{SO}_3\text{H}$ .

It is surprising that the 7.55 ppm signal no longer appears after neutralization with sodium acetate or rubidium acetate as shown in Figure 2-2. This indicates that the sulfonate group does not show strong electron-withdrawing property. The extent of sulfonation for these samples was determined by NMR before neutralization or by elemental analysis after neutralization.

IR spectra also reveal the characteristics of sulfonic acid, as shown in the IR spectra of sulfonated polystyrene and pure polystyrene (Figure 2-3). The peak at  $834\text{ cm}^{-1}$  is characteristic of disubstituted benzene ring; and the peaks at  $1250\text{--}1150\text{ cm}^{-1}$  and  $1040\text{--}1005\text{ cm}^{-1}$  are characteristic of sulfonic acid [21].

Figure 2-4 is an IR spectrum of 15 percent sulfonated polystyrene. The resolution of IR is better for low sulfonation level (see Figure 2-5 for 60 percent of sulfonated polystyrene). However, intense IR peak,  $3500\text{ cm}^{-1}$ , from water persists even for film sample dried in vacuum oven at  $35\text{ }^\circ\text{C}$  for 24 h (Figure 2-6). Water was used as solvent for preparation of the film and is difficult to remove.

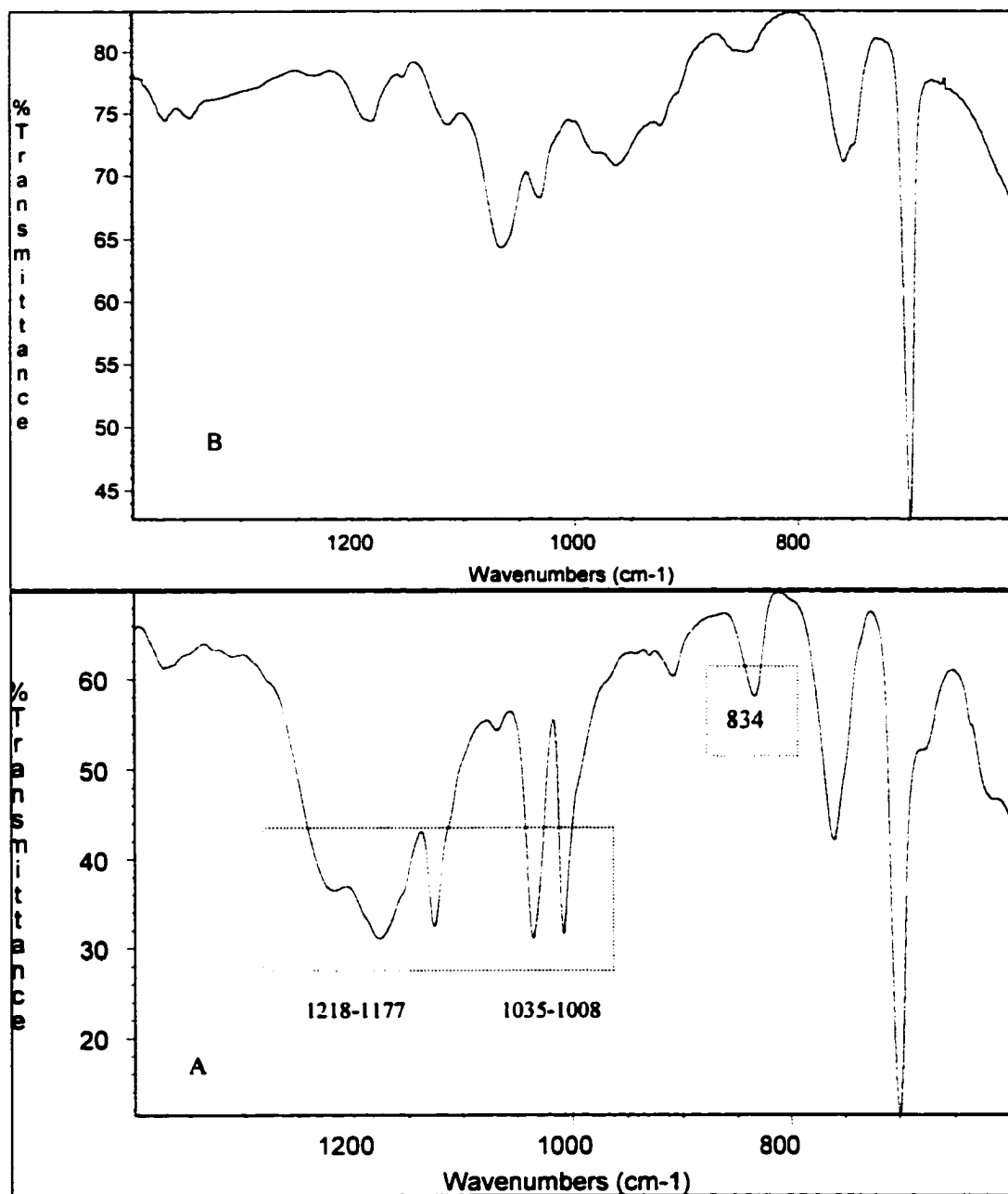


Figure 2-3. Comparison of FT-IR spectrum between sulfonated polystyrene(A) and original polystyrene(B).

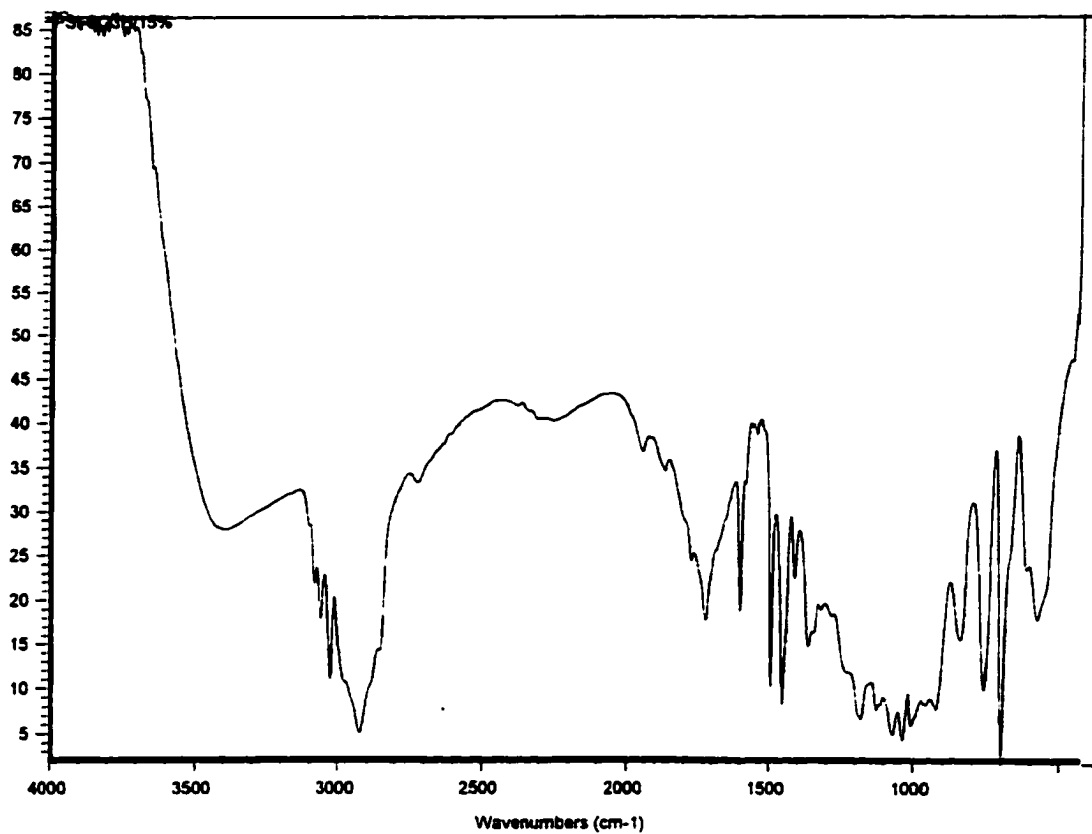


Figure 2-4. FT-IR spectrum of sulfonated polystyrene (5 mole % sulfonation)

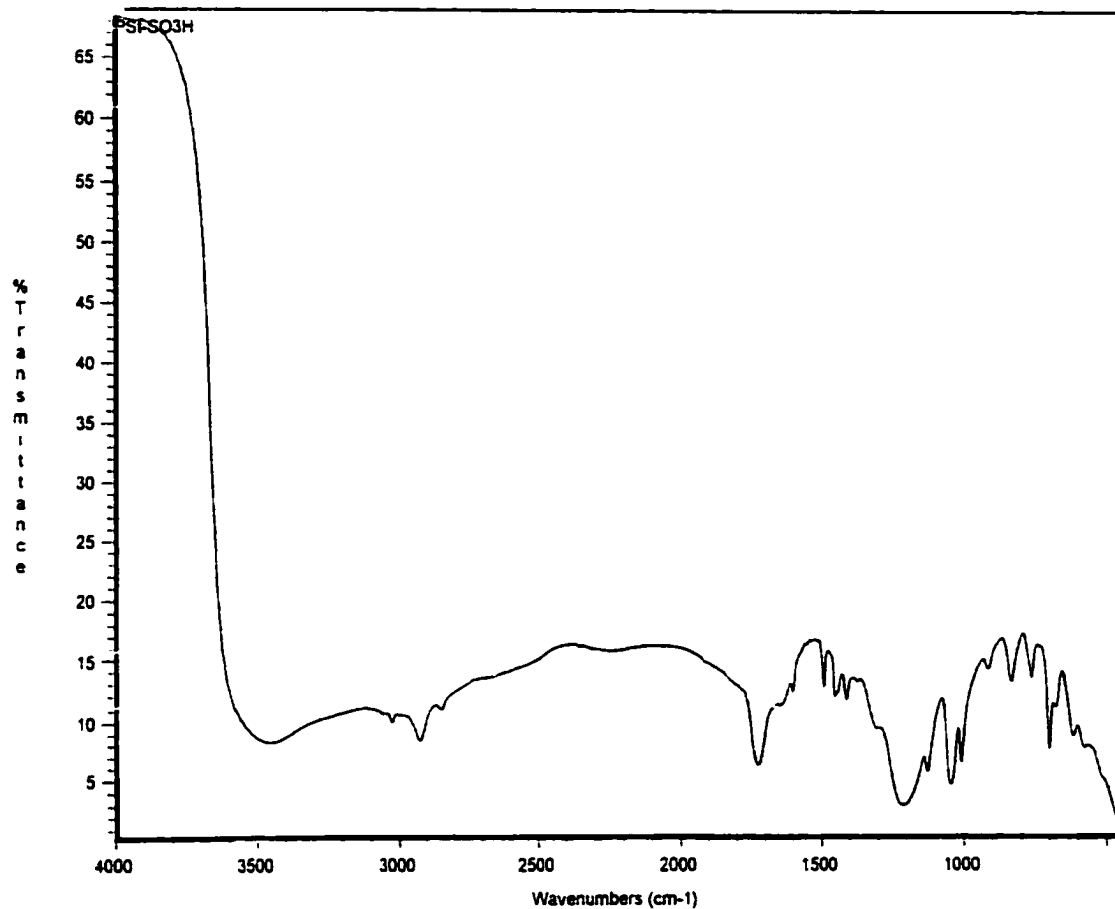


Figure 2-5. FT-IR spectrum of 60 % sulfonated polystyrene product.

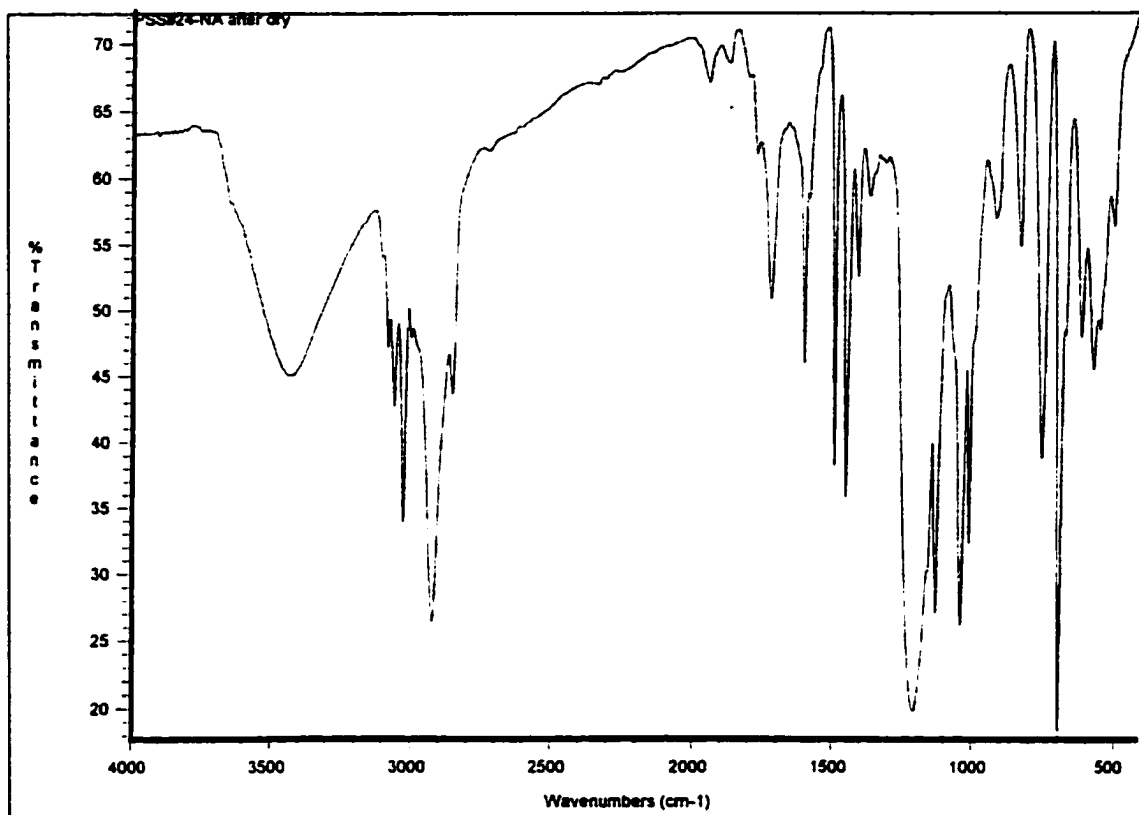


Figure 2-6. the FT-IR spectrum of higher sulfonated polystyrene dried in vacuum oven at 35°C, for 24h.

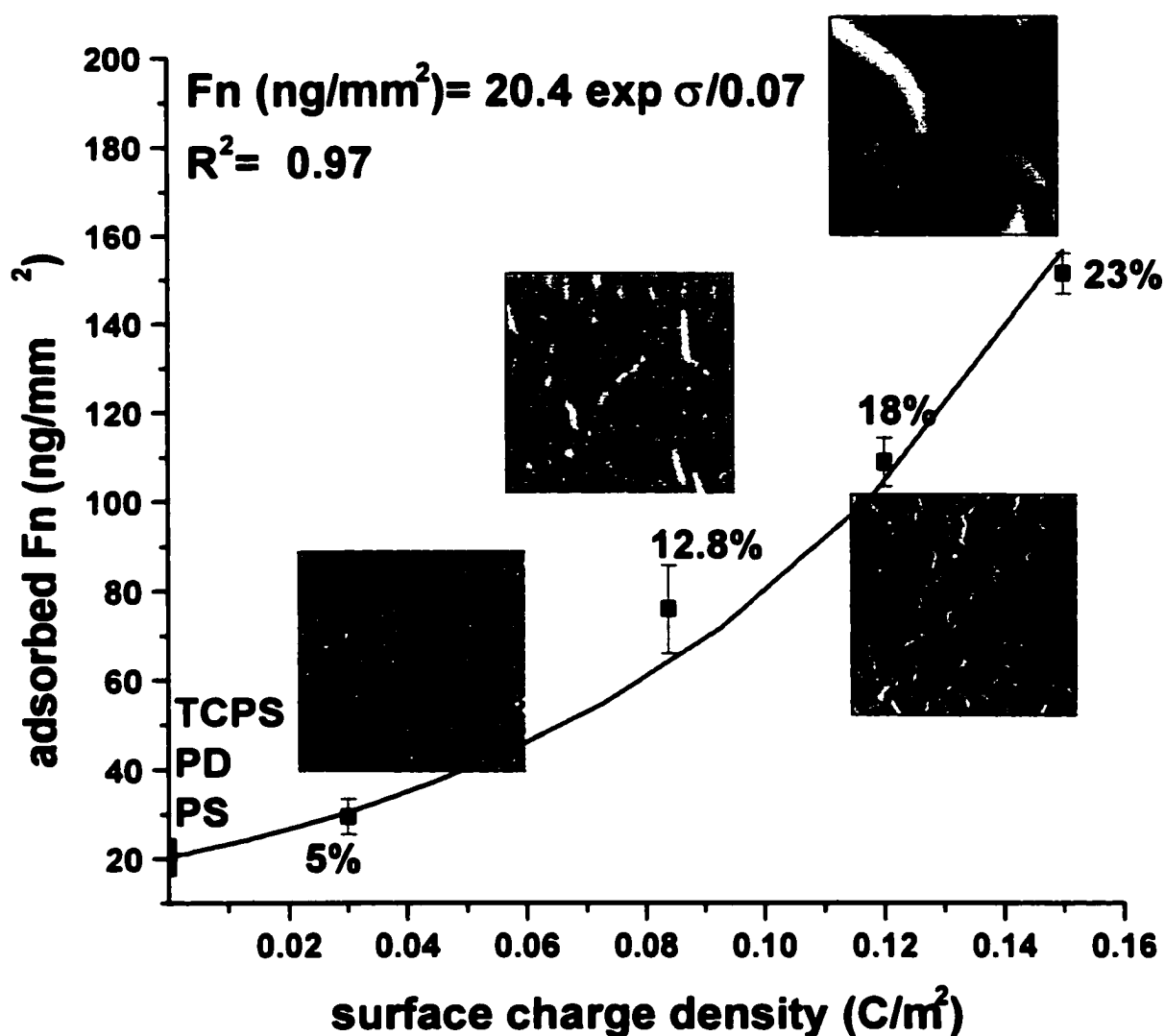


Figure 2-7. Adsorbed fibronectin mass as a function of surface charge density. <sup>[32]</sup>

AFM image of fibronectin adsorbed on PS surface ( $50 \times 50 \mu m$ ). Monolayer adsorption ( $\sim 20 \text{ ng/mm}^2$ ) was observed on all non-sulfonated polystyrene surfaces. At a charge density of  $-0.03 \text{ C/m}^2$  an adsorption transition is evident, and at increased charge densities significant increases in adsorbed protein occur for small changes in fixed surface charge density. (The absolute magnitude of the charge density is represented on the abscissa; sulfonated surfaces have a net negative charge).

### **Sulfonated Polystyrene as an extracellular matrix (ECM) model** <sup>[32]</sup>

(Figure 2-7)

Our establishment of an efficient synthetic procedure for the fine tuning of charge on polymer allows detailed investigations on *biomacromolecule* interaction with well-controlled surface. To gain fundamental information for processes involved in tissue engineering, polystyrene sulfonated at different levels was applied as a synthetic model of extracellular matrix (ECM) for protein adsorption and organization. Fibronectin, a critical component of the ECM, undergoes fibrillogenesis in the presence of cells. Using sulfonated polystyrene surfaces to mimic ECM charge density, fibronectin was observed to undergo a transition from monolayer to multilayer adsorption at surface charge densities above  $0.03 \text{ C/m}^2$ . At charge densities above approximately  $0.08 \text{ C/m}^2$ , distinct fibronectin fibrillar networks are observed to form, with the fibril morphology similar to that forms *in situ* on cell surfaces. The polarization of charge domains on the polyampholytic fibronectin molecules near high charge density sulfonated polystyrene surfaces is sufficient to initiate multilayer adsorption and the organization of these fibrillar structures. The process of tissue development is inherently dependent on the interaction of cells with extracellular matrix (ECM) proteins, many of the critical ECM proteins require surface interactions to initiate nucleation. In tissue engineering, it is important to synthesize surfaces with properties appropriate for the initiation of ECM self-organization. Fibronectin, a major ECM adhesive

protein, will not spontaneously organize into proper organization in solution. Attachment of fibronectin to a surface is necessary to initiate fibril formation.

Adsorption of fibronectin onto surfaces commonly utilized in biomedical applications does not permit the formation of fibronectin fibrils, instead, fibronectin adsorbs as isolated molecules or as a monolayer. An active force is apparently required to unfold the protein domains in order to initiate fibrillogenesis.

One hypothesis for the mechanism of fibronectin molecular unfolding and fibrillogenesis is that high substrate surface electrical charge densities may be sufficient to initiate this process. While fibronectin supports a net negative charge density at neutral pH, like most proteins, fibronectin is polyampholytic, supporting both positive and negative charge groups. High charge density surfaces are capable of significantly deforming polyampholytes, thus influencing their adsorption properties. As estimates of cell surface charge density approach or exceed  $0.1 \text{ Coulombs/m}^2 \text{ (C/m}^2\text{)}$  appears to be sufficiently large electrostatic interactions at the cell surface to drive fibronectin unfolding. Thus, polystyrene sulfonated at levels covering a range including high charge density was synthesized.

To determine the extent to which the surface charge density of a substrate might influence fibronectin adsorption and fibril formation, sulfonated polystyrene surfaces on rigid silicon wafers were used to produce charge densities on the order

of those existing on cell surfaces. Degrees of sulfonation with charge densities ranging from 0 to  $0.15 \text{ C/m}^2$  were produced in aqueous solution. Atomic force microscopy of adsorbed fibronectin morphology demonstrated that a high charge density surface is sufficient to induce fibronectin fibrillogenesis. (Figure II-6).

Each percentage of sulfonation yields a  $0.0065 \text{ Coulomb/m}^2$  charge density. Sulfonation levels of 0-23% provided surface charge densities ranging from 0 to  $-0.15 \text{ C/m}^2$ .

Following 48 hours of adsorption, the total mass of adsorbed fibronectin was found to be essentially independent of surface charge density for densities up to  $0.03 \text{ C/m}^2$ . No significant differences in total fibronectin adsorption as found between pure PS surfaces (i.e. essentially zero charge density surfaces), PD, or TCPS. (Figure II-6). A total protein adsorption of approximately  $20 \text{ ng/mm}^2$  was observed in this range. At a charge density of  $0.03 \text{ C/m}^2$ , total protein adsorption was increased significantly over levels observed on native PS, this represented approximately a 50% increase to  $30 \text{ ng/mm}^2$ . Accompanying increasing surface charge density, fibronectin adsorption entered a transition region where the total adsorbed fibronectin increased significantly with small increases in surface charge density. At a charge density of  $0.15 \text{ C/m}^2$  total protein adsorption increases eight-fold, to over  $160 \text{ ng/mm}^2$ . Adsorption over the full experimental charge density range ( $10^{-7} - 0.15 \text{ C/m}^2$ ) closely follows an exponential dependence on charge density.

Increased surface charge density induced not only a rapid increase in the mass of fibronectin adsorption, but also a dramatic change in adsorbed protein morphology. Adsorbed protein surfaces on a pure polystyrene surface (charge density  $\sigma \sim 10^{-7} \text{ C/m}^2$ ) showed evidence of only a uniform adsorption layer of fibronectin. Fibronectin appeared in a globular form on  $0.03 \text{ C/m}^2$  as well as on  $0.08 \text{ C/m}^2$  surfaces, though on the latter, globules of increased size and small fibril-like structures were observed. With increasing surface charge density a progressively more extensive fibrillar matrix of fibronectin was seen to evolve, such that at charge densities of  $0.12 \text{ C/m}^2$  and  $0.15 \text{ C/m}^2$  surfaces, the adsorbed fibronectin forms a distinct network. On the  $0.15 \text{ C/m}^2$  sulfonated surface, fibrils up to  $10 \mu\text{m}$  wide,  $40 \mu\text{m}$  long, and close to  $1 \mu\text{m}$  high could be found. The fibrillar structures are similar both to those assembled on cell surfaces *in vitro* and to those found to assemble on deformable biomimetic surfaces.

On the sulfonated polystyrene surfaces, the adsorbed protein appears to take on a distinctly different morphology. At the lowest sulfonated polystyrene surface charge density utilized (5%), the adsorbed fibronectin layer thickness was seen to double (to approximately  $60 \text{ nm}$ ) over that seen for native polystyrene, yet the total amount of adsorbed protein increased by only 50% (to approximately  $30 \text{ ng/mm}^2$ ), suggesting a less compact form on the adsorbed molecule on the surface. With further increases in surface charge density, the relationship between total adsorbed protein and protein layer thickness continued this pattern, such that on  $0.15 \text{ C/m}^2$

surfaces fibronectin layer thickness reached 675 nm, for a total adsorbed protein mass of 160 ng/mm<sup>2</sup>.

Our observation on the sulfonated polystyrene surface suggest that high charge density surfaces may be sufficient to initiate fibril formation by fibronectin molecules. Utilizing sulfonated polystyrene surface coating to produce controlled charge density substrates, it was shown that surface charge density does significantly affect the amount of adsorbed fibronectin onto the surface as well as significantly altering the adsorbed fibronectin conformation. At high surface charge densities ( $> \sim 0.1 \text{ C/m}^2$ ) spontaneous fibronectin fibrillogenesis is observed.

In the presence of the sulfonated polystyrene surface, the electric field created by the negative surface charge can polarize the molecule changing the protein conformation into a more elongated structure, exposing positive domains for adsorption and matrix formation. The adsorption of fibronectin to the negatively charged substrate can be thought of as largely electrostatic, the positive charge domains on the fibronectin molecule serving as the counter ions to the substrate charge. Because fibronectin supports an average net negative charge density close to  $0.025 \text{ C/m}^2$ , a four to five fold concentration of these domains above the surface would result in the creation of a new adsorption "surface" with a charge density exceeding  $0.1 \text{ C/m}^2$ . Thus, it is evident how increasing surface charge density can lead to the abrupt transition to multilayer adsorption.

At high surface charge densities, the created electric field would repel the negative domains and strongly attract the positive domains, leaving open and accessible the domains implicated in the fibrillogenesis process.

Moreover, the networks spontaneously formed are similar to the networks induced by the presence of cells when the surface charge densities initiating the network formation is comparable to the surface charge density of cell surfaces. This observation suggests that control of the surface charge density of biomaterials can play a critical role in regulating extracellular matrix self-organization.

### **Conclusion**

The polystyrene sulfonated at the range of 2-30 mole % was prepared successfully by homogeneous sulfonation with acetyl sulfate in dichloroethane. The sulfonation level can be controlled by adjusting the amount of acetyl sulfate.

Depending on sulfonation levels, sulfonated polystyrene can be dissolved in non-polar solvent, such as chloroform, partially polar solvent, such as mixture of chloroform/methanol, and polar solvent such as methanol and water, i.e. as expected, polystyrene with higher sulfonation level requiring more polar solvent

Copolymer ionomers were prepared by sulfonating the polystyrene and followed by neutralization of sulfonic acid groups with either sodium or rubidium.

These negative charged polystyrene serve as an important model surface for tissue engineering investigation.

## **2. Polystyrene with acetyl group**

### **Introduction**

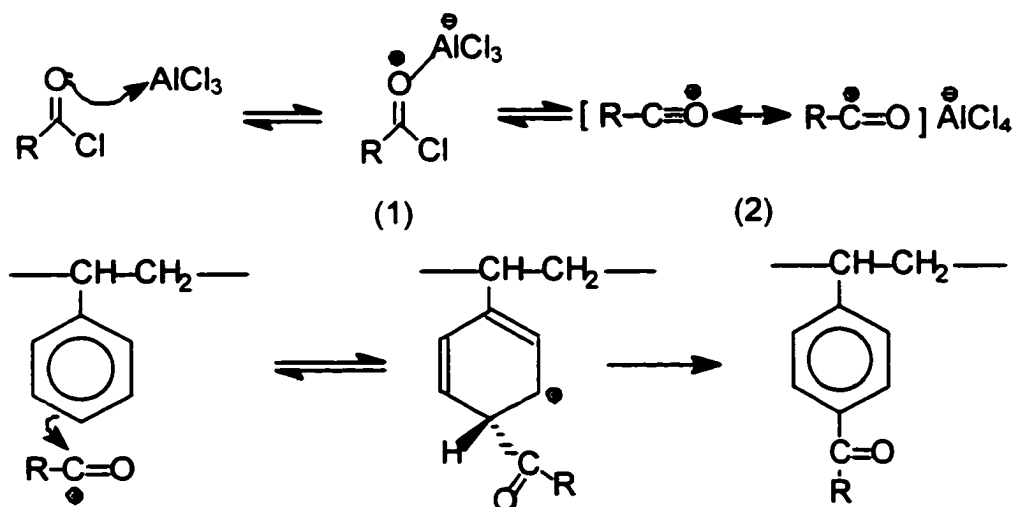
Only a few publications on acetylation of polystyrene are available. Results from a Chemical Abstracts (since 1970) search indicates only a modest interest in polystyrene with acetyl group.

Poly(4-acetylstyrene) can be prepared by Friedel-Crafts acylation of polystyrene with acetic chloride<sup>[33 - 36]</sup> or acetic anhydride as acetylating reagent with anhydrous aluminum chloride as a catalyst.

The mechanism of the Friedel-Crafts acylation reaction, formulated below for reaction using acid chloride, probably involves the acylium ion (2) as the reactive electrophilic species, although an electrophilic complex (1) between the acid chloride and aluminum chloride may also be involved.<sup>[37]</sup>

The use of aliphatic carboxylic anhydrides in place of the corresponding acid chloride offers many advantages including:

- (a) The greater ease of obtaining the anhydrides in a state of purity, and their availability as commercial products;
- (b) The handling of disagreeable acid chloride is avoided;



Scheme 2-5. Mechanism of acetylation of polystyrene through Friedel-Crafts reaction.

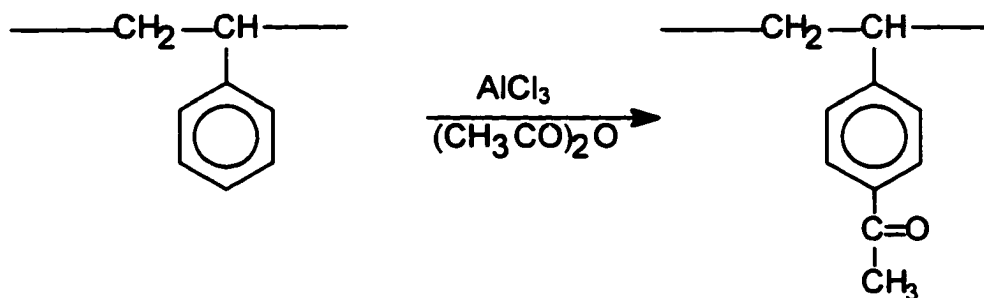
(c) The absence of any appreciable quantities of by-products and resinous substances:

(d) The reaction is smooth and the yield is generally good.

The acetylation of polystyrene in this work was carried out with acetic anhydride and the product was characterized using NMR.

## Experimental section

### 1). Synthesis - Acetylation of polystyrene



### Experimental procedure

Polystyrene (1.0g) was dissolved in 40 ml of  $\text{CCl}_4$  with  $\text{AlCl}_3$  in 100 ml-round flask to form a dark red solution. Acetic anhydride was added dropwise into the solution under stirring. The molar ratio of  $\text{AlCl}_3$  and anhydride was 1:1. The reaction was allowed to proceed at room temperature for 2 h and then the polymer product was precipitated in methanol and dried at a vacuum oven at  $40^\circ\text{C}$  for 24 h.

### 2). Structural characterization

The acetylation result of polystyrene was characterized with  $^1\text{H-NMR}$  spectroscopy and FT-IR spectrometry.

## Result and discussion

Acetylated polystyrene gives a characteristic  $-\text{CH}_3$  singlet in  $^1\text{H-NMR}$  spectrum at 2.60 ppm from acetyl group (Fig. 2-8). Calculation of the acetylating extent from the NMR spectra was based on the equation below:

$$\text{Acetylated units \%} = \frac{I_{2.60}}{I_{1.40} + I_{1.91}} \times 100$$

Where,  $I_{2.60}$ ,  $I_{1.40}$  and  $I_{1.91}$  are the integrated intensity of signal at 2.60 ppm from acetyl group and that of signal of 1.40 and 1.91 ppm from the hydrogen of backbone of polystyrene -  $\text{CH}_2$  -  $\text{CH}$  -.

The carbonyl group  $\text{C}=\text{O}$  in aryl ketone functionality of acetylated polystyrene has strong IR adsorption at  $1680\text{ cm}^{-1}$  (Figure 2-9).

## Conclusion

The partial acetylation of polystyrene was successfully carried out by the Friedel-Crafts acylation reaction.

The NMR and FT-IR spectra can be employed for structure characterization of acetylated polystyrene. The degree of acetylation of polystyrene can be determined through  $^1\text{H-NMR}$  data.

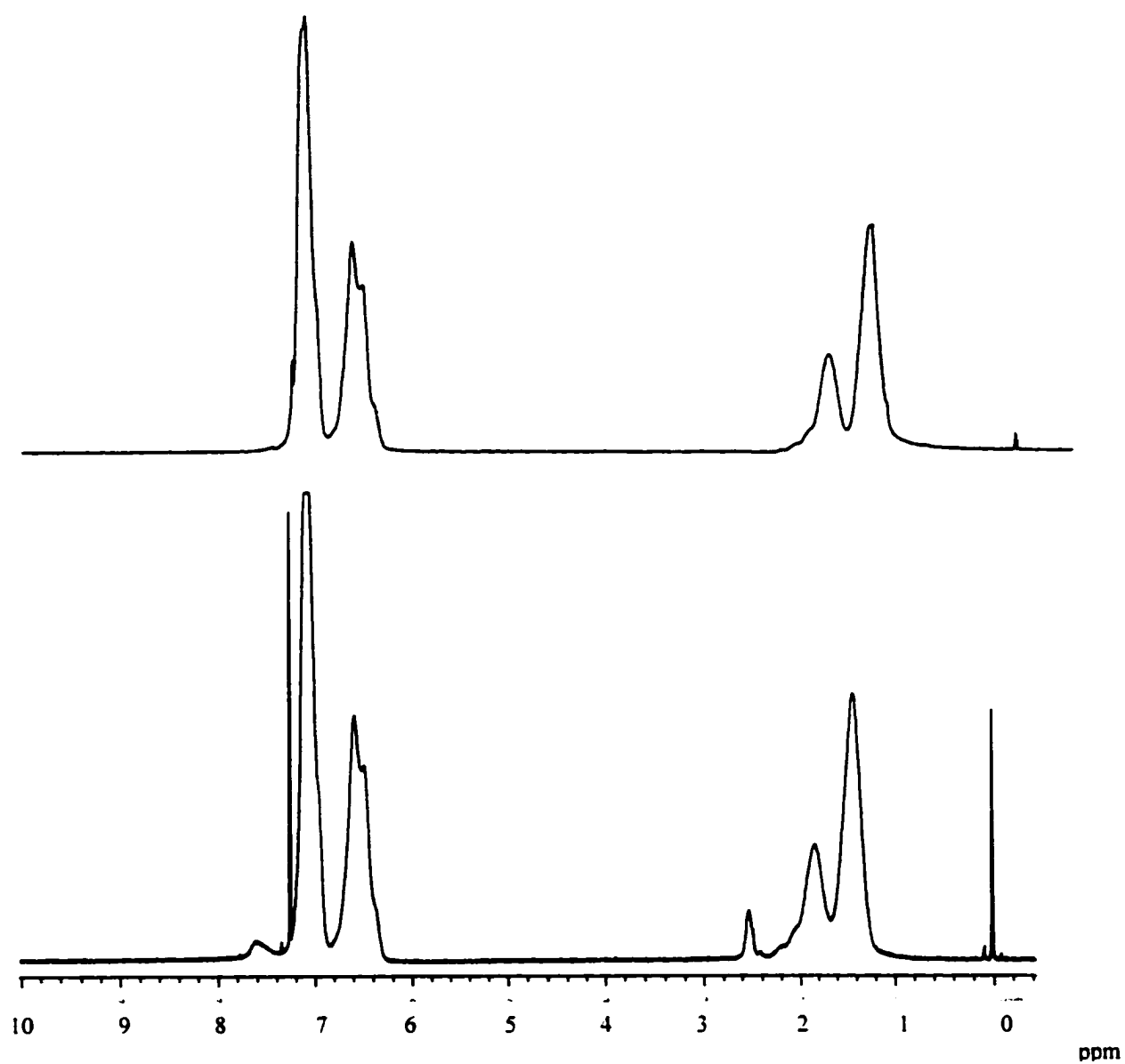


Figure 2-8.  $^1\text{H-NMR}$  spectra of acetylated polystyrene (7 mole %) and its original polystyrene (top).

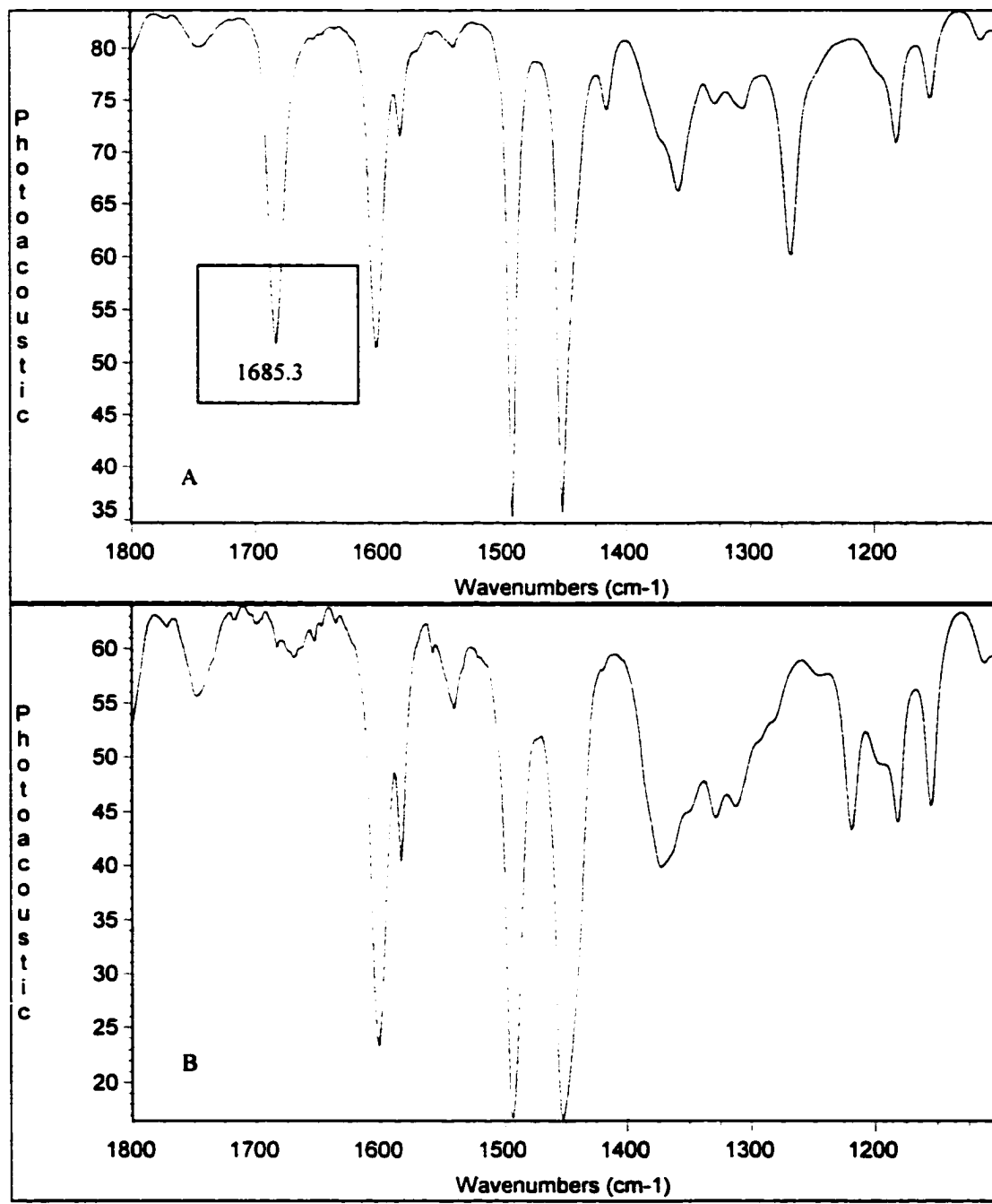


Figure 2-9. FT-IR spectra of acetylated polystyrene (A) and its original polystyrene( B)

### 3. Polystyrene with hydroxyl group

#### Introduction

Both poly-4-hydroxystyrene and poly-styrene-co-4-hydroxystyrene have been ones among the most attractive polymeric materials for years due to their significance in both fundamental research as well as and technological applications. Owing to the outstanding abilities of proton-donating and proton transfer from the phenolic hydroxyl to form hydrogen bonding with carbonyl-containing polymers and acid-base interaction with pyridyl unit-containing polymers. The polymers have also been widely used in the studies of polymer-polymer miscibility in blends<sup>[38,39]</sup>. In addition; the polymer has been extensively investigated as main component in both positive and negative photoresist systems<sup>[40,41]</sup>.

Polystyrene with hydroxyl group was prepared directly from monomer 4-vinylphenol in 1950's. Monomer, 4-vinylphenol, was prepared by a number of different methods<sup>[42-44]</sup>.

However, free-radical polymerization of 4-hydroxystyrene generally produces ill-defined, highly colored, low molecular weight polymer, mainly due to chain transfer and other side reactions (e.g. oxidation) of the phenolic hydroxyl.

In order to prepare high molecular weight poly(4-hydroxystyrene) and its styrene copolymer, many synthesis procedures have been developed, with the general strategy of protecting OH group during the (co)polymerization of 4-hydroxystyrene followed by transforming the resulting polymer to poly(4-hydroxystyrene) and its copolymer.

A number of protective groups have been employed for this purpose including acetyl,<sup>[45,46]</sup> *tert*-butoxycarbonyl,<sup>[47]</sup> trialkylsilyl,<sup>[48-51]</sup> and methyl.<sup>[52,53]</sup>

A large volume of publications about properties and applications of poly-4-hydroxystyrene and its copolymer with styrene has been published. The most interesting of investigation is on the interaction of -OH group with other functional group in the polymer-polymer blends.

Recently works of the miscibility of blends involved in poly-4-hydroxystyrene include:

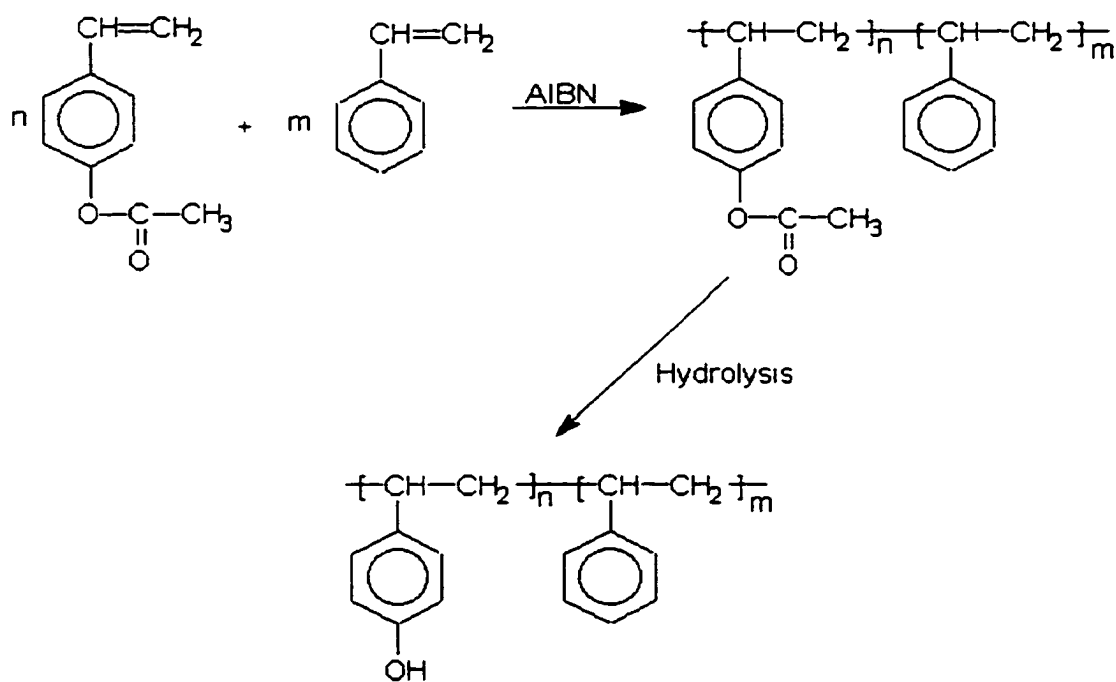
1. Miscibility of poly(1-vinylimidazole)/poly(4-hydroxystyrene) blends<sup>[54]</sup>;
2. Association equilibrium and miscibility in blends of poly(4-hydroxystyrene) with poly(hydroxybutyrate)<sup>[55,60]</sup>;
3. Miscibility of poly(styrene-co-vinylphenol)/poly(n-butyl methacrylate) by NMR<sup>[56]</sup>;
4. Phase behavior of blends of poly(glutamates) with poly(vinylphenol)<sup>[57]</sup>;
5. Hydrogen bonding blends of poly(4-vinylphenol) with poly(butyl methacrylate), or poly(butyl acrylate), or poly(vinyl butylether)<sup>[58]</sup>;

6. Crystallization of poly(ethylene oxide) in binary blends containing poly(p-vinylphenol) <sup>[59,63]</sup>;
7. Miscibility of poly(p-vinylphenol) with poly(dialkyl itaconate) and poly(methoxycarbonylmethyl methacrylate) <sup>[61]</sup>;
8. Miscibility and inter-polymer hydrogen bonding of poly(methyl acrylate)/poly(vinylphenol) by 2-D <sup>1</sup>H-<sup>13</sup>C NMR <sup>[64]</sup>;
9. IR and thermal analysis of blend of poly(vinyl methyl ether) with an ethyl methacrylate-co-4-vinylphenol copolymer <sup>[65]</sup>;
10. Melting behavior and miscibility of nylon-6/poly(4-hydroxystyrene) <sup>[67]</sup>;
11. Miscibility of Poly(methyl methacrylate) <sup>[45,68,69]</sup>;
12. Compatibility of copolymer containing styrene, 4-hydroxystyrene and 4-pyridine <sup>[47]</sup>;
13. Thermodynamics of hydrogen bonding in blends of poly(vinylphenol) with poly(vinyl acetate), or poly-ethylene-co-vinyl acetate, or poly(caprolactone), or polyacrylates <sup>[39]</sup>.

The copolymer containing 4-hydroxystyrene can not be prepared directly through the copolymerization of 4-hydroxystyrene with other monomer, because of the chain transfer reaction of 4-hydroxystyrene, leading to low molecular weight product with color. <sup>[72]</sup> Practically, protected 4-hydroxystyrene was used for synthesis of copolymers with hydroxyl group, which could be recovered through hydrolysis.

## Experimental section

### Synthesis route - copolymerization and hydrolysis



Scheme 2-6. Preparation of polystyrene with *p*-hydroxyl group.

## **Experimental procedure**

### **1). Polymerization.**

Acetoxystyrene and styrene with the required ratios were added to a 100-ml three-necked round flask with 20 ml of solvent ( benzene, or toluene, or dioxane) under a slow flowing nitrogen stream. A radical initiator, azobisisobutylnitrile was added under stirring and the polymerization was allowed to proceed at a temperature of 60 °C and a reaction time of 4 h for copolymerization and 16 h for homopolymerization. The polymer products were precipitated from methanol. The polymer molecular mass is ca.  $2.0 \times 10^4$  g/mole determined by GPC.

To obtain the copolymer with high molecular weight, the polymerization temperature should be lowered to 50 °C with the polymerization time extended longer to 48 h. Benzene is used as solvent, because of its low chain transfer constant. The molecular mass of copolymer is about  $2.0 \times 10^5$  g/mole.

### **2). Hydrolysis.**

The best way to hydrolyze the acetyl group of the copolymer is to use the hydrazine as a hydrolysis reagent and tetrahydrofuran as solvent, because the polar THF can dissolve the polymer and can be mixed with the hydrazine hydrate.

The copolymer of acetoxyl styrene and styrene was separated from benzene through precipitation with methanol and then air dried for a few hours, followed by

dissolving in THF. Hydrazine hydrate was added dropwise into the solution under stirring at room temperature overnight. HCl was then added to neutralize the reaction solution and then methanol was used to precipitate the polymer.

### 3) Structure characterization

The  $^1\text{H-NMR}$  and IR were employed for characterizing the polystyrene-*co-p*-acetoxystyrene and polystyrene-*co-p*-hydroxystyrene.

## Results and discussion

The  $^1\text{H-NMR}$  signal of hydrogen of hydroxyl group is broad and was not used for calculating the amount of hydroxy styrene( Figure 2-10-B). Therefore, the amount of *p*-hydroxystyrene was determined by  $^1\text{H-NMR}$  spectrum of copolymer before hydrolysis. The figure 2-9-C represents the  $^1\text{H-NMR}$  spectrum of unhydrolyzed poly(acetoxy styrene-*co*-styrene).

Acetoxystyrene unit gives a characteristic  $-\text{COCH}_3$  singlet in  $^1\text{H-NMR}$  spectrum at 2.30 ppm, which is different from acetyl group (Fig. 2-8). Calculation of the hydroxyl extent from the NMR spectra was based on the equation below:

$$\text{Hydroxyl units \%} = \left[ \frac{I_{2.30}}{I_{1.40} + I_{1.91}} \times 100 \right]_{\text{unhydrolyzed}} - \left[ \frac{I_{2.30}}{I_{1.40} + I_{1.91}} \times 100 \right]_{\text{hydrolyzed}}$$

where,  $I_{2.30}$ ,  $I_{1.40}$  and  $I_{1.91}$  are the integrated intensity of signal at 2.30 ppm from acetyl group and that of signal of 1.40 and 1.91 ppm from the hydrogen of backbone of polystyrene - CH<sub>2</sub> - CH -.

Figure 2-11 shows an IR spectrum of poly (hydroxy styrene). From IR spectrum of the hydrolyzed product gave strong absorption peak of hydrogen-bonding of hydroxyl groups.

### **Conclusion**

The polystyrene with partial hydroxyl functional group was prepared successfully through radical polymerization of styrene and acetoxystyrene and then ester hydrolysis of acetoxystyrene units.

The quantitative characterization of hydroxyl group can be completed through calculation of the integrated intensity of proton NMR signal of the acetyl group of acetoxystyrene unit in original copolymer and hydrolysis product.

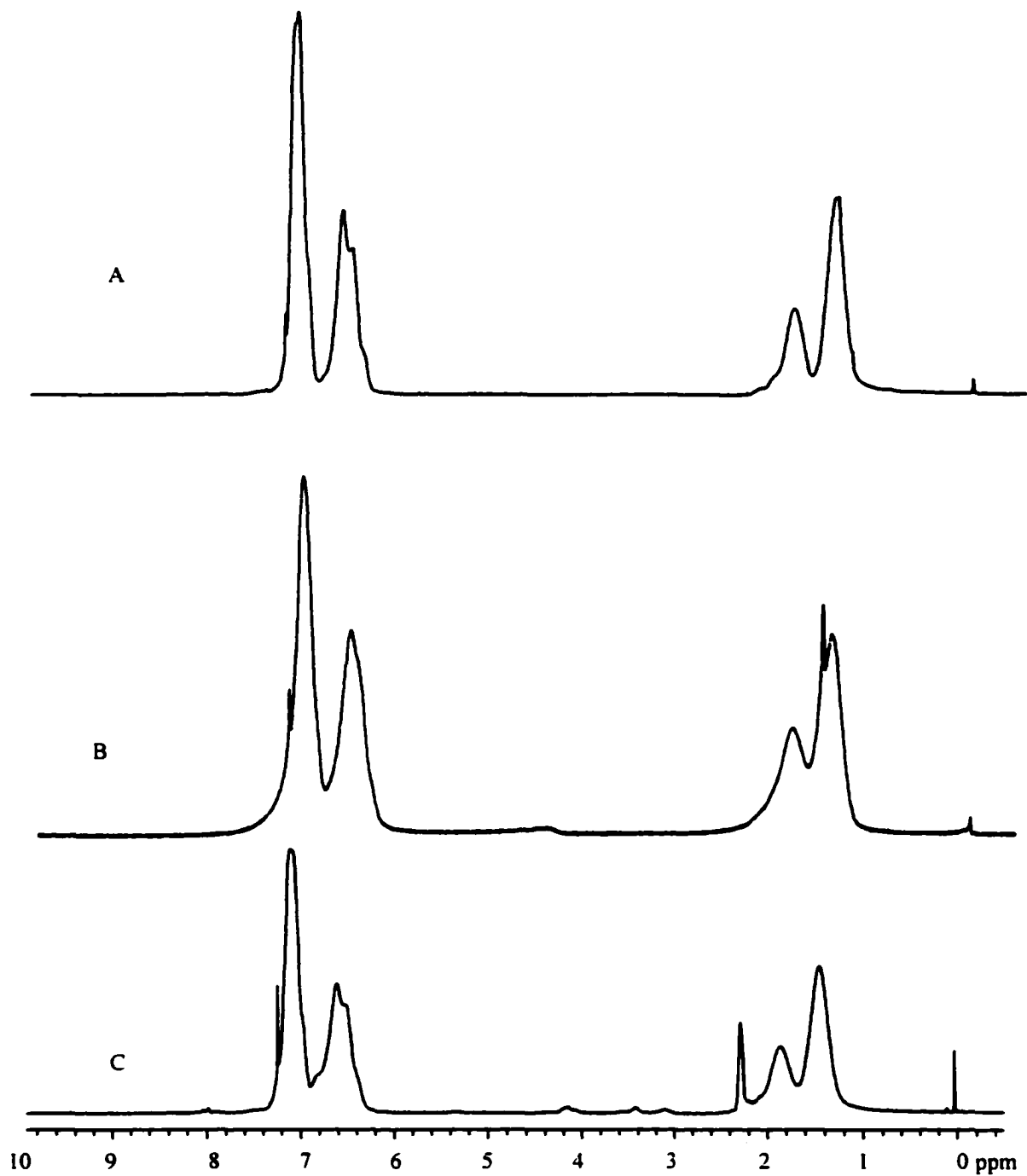


Figure 2-10.  $^1\text{H-NMR}$  spectra of polystyrene (A), poly-styrene-co-4-acetoxystyrene(C) and polystyrene-co-4-hydroxystyrene (10 mole %)(B).

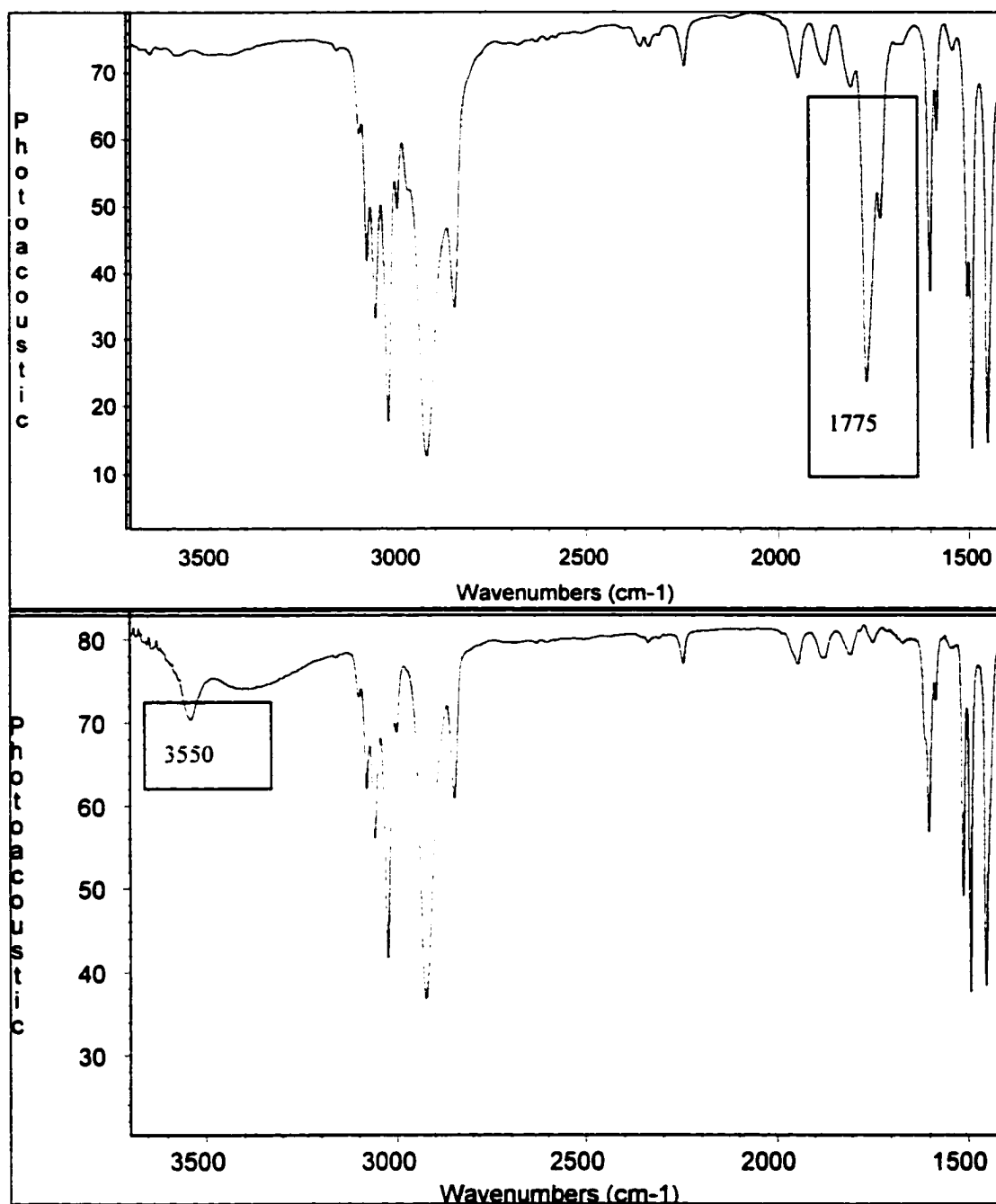


Figure 2-11. FT-IR spectra of polystyrene-co-4-acetoxystyrene (A) and its hydrolyzed product, polystyrene-co-4-hydroxystyrene (B)

### **Chapter 3.**

## **Polymethacrylate with POSS Side Group by Atom Transfer Radical Polymerization, ATRP**

### **Introduction**

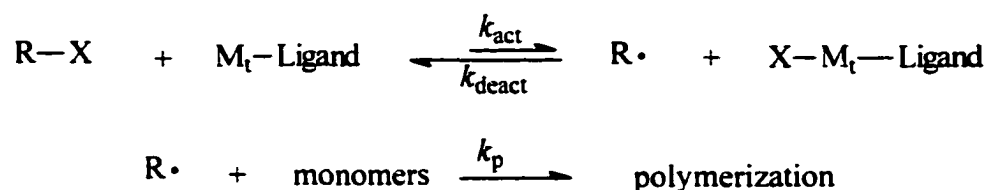
Polyhedral oligomeric silsesquioxane, POSS, is an interesting building unit for organic-inorganic hybrid materials, in which the incorporated inorganic segment is expected to lead to unusual properties. POSS molecules, first reported in 1946, have a cage-like structure with a polyhedral silicon-oxygen nanostructured skeleton. The major advantage of POSS copolymers is that a variety of substituents can be incorporated, thereby providing a large number of chemical functionalities attached to the chain. These attachments contribute only to the enthalpy of the chain interaction without changing the entropic interactions at the interface. This is in contrast to graft copolymers with long grafts, which have also been shown to be effective compatibilizers at low grafting densities. As the number of grafts is increased, however, the large unfavorable entropy quickly overcame enthalpic gains and the interfacial tension actually increases thereby enhancing phase segregation <sup>[1]</sup>.

POSS copolymers are now used in various applications ranging from windshields to flame retardant polymer composites. Since these applications frequently require blending or interfacial adhesion with other polymers, it is important to understand the effect of the POSS on the miscibility of polymer blends. For this purpose, random copolymers, containing POSS units, with narrow molecular weight distribution are desirable.

The synthesis of polymers with well-defined compositions, architectures, and functionalities has long been of great interest in polymer chemistry. The preparation of random polymethacrylate with POSS side group having narrow dispersity of chain size has not been reported before. For controlled molecular weight distribution, living polymerization techniques typically are employed where the polymerization proceeds in the absence of irreversible chain transfer and chain termination. Much of the academic and industrial research on living polymerization has been focused on anionic, cationic, coordination, ring-opening polymerization and controlled/living radical polymerization methods<sup>[2]</sup>.

Among living radical polymerization methods, atom transfer radical polymerization (ATRP) has been studied extensively recently<sup>[2]</sup>. ATRP has been successful in controlling polymerization of styrene<sup>[3-9]</sup>, acrylate<sup>[10-12]</sup>, and methacrylate<sup>[13-24]</sup> and several other relatively reactive monomers such as acrylamide, vinylpyridine, and acrylonitrile. As a multicomponent system, ATRP is composed of the monomer, an initiator with a transferable (pseudo) halogen, and a catalyst (composed of a transition metal species with any suitable ligand). In some

cases an additive is used. For a successful ATRP, other factors, such as solvent and temperature, must also be optimized.

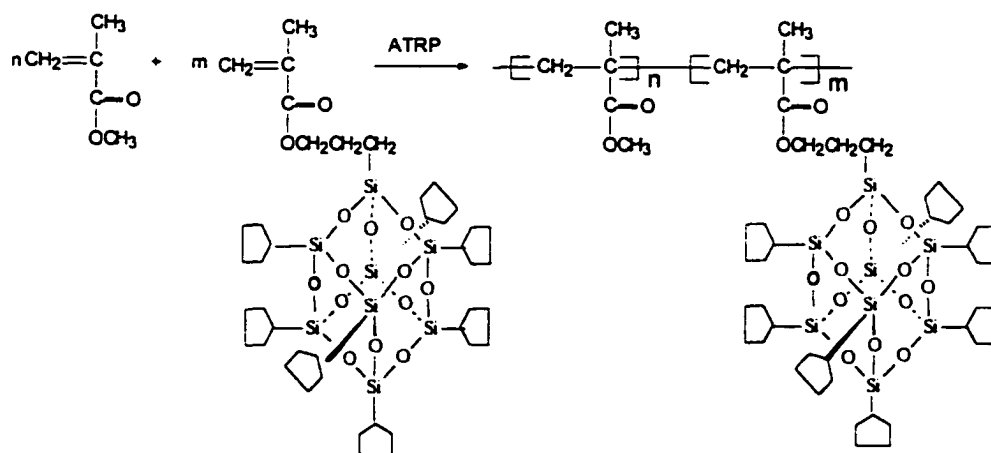


Scheme 3-1. Transition-metal-catalyzed ATRP

A general mechanism for ATRP is depicted in Scheme 3-1. The radicals, or the active species, are generated through a reversible redox process catalyzed by a transition metal complex ( $\text{M}_t^n\text{-Ligand}$ ,) undergoing a one-electron oxidation with concomitant abstraction of a (pseudo) halogen atom, X, from a dormant species, R-X. This process occurs with a rate constant of activation,  $k_{\text{act}}$ , and deactivation,  $k_{\text{deact}}$ . Polymer chains grow by the addition of the intermediate radicals to monomers with the rate constant of propagation,  $k_p$ , in a manner similar to a conventional radical polymerization. Termination reactions can also occur in ATRP, mainly through radical coupling and disproportionation

Pyun J. <sup>[25]</sup> *et al.* prepared the homopolymer and block polymers from polyhedral oligomeric silsesquioxane monomer using ATRP method with 4-methylphenyl 2-bromoisobutyrate as initiator.

In this work, a random copolymer of methyl methacrylate and 3-(3, 5, 7, 9, 11, 13, 15-heptacyclopentylpentacyclo [9. 5. 1.<sup>3,9</sup>. 1<sup>5,15</sup>. 1<sup>7,13</sup>] octasiloxa-1-nyl) propyl methacrylate (POSS-propyl methacrylate) was synthesized through atom transfer radical polymerization.



Scheme 3-2. Copolymerization of methyl methacrylate and POSS-propyl methacrylate.

### Synthesis procedure

Methyl methacrylate was stirred over calcium hydride for 24 h and vacuum distilled. Toluene was stirred over sodium for 24 h. and distilled. 3-(3, 5,7, 9, 11, 13, 15-heptacyclopentylpentacyclo [9. 5. 1.<sup>3,9</sup>. 1<sup>5,15</sup>. 1<sup>7,13</sup>] octasiloxa-1-nyl) propyl methacrylate (POSS-propylmethacrylate), copper (I) chloride, N, N, N', N', N"-pentamethyldiethylenetriamine (PMDETA) and ethyl 2-bromoisobutyrate were purchased from Aldrich co. and used without purification.

Methyl methacrylate (2.92 g, 29.2 mmol.) and POSS-propylmethacrylate (0.3 g 0.292 mmol for 1 mole % of POSS; 0.6 g, 0.584 mmol for 2 mole % of POSS.) were placed in a vial with a magnetic stirring bar, followed by addition of purified toluene (3.0 g) to dissolve the monomers. The solution was bubbled slowly with nitrogen for about 1 min. and capped. Cu (I) Cl (0.0058 g, 0.058 mmol) and PMDETA (0.048 g, 0.34 mmol) were added into the vial under N<sub>2</sub>. The solution turned blue after stirring for about 20 min. Then, 8.5 µl of initiator and ethyl 2-bromoisobutyrate (0.058 mmol.) were added to the solution under N<sub>2</sub>. The vial cap was sealed with parafilm. The reaction solution was stirred 10 min at room temperature and then heated to 60 °C for 24h in an oil bath. The solution was then kept at 80 °C for desired polymerization time, usually 24 h or longer. The conversion of polymerization was controlled under 80 % to avoid radical coupling reaction.

The copolymer was precipitated in methanol and then dissolved in chloroform and reprecipitated at least twice in cyclohexane to remove unreacted POSS monomer and twice in methanol to remove transition metal catalyst. This purification procedure was continued until copolymer appeared white and no NMR signal of  $\text{CH}=\text{C}$  was present.

### **Results and discussion**

In order to avoid the coupling of radicals, the polymerization conversion of the monomers should be controlled below 80 %.  $^1\text{H-NMR}$  was employed for tracking conversion of the living polymerization using chemical shifts of methyl,  $-\text{OCH}_3$ , of MMA at 3.8 ppm for monomer and 3.6 ppm for polymer (Figure 3-1). From the integral ratio of both signals, the conversion of monomer was calculated.

Figure 3-2 shown the  $^1\text{H-NMR}$  spectrum of purified random copolymer of methyl methacrylate and POSS-propyl methacrylate.

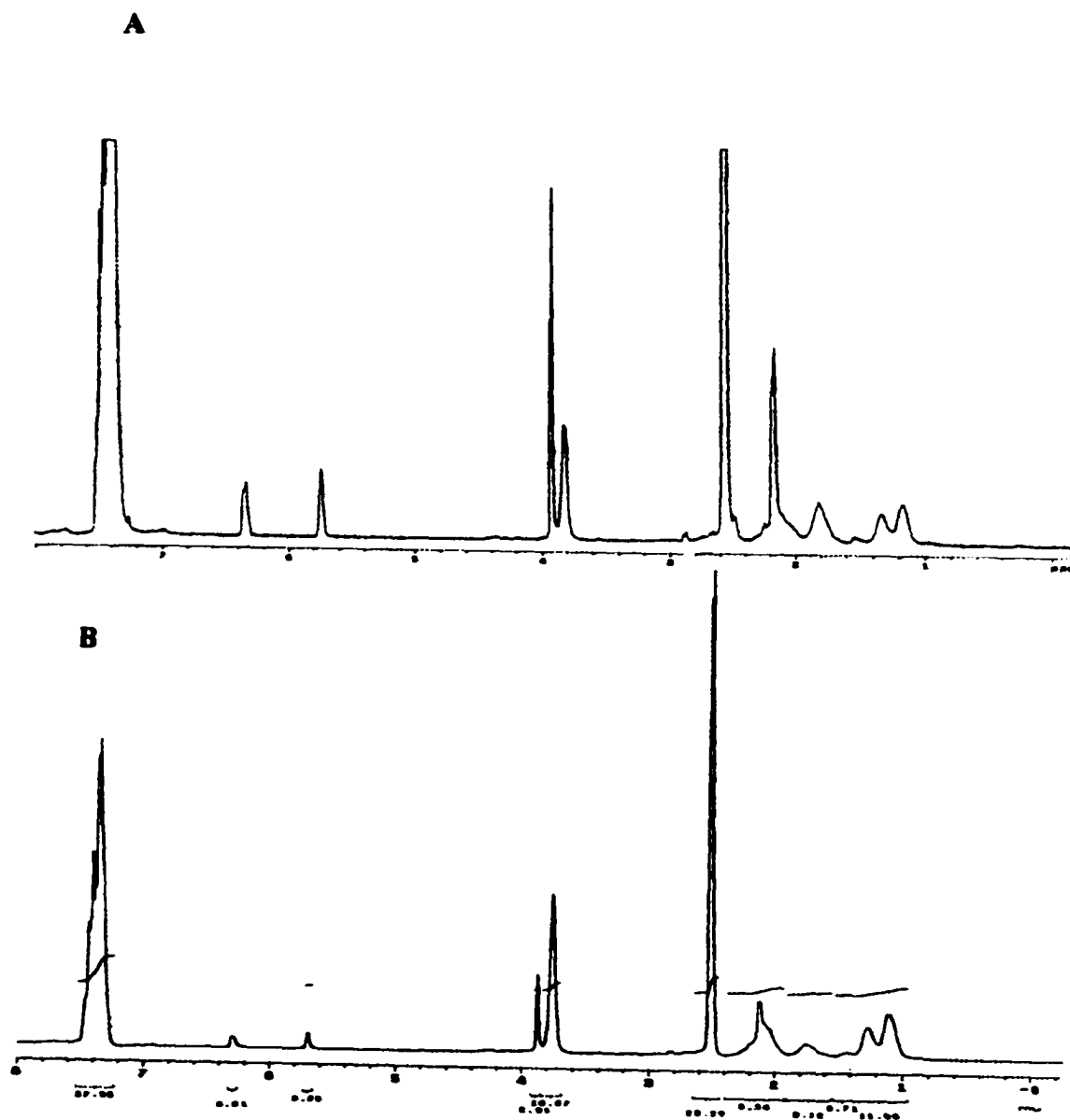


**Figure 3-1.**  $^1\text{H-NMR}$  spectra of ATRP copolymerization solution of methyl methacrylate and propyl-POSS methacrylate (toluene as solvent, A is that after 36 h; and B is that after 72 h)

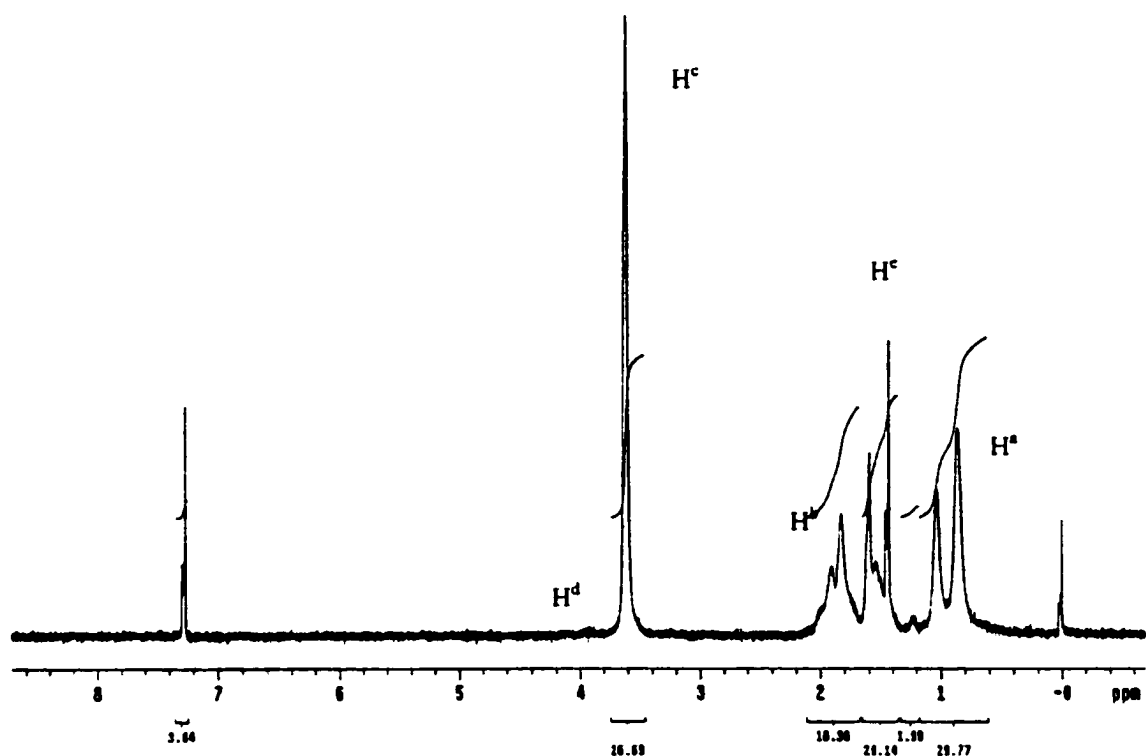
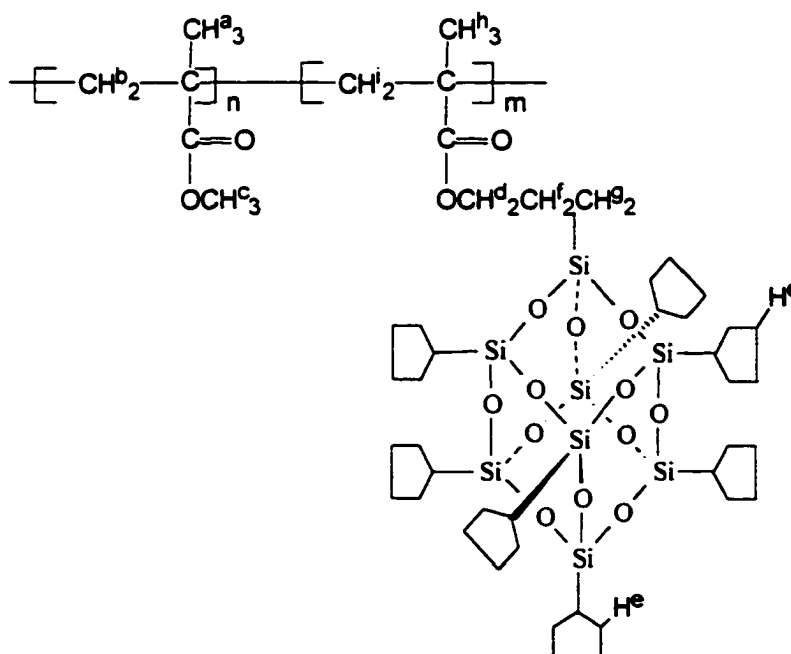


Figure 3-2.  $^1\text{H-NMR}$  spectrum of random copolymer of methyl methacrylate and POSS-propyl methacrylate ( 3 mole %).

The chemical shift of H<sup>a</sup>, H<sup>b</sup> and H<sup>c</sup> of  $\alpha$ -methyl, methylene and methyl of methyl methacrylate are ca 1.0 ppm, 1.9 ppm and 3.6 ppm, respectively, according to the reference on homopolymer of MMA<sup>[26]</sup>. H<sup>a</sup> gives detail three signals at 0.91 ppm, 1.05 ppm and 1.22 ppm from syndiotactic, heterotactic and isotactic microstructures. For POSS-propyl methacrylate unit, however, only chemical shift of hydrogen of cyclopentyl on POSS site of POSS-propyl methacrylate can be observed at 2.5 ppm. The H<sup>d</sup> of propyl gives a weak signal at 3.90 ppm; the signals of H<sup>f</sup> and H<sup>g</sup> of propyl, H<sup>i</sup> of methylene and H<sup>h</sup> of  $\alpha$ -methyl of POSS were covered by the signals of MMA.



The molecular weight and molecular weight distribution was determined by GPC, used linear polystyrene as standard. The GPC results were listed in table 1.

Table 3-1. The GPC results of copolymers (polystyrene as standard.)

Samples	Mw	Mn	Mw/Mn
MMA-POSS#1	28.3K	22.8K	1.24
MMA-POSS#2(36 hr)	12.4K	10.5K	1.18
MMA-POSS#2( 72 hr)	27.1K	22.6K	1.20
MMA-POSS#3( 120 hr)	35.0K	26.1K	1.34
MMA-POSS#4( 1 week)	34.9K	23.7K	1.47

The GPC results indicated that ATRP is a living radical polymerization process and gave narrow distribution products when the polymerization conversion of monomers was below 80 % (1.18-1.24, for conversion below 50 %). But the molecular weight distribution became broader if polymerization was over-extended and the conversion of monomer was higher than 80 %, due to increased coupling reaction of living radicals. Figure 3-3 shown a GPC spectrum for the copolymer containing 2 mole % POSS units.

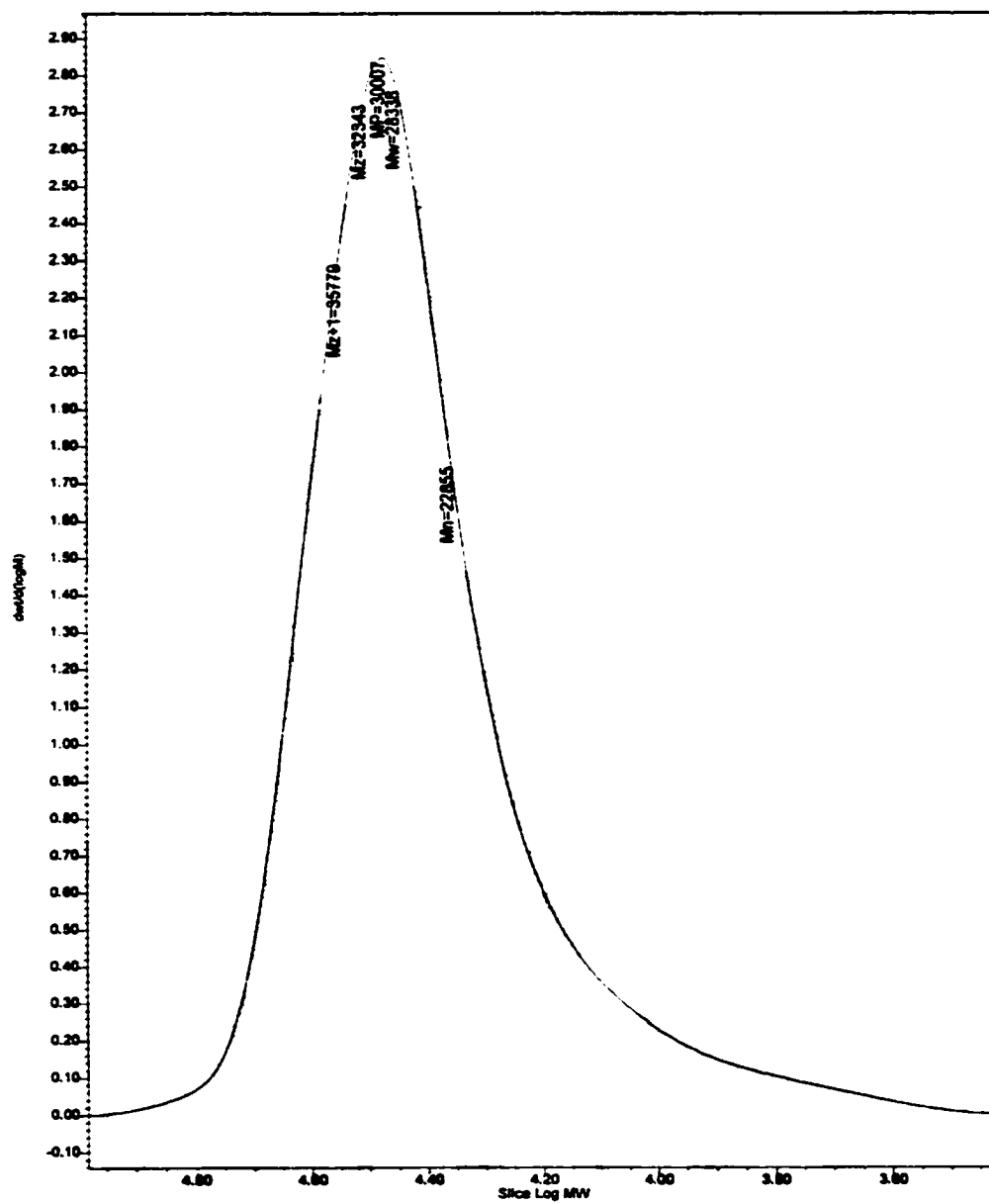


Figure 3-3. GPC chromatogram of copolymer of methyl methacrylate and propyl-POSS methyl methacrylate (2 mole %).

**Polymethacrylate with POSS side group as a compatibilizer  
for Polystyrene/ Poly(methyl methacrylate) Blend<sup>[27]</sup>**

The polymethacrylate with POSS side group having narrow molecular weight distribution from ATRP was examined as a compatibilizer for polystyrene/poly(methyl methacrylate) blend. The results showed these copolymers could be very efficient at compatibilizing immiscible polymer blends. Compatibilization only occurred if the POSS was grafted onto the backbone and favorable interaction existed between the POSS functional groups and the PS homopolymers. To study the effects on miscibility, we used POSS molecules having seven cyclopentyl groups. Cyclopentyl interacts more favorably with PS than PMMA, hence increasing the favorable enthalpy component. We therefore compare the effects on interfacial properties when cyclopentyl POSS is introduced as individual particles or grafted onto high and low  $M_w$  PMMA backbones. Contact angles for the blends were studied.

The results are plotted in Figure 3-4 in terms of interfacial tension ( $\gamma$ ), where we see that  $\gamma$  decreases by 20% or more with the grafting of little as 10% cyclopentyl-POSS onto the PMMA backbone. Addition of free particles on the other hand has no effect on the surface tension. On the basis of these data, we can make the qualitative model depicted in Figure 3-5.

PS and PMMA are immiscible for the molecular weights used here. When POSS is grafted onto the PMMA, the POSS functionalities can interact separately

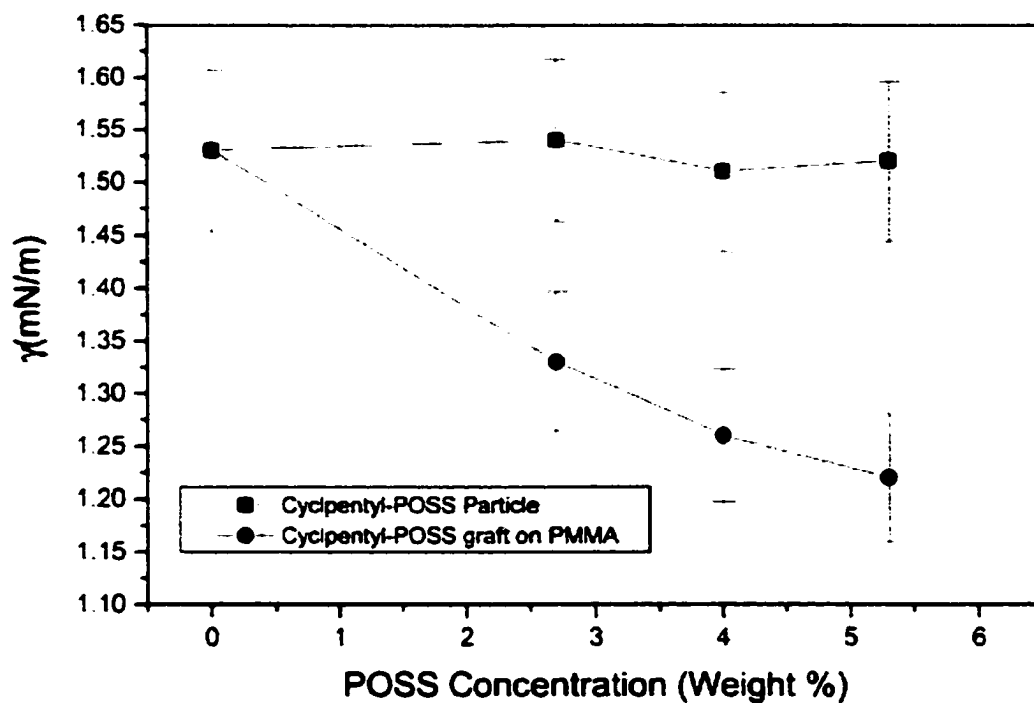


Figure 3-4 Interfacial tension calculated from observed contact angles as a function of POSS concentrations. Note that the POSS can be either grafted onto the PMMA backbone (dot) or introduced as unbound particles (squares).<sup>[27]</sup>

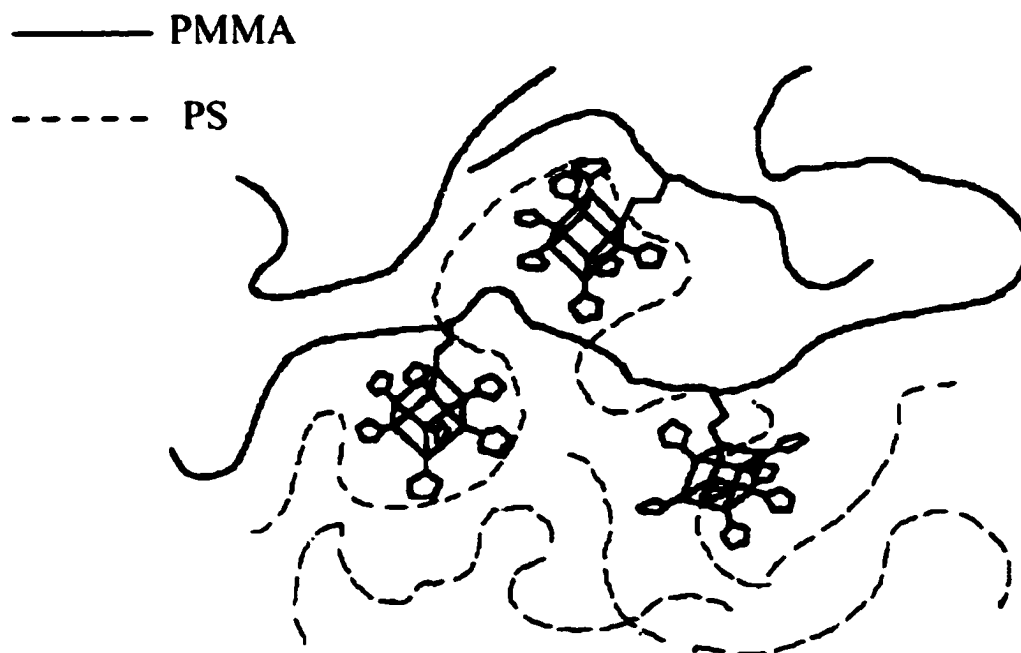


Figure 3-5. Schematic of PMMA (solid) and PS (dashed) chains in a blend when functionalized POSS is grafted onto the PMMA chains. In this case, the functional groups (cyclopentyl) interact more favorably with the PS than the PMMA monomers. <sup>[27]</sup>

with the PS homopolymers. If the interactions are favorable and then if sufficient functional groups are present on the chain, the unfavorable interactions between the PS and PMMA monomers can be overcome and commingling can result between the chains. Conversely, if the interactions with the R group are unfavorable, phase segregation of the polymers may even be slightly enhanced. Hence, for this mechanism to work it is important for the particles to be attached to the backbone. Otherwise, since the interaction between particles is always more favorable than that of at least one of the components, particle aggregation will occur and the polymer phase separation will not be affected.

### Conclusion

Random copolymers based on polyhedral oligomeric silsesquioxanes, i.e., methyl methacrylate (MMA) and 3-(3, 5,7, 9, 11, 13, 15-heptacyclopentylpentacyclo [9. 5. 1.<sup>3.9</sup>. 1<sup>5.15</sup>. 1<sup>7.13</sup>] octasiloxa-1-nyl) propyl methacrylate (POSS-propyl methacrylate) were prepared through atom transfer radical polymerization. Narrow molecular weight distribution products (PD: 1.18-1.24) were obtained when the polymerization conversion was below 50 %. The molecular weight distribution became broader with the higher conversion.

Polymethacrylate with POSS side group having low chain size dispersity was established as a very efficient compatibilizer for polystyrene/ poly (methyl methacrylate) blend.

## Bibliography

### Chapter 1.

- [1] Bassler, H.; Schweitzer, B.; *Acc. Chem. Res.* **1999**, *32*, 173.
- [2] Ahn, T.; Jang, M. S.; Shim, H.-K.; Hwang, D.-H.; Zyung, T.; *Macromolecules* **1999**, *32*, 3279.
- [3] Ahn, T.; Song, S.-Y.; Shim, H.-K.; *Macromolecules* **2000**, *33*, 6764.
- [4] Remmers, M.; Neher, D.; Gruner, J.; Friend, R. H.; Gelinck, G. H.; Warman, J. M.; Quattrocchi, C.; dos Santos, D. A.; Bredas, J.-L.; *Macromolecules* **1996**, *29*, 7432.
- [5] Meng, H.; Yu, W.-L.; Huang, W.; *Macromolecules* **1999**, *32*, 8841.
- [6] Kim, Y.; Kwon, S.; Yoo, D.; Rubner, M. F.; Wrighton, M. S.; *Chem. Mater.* **1997**, *9*, 2699.
- [7] Zhang, X.; Jenekhe, S. A.; *Macromolecules* **2000**, *33*, 2069.
- [8] Shim, H. K.; Kang, I. N.; Jang, M. S.; Zyung, T.; Jung, S. D.; *Macromolecules* **1997**, *30*, 7749.
- [9] Peeters, E.; Christiaans, M. P. T.; Janssen, R. A. J.; Schoo, H. F. M.; Dekkers, H. P. J. M.; Meijer, E. W.; *J. Am. Chem. Soc.* **1997**, *119*, 9909.
- [10] Tarkka, R. M.; Zhang, X.; Jenekhe, S. A.; *J. Am. Chem. Soc.* **1996**, *118*, 9438.

- [11] Jenekhe, S. A.; Zhang, X.; Chen, X. L.; Choong, V.-E.; Gao, Y.; Hsieh, B. R.; *Chemi. Mater.* **1997**, *9*, 409.
- [12] Detriau, G.; *J.Chem. Phys.* **1936**, *33*, 620.
- [13] Pope, M.; Kallmann, H.P.; Magnantz, P.; *J. Chem. Phys.* **1977**, *38*, 2024.
- [14] Tang, C. W.; VanSlyke S. A.; *Appl. Phys. Lett.* **1987**, *51*, 913.
- [15] Kido, J.; Kimura, M.; Nagai, K.; *Science* **1995**, *267*, 1332.
- [16] Sheats, J. R.; Antoniadis, H.; Hueschen, M.; Leonard, W.; Miller, J.; Moon, R.; Roitman, D.; Stocking, A.; *Science* **1996**, *273*, 884.
- [17] Adachi, C.; Tsutsui, T.; Saito, S.; *Appl. Phys. Lett.* **1989**, *55*, 1489.
- [18] Adachi, C.; Nagai, K.; Tamoto, N.; *Appl. Phys. Lett.* **1995**, *66*, 2679.
- [19] Matsumura, M.; Akai, T.; Saito, M.; Kimura, T.; *J. Appl. Phys.* **1996**, *79*, 264.
- [20] Adachi, C.; Tsutsui T. and Saito S.; *Appl. Phys. Lett.* **1990**, *56*, 799.
- [21] J.kido; K. Nagai; Y. Okamoto; T. Skoheim; *Chemistry Letters ( Chem. Soc. Japan)* **1991**,1267.
- [22] T. Fujii; M.Fujita; Y. Hamada; K. Shibata; Y. Tsujino; K. Kuroki; *J. Photopolym. Sci. Technol.* **1991**, *4*,135.
- [23] Takahashi, Y.; Iijima, M.; Oishi, Y.; Kamimoto, M.; Imai, Y.; *Macromolecules* **1991**, *24*, 3543.
- [24] J. Kido; K. Okuyama; K. Nagai; *Appl. Phys. Lett.* **1992**, *61*, 761.
- [25] Wen, W.-K.; Jou, J.-H.; Wu, H.-S.; Cheng, C.-L.; *Macromolecules* **1998**, *31*, 6515.

- [26] Mori, Y.; *Organic Electroluminescent Material and Device*; Miyata, S., Nalwa, H. S., Eds.; Gordon and Breach Publishers: New York, **1997**; p 391.
- [27] Burroughes, J.H.; Bradley, D.D.C.; Brown, A. R.; Marks, R.N.; Mackay, K.; Friend, R. H.; Burnst P.L.; Holmes A.B.; *Nature*, **1990**, *347*, 539.
- [28] Nakano. T. ; Eur. Pat. Appl. EP 443861, Aug. 28, **1991**; CA 116:P71721k.
- [29] Braun, D.; Heeger,A.; *J. Appl. Phys.Lett.* **1991**, *58*, 1982.
- [30] Braun,D.; Heeger,A. J.; Kroemer, H.; *J. Electron. Mater.* **1991**, *20*, 945.
- [31] Burn, P. L.; Holmers,A.B.; Kraft, A.; Bradley, D.D.C.; Brown,A.R.; Friend,R.H.; *J. Chem. Soc. Chem. Commun.* **1992**, 32.
- [32] Burn, P. L.; Holmers,A.B.; Kraft, A.; Bradley, D.D.C.; Brown,A.R.; Friend,R.H.; Gymer, R.W. ; *Nature*, **1992**, *356*, 47.
- [33] Gustafsson,G.; Cao, Y.; Treacy G. M.; Klavetter, F.; Colaneri, N.; Gustafsson, G. *Nature*, **1992**, *357*, 477.
- [34] Braun,D.; Gustafsson,G; McBranch D. and Gustafsson,G.; *J. Appl. Phys.* **1992**, *72*, 564.
- [35] Ohmori, Y. Uchida,M., Muro, K. and Yoshino, K.; *Jpn. J. Appl. Phys.* **1991**, *30*, L1941.
- [36] Grem, G.; Leditzky, G.; Ullrich, B.; Leising, G.; *Adv. Mater.* **1992**, *4*, 36.
- [37] Bradley, D.D. C.; *Chem. Br.***1991**, *27*, 719.
- [38] Berggren. M.: Inganas. O.; Gustafsson. G.: Rasmusson. J.; Andersson. M. R.; Hjertberg. T.: Wennerstrom. O.; *Nature* **1994**, *372*, 444.
- [39] Schlueter. A.-D.; Wegner. G. ; *Acta PoJym.* **1993**, *44*, 59.

- [40] Wallow.T.I.; Novak.B.M.; *J. Am. Chem. Soc.* **1991**, *113*, 7411.
- [41] Connolly. M.; Karasz. F.; Trimmer. M.: *Macromolecules* **1995**, *28*, 1872.
- [42] Hillberer. A.; Brouwer. H. J.; Scheer. B. J.; Wildeman. J.; Hadzlioannou. G.;  
*Macromolecules* **1995**, *28*, 4525.
- [43] Z. Yang, I Sokolik ; F.E. Karasz, ; *Macromolecules* **1993**, *26*, 1188.
- [44] Sokolik,I.; Z. Yang; D. Morton; Karasz,F.E. ; *J. Appl. Phys.* **1993**, *74*, 3584.
- [45] Yang, Z.; Geise, H.J.,Karasz, F.E.; *Polymer* **1994**, *35*, 391.
- [46] Hu,B..Morton, D.C., Sokolik, I., Yang Z. Karasz, F.E.; *J. Luminescence* **1994**,  
*60&61*. 919.
- [47] Yang, Z., Hu, B., Karasz F. E.; *Macromolecules*, **1995**, *28*, 6165.
- [48] Ahn, T.; Jang, M. S.; Shim, H.-K.; Hwang, D.-H.; Zyung, T.; *Macromolecules*  
**1999**, *32*. 3279.
- [49] Kang, I.-N.; Hwang, D.-H.; Shim, H.-K.; Zyung, T.; Kim, J.-J.;  
*Macromolecules* **1996**, *29*. 165.
- [50] Sonoda, Y.; Kaeriyama, K.; *Bull. Chem. Soc. Jpn.* **1992**, *65*, 853.
- [51] Sonoda, Y.; Suzuki, Y.; Van Keuren, E.; Matsuda, H.; *Macromolecules* **1996**,  
*29*, 288.
- [52] Gurge, R. M.; Sarker, A.; Lahti, P. M.; Hu, B.; Karasz, F. E.; *Macromolecules*  
**1996**, *29*, 4287.
- [53] Gurge, R. M.; Sarker, A. M.; Lahti, P. M.; Hu, B.; Karasz, F. E.;  
*Macromolecules* **1997**, *30*, 8286.

- [54] Ahn, T.; Jang, M. S.; Shim, H.-K.; Hwang, D.-H.; Zyung, T.;  
*Macromolecules*, **1999**, *32*, 3279 .
- [55] Pasco, S. T.; Lahti, P. M.; Karasz, F. E.; *Macromolecules* **1999**, *32*, 6933.
- [56] Zheng, M.; Sarker, A. M.; Gurel, E. E.; Lahti, P. M.; Karasz, F. E.;  
*Macromolecules* **2000**, *33*, 7426.
- [57] Wittig, G.; *Pure Appl. Chem.* **1964**, *9*, 245.
- [58] Pope, M.; *Electronic Processes in Organic Crystals*; Oxford University press;  
Oxford, U.K.. **1982**.
- [59] Kido, J.; Kohada, M.; Nagai, K.; Okuyama, K.; *Appl. Phys. Lett.* **1992**, *61*,  
761.
- [60] Jerry March; *Advanced Organic Chemistry: Reaction Mechanism, and  
Structure*, McGraw-Hill Book Co. New York, pp702-709(**1968**)
- [61] Horner, Hoffman, and Wippel, ; *Chem.Ber.* **1958**, *91*, 61.
- [62] Harald Gunther; *NMR Spectroscopy*, 2<sup>nd</sup>, John Wiley & Sons, New York, **1995**
- [63] Y. Pang; J. Li; *Macromolecules* **1998**, *31*, 6730.

## **Chapter 2.**

- [1] Ladam, G.; Gergely, C.; Senger, B.; Decher, G.; Voegel, J.-C.; Schaaf, P.;  
Cuisinier, F. J. G.; *Biomacromolecules* **2000**, *1*, 674.
- [2] Kim, S. D.; Klein, A.; Sperling, L. H.; Boczar, E. M.; Bauer, B. J.;  
*Macromolecules* **2000**, *33*, 8334.
- [3] D. Huang; Y. Yang; G. Zhuang; Binyao Li ; *Macromolecules* **2000**, *33*, 461.

- [4] Mani, S.; Weiss, R. A.; Williams, C. E.; Hahn, S. F.; *Macromolecules* **1999**, *32*, 3663.
- [5] Orlor, E. B.; Gummaraju, R. V.; Calhoun, B. H.; Moore, R. B.; *Macromolecules* **1999**, *32*, 1180.
- [6] Chakrabarty, K.; Weiss, R. A.; Sehgal, A.; Seery, T. A. P.; *Macromolecules* **1998**, *31*, 7390.
- [7] Chakrabarty, K.; Seery, T. A. P.; Weiss, R. A.; *Macromolecules* **1998**, *31*, 7385.
- [8] Innis, P. C.; Norris, I. D.; Kane-Maguire, L. A. P.; Wallace, G. G.; *Macromolecules* **1998**, *31*, 6521.
- [9] Boris, D. C.; Colby, R. H.; *Macromolecules* **1998**, *31*, 5746.
- [10] Feng, Y.; Karim, A.; Weiss, R. A.; Douglas, J. F.; Han, C. C.; *Macromolecules* **1998**, *31*, 484.
- [11] Orlor, E. B.; Calhoun, B. H.; Moore, R. B.; *Macromolecules* **1996**, *29*, 5965.
- [12] O'Connell, E. M.; Peiffer, D. G.; Root, T. W.; Cooper, S. L.; *Macromolecules* **1996**, *29*, 2124.
- [13] Lu, X.; Weiss, R. A.; *Macromolecules* **1996**, *29*, 1216.
- [14] Szczubialka, K.; Ishikawa, K.; Morishima, Y.; *Langmuir* **2000**, *16*, 2083.
- [15] Inagaki, Y.; Kuromiya, M.; Noguchi, T.; Watanabe, H.; *Langmuir* **1999**, *15*, 4171.
- [16] Roberts, J. M.; Linse, P.; Osteryoung, J. G.; *Langmuir* **1998**, *14*, 204.

- [17] Roberts, J. M.; Sierzputowska-Gracz, H.; Stejskal, E. O.; Osteryoung, J. G.; *J. Phys. Chem. B*; **1998**, *102*, 7735.
- [18] Phillies, G. D. J.; Lacroix, M.; Yambert, J.; *J. Phys. Chem. B*; **1997**, *101*, 5124.
- [19] Johnathan Z. Knaul; Van Tam Bui; Katherine A. M. Creber ; *J. Chem. Eng. Data*, **2000**, *45*, 508.
- [20] Thielking, H.; Kulicke, W.-M.; *Anal. Chem.* **1996**, *68*, 1169.
- [21]. Tan. N. C.Beck, Peifer D.G. ,Briber R. M. ; *Macromolecules* **1996**, *29*, 4969.
- [22]. Jung. S.-D.; Hwang, W.-Y.; Song, S.H.; *Opt. Lett.* **1995**, *20*, 1236.
- [23]. E. B. Orler; D.J. Yontz; R.B. Moore; *Macromolecules* **1993**, *26*, 5157.
- [24]. M.J.Sullivan; R.A. Weiss; *Polym. Eng. Sci.* **1992**, *32*, 517.
- [25]. A. Molnar; A. Eisenberg; *Polym. Commun.* **1991**, *32*, 370.
- [26]. X.S.Zhang; A. Natansohn; A. Eisenberg; *Macromolecules* **1990**, *23*, 412.
- [27]. A.F. Turbak, *Ind. Eng. Chem.Prod. Res. Dev.* **1962**, *1*, 275; Patent US3072618 (1963)
- [28]. W.R. Carroll; H.Eisenberg,; *J. Polym. Sci. Part A-2*, **1966**, *4*, 599.
- [29]. H. Vink; *Makromol. Chem.* **1981**, *182*, 279.
- [30]. K. Matsuzaki; T. Uryu; K. Osada; T. Kawmura; *Macromolecules* **1972**, *5*, 816.
- [31]. W.A. Thaler,; *Macromolecules* **1983**, *16*, 623.
- [32]. Nadine Pernodet, Miriam Rafailovich Jonathan Sokolov, Dilip Gersappe, Dayi. Xu, Nan-Loh Yang, and Kenneth McLeod, *J. Biomed. Mat. Res.*, 2002 (in Press)
- [33]. W.O. Kenyon; G. P. Waugh; *J. Polym. Sci.*, **1958**, *32*, 83.

- [34]. D.L. Trumbo; T.K. Chen; H.J. Harwood; *Macromolecules* **1981**, *14*, 1138.
- [35]. S. Machida; N. Tani; T. Tazaki, Japan patent, JP 05320250 (**1992**)  
CA120:271535.
- [36]. J. J. Sun; J.S. Fritz; *J. Chromatogr*, **1981**, *590*, 197.
- [37]. B. S. Furniss ; *Textbook of Practical Organic Chemistry*, 5<sup>th</sup> edition,  
Longman, John Willey & Sons, New York, 1006(**1989** ).
- [38]. M.M.coleman, J. F. Graf, P.C. Painter, "*Specific Interactions and the Miscibility of Polymer Blends*", Technomic Publishing Inc., Lancaster, PA, USA **1991**.
- [39]. M.M. Coleman; A.M. Lichkus; P. C. Painter; *Macromolecules* **1989**, *22*, 586.
- [40]. T. Yamaoka; M.Nishiki; K.Koseki; M.Koshiba; *Polym. Eng. Sci.* **1989**, *29*, 856.
- [41]. J.T.Fahey; K. Shimizu; J.M. J. Frechet; N. Clecak; C. G. Willson; *J Polym. Sci., Polym. Chem. Ed.*, **1989**, *31*, 1.
- [42]. B.B.Corson; W. J. Heintzelman; L. H. Schwartzman; H. E. Tiefenthal; R. J. Lokken; J. E. Nickels; G. R. Atwood; F. J. Pavlik; *J. Org.Chem.* **1958**, *23*, 544.
- [43]. W. J. Dale; H. E. Hennis; *J. Am.Chem. Soc.* **1958**, *80*, 3645.
- [44]. R. C. Sovish; *J. Org. Chem.* **1959**, *24*, 1345.
- [45]. C.T. Chen; H.Morawetz; *Macromolecules* **1958**, *22*, 159.
- [46]. K. J. Zhu; S.F. Chen; T. Ho; E.M. Pearce; T. K. Kwei; *Macromolecules* **1958**, *23*,150.

- [47]. M. V. de Meftahi; J. M. J. Frechet; *Polymer* **1958**, *29*, 477.
- [48]. Y. Xu; P.C.Painter; M.M. Coleman; *Polymer* **1958**, *34*, 3010.
- [49]. A. Hirao; K. Kitamura; K. Takenaka; S. Nakahama; *Macromolecules* **1993**, *26*, 4995.
- [50]. A.Hirao; K. Takenaka; S. Packirisamy; K. Yamaguchi; S.Nakahama; *Makromol. Chem.*, **1985**, *186*,1157.
- [51]. M.Xiang; M. Jiang; L. Feng; *Macromol. Rapid Commun.* **1995**, *16*, 477.
- [52]. S.D.Clas; A.Eisenberg; *J. Polym. Sci., Part B: Polym. Phys.* **1985**, *24*, 2743.
- [53]. R.Arshady, *Angew. Makromol. Chem.* **1985**, *106*, 191.
- [54]. Goh, S.H.; S.Y. Lee; L.I.K. Tan; *Polym. Bull.* **1985**, *37*, 253.
- [55]. P. Iriondo; J. J. Iruin; M.J. Fernandez-Berridi; *Macromolecules* **1985**, *29*, 5605.
- [56]. L. Jong; E.M. Pearce; T.K.Kwei; L.C.Dickinson; *Macromolecules* **1985**, *23*, 5017.
- [57]. W.L.Tang; B. Thompson; M.M. Coleman; P.C. Painter; *Polym. Prepr.* **1985**, *31*,541.
- [58]. J.F. Graf; P.C. Painter; M.M.Coleman; *Polym. Prepr.*, **1990**, *31*, 537.
- [59]. P. Pedrosa; J.A. Pomposo; E. Calahorra; M. Cortazar; *Polymer* **1990**, *36*, 3889.
- [60]. P. Iriondo; J. J. Iruin; M.J. Fernandez-Berridi; *Polymer* **1990**, *36*, 3235.
- [61]. J. Hong; S.H. Goh; S. Y. Lee; K. S. Siow; *Polymer*. **1990**, *36*, 143.
- [62]. K. Takegoshi; K. Hikichi; *Polymer J.* **1994**, *26*, 1377.

- [63]. C. Qin; A.T.N. Pires; L. A. Belfiore; *Polym. Commun.*, **1990**, *31*, 177.
- [64]. P. A. Mirau; J.L. White, Magn; *Reson. Chem.* **1990**, *32*,s23.
- [65]. Y. Xu, D. E. Bhagwagar, P.C. Painter;M.M. Coleman; *Macromol. Symp.* **1994**, *84*, 307.
- [66]. W.L. Tang; M. M.Coleman; P. C. Painter; *Macromol. Symp.* **1994**, *48*, 315.
- [67]. E.G. Lezcano; C. S. Coll; M. G. Prolongo; *Polymer.* **1996**, *37*, 3603.
- [68]. M. Jiang; X.P.Qiu; W.Qin; L.Fei; *Macromolecules* **1995**, *28*, 730.
- [69]. X. P. Qiu; M Jiang; *Polymer* **1996**, *35*, 5084.
- [70] Shin, K.; Rafailovich, M. H.; Sokolov, J.; Gersappe, D.; Kim, M. W.; Satija, S. K.; Nguyen. D.: Xu, Dayi, Yang Nan.-Loh.; Eisenberg, A.; *Langmuir*; **2001**, *17*, 6675.
- [71] N. Pernodet. L. Collazo. M. Rafailovich, J. Sokolov, Dayi Xu, Nan Loh Yang, K.J. McLeod ; *American Journal of Physiology- Cell Physiology*, (**2002**) (submitted).
- [72] R. Arshady; G. W. Kenner; *J. Polym. Sci. Polym. Chem. Ed.* **1974**, *12*, 2017.

### **Chapter 3.**

- [1] Ge, S.; Guo. L.; Rafailovich, M.; Sokolov, J.; Overney, R.; Buenviajie, C. Peiffer, D.; Schwarz; *Langmuir* **2001**, *17*, 1687.
- [2] Matyjaszewski, K.; Jianhui Xia; *Chem. Rev.* **2001**,*101*, 2921.

- [3] Matyjaszewski, K.; Wei, M.; Xia, J.; McDermott, N. E. ;*Macromol.*, **1997**, *30*, 8161.
- [4] Kotani, Y.; Kamigaito, M.; Sawamoto, M.; *Macromolecules* **1999**, *32*, 2420.
- [5] Kotani, Y.; Kamigaito, M.; Sawamoto, M.; *Macromolecules* **2000**, *33*, 6746.
- [6] Matyjaszewski, K.; Wang, J. S. WO Pat. 9630421, U.S. Pat. 5,763,548.
- [7] Wang, J.-S.; Matyjaszewski, K. ;*Macromolecules* **1995**, *28*, 7901.
- [8] Percec, V.; Barboiu, B.; *Macromolecules* **1995**, *28*, 7970.
- [9] Matyjaszewski, K.; Patten, T. E.; Xia, J.; *J. Am. Chem. Soc.* **1997**, *119*, 674.
- [10] Wang, J.-S.; Matyjaszewski, K.; *Macromolecules* **1995**, *28*, 7901.
- [11] Wang, J. S.; Matyjaszewski, K.; *J. Am. Chem. Soc.* **1995**, *117*, 5614.
- [12] Wang, J.-L.; Grimaud, T.; Matyjaszewski, K.; *Macromolecules* **1997**, *30*, 6507.
- [13] Kato, M.; Kamigaito, M.; Sawamoto, M.; Higashimura, T.; *Macromolecules* **1995**, *28*, 1721.
- [14] Simal, F.; Demonceau, A.; Noels, A. F. ; *Angew. Chem., Int. Ed. Engl.* **1999**, *38*, 538.
- [15] Grimaud, T.; Matyjaszewski, K. ; *Macromolecules* **1997**, *30*, 2216.
- [16] Haddleton, D. M.; Jasieczek, C. B.; Hannon, M. J.; Shooter, A. J.; *Macromolecules* **1997**, *30*, 2190.
- [17] Granel, C.; Dubois, P.; Jerome, R.; Teyssie, P.; *Macromolecules* **1996**, *29*, 8576.

- [18] Uegaki, H.; Kotani, Y.; Kamigaito, M.; Sawamoto, M.; *Macromolecules* **1998**, *31*, 6756.
- [19] Moineau, G.; Minet, M.; Dubois, P.; Teyssie, P.; Senninger, T.; Jerome, R.; *Macromolecules*, **1999**, *32*, 27.
- [20] Ando, T.; Kamigaito, M.; Sawamoto, M.; *Macromolecules* **1997**, *30*, 4507.
- [21] Louie, J.; Grubbs, R. H.; *Chem. Commun.* **2000**, 1479.
- [22] Lecomte, P.; Drapier, I.; Dubois, P.; Teyssie, P.; Jerome, R.; *Macromolecules*, **1997**, *30*, 7631.
- [23] Moineau, G.; Granel, C.; Dubois, P.; Jerome, R.; Teyssie, P.; *Macromolecules* **1998**, *31*, 542.
- [24] Ando, T.; Kamigaito, M.; Sawamoto, M.; *Tetrahedron* **1997**, *53*, 15445.
- [25] Pyun, J.; Matyjaszewski, K.; *Macromolecules* **2000**, *33*, 217.
- [26] *Handbook of polymer analysis*, Japan chemical society, **1986**, pp313.
- [27] Zhang, W.; Fu, B. X.; Seo, Y.; Schrag, E.; Hsiao, B.; Mather, P.; Yang, N.-L.; Xu, Dayi.; Ade, H.; Rafailovich, M.; Sokolov, J.; *Macromolecules* **2002**, in press.